

UKNDC(83)P109
NEANDC(E)242 Vol.8
INDC(UK)-37/LN

UNCLASSIFIED

UKNDC(83)P109
NEANDC(E)242 Vol.8
INDC(UK)-37/LN

United Kingdom Atomic Energy Authority

HARWELL

**U.K. Nuclear Data
Progress Report for the Period
January-December 1982**

Editor: D.J.S. Findlay
Nuclear Physics Division
AERE Harwell, Oxfordshire
April 1983

MDS LIBRARY COPY

UNCLASSIFIED

© - UNITED KINGDOM ATOMIC ENERGY AUTHORITY - 1983
Enquiries about copyright and reproduction should be addressed to the
Publications Office, AERE Harwell, Oxfordshire, England OX11 0RA.

UNCLASSIFIED

UKNDC(83)P109
NEANDC(E)242 VOL.8
INDC(UK)-37/LN

U.K. NUCLEAR DATA PROGRESS REPORT FOR THE PERIOD
JANUARY - DECEMBER 1982

Editor: D.J.S. Findlay

Nuclear Physics Division
AERE Harwell

April 1983

HL83/1284

CONTENTS

| | <u>Accelerator*</u> | <u>Page No.</u> |
|--|---------------------|-----------------|
| CONTENTS | | 2 |
| PREFACE | | 6 |
| NUCLEAR DATA FORUM LECTURES | | 7 |
| Evaluation of the thermal neutron constants of ^{233}U , ^{235}U , ^{239}Pu and ^{241}Pu and the fission neutron yield of ^{252}Cf (E.J. Axton) | | 8 |
| Neutron fluence and spectrum determination in fast reactors (J.L. Rowlands) | | 22 |
| CINDA-TYPE INDEX | | 34 |
| 1. <u>NUCLEAR PHYSICS DIVISION, AERE HARWELL</u> | | 36 |
| Introduction | | 36 |
| 1.1 The new machine for the electron linac laboratory E | | 37 |
| 1.2 Resonance analysis of transmission data for the 1.15 keV resonance in ^{56}Fe | H | 37 |
| 1.3 Average neutron transmission and thin sample capture of ^{238}U in the 1 to 40 keV energy range | | 38 |
| 1.4 Measurements of the performance of the fast neutron target of HELIOS | E | 39 |
| 1.5 Background and resolution functions in neutron time-of-flight spectrometers | | 43 |
| 1.5.1 Response function of detectors in shields to pulsed neutron beams | | 44 |
| 1.5.2 Region of interest estimator | | 46 |
| 1.6 Fission chambers for the intercomparison of fast neutron flux density measurements | | 47 |
| 1.7 The $^{93}\text{Nb}(n,n')^{93\text{m}}\text{Nb}$ reaction | | 48 |
| 1.8 (n,α) cross-sections | A | 48 |
| 1.9 Suggested improvements to the procedures used in making accurate nuclear data measurements | | 48 |
| 1.10 Evaluation of neutron nuclear data | | 49 |
| 1.10.1 Nuclear data files | | 49 |
| 1.10.2 Nuclear data codes | | 49 |
| 1.10.3 Joint Programme on neutron data evaluation | | 50 |

*For key see p. 36

| | <u>Accelerator*</u> | <u>Page No.</u> |
|---|---------------------|-----------------|
| 1.10.4 The status of FISPIN on the Harwell computer | | 50 |
| 1.10.4.1 FISPIN coding | | 50 |
| 1.10.4.2 FISPIN data libraries | | 51 |
| 1.11 Selection of low-activity elements for inclusion in structural materials for fusion reactors | | 51 |
| 1.12 Safeguards research | | 52 |
| 1.12.1 Fissile material assay by neutron die-away | | 52 |
| 1.12.1.1 The design of neutron die-away chambers | | 52 |
| 1.12.1.2 Assay of fissile material in 208 l barrels | | 54 |
| 1.12.1.3 A monitor for observing enriched uranium in large volume packages | | 57 |
| 1.12.1.4 Pulsed neutron source assessment | | 58 |
| 1.12.2 Non-invasive determination of the U content in a centrifuge plant dump tank | | 59 |
| 1.12.3 The ²⁵² Cf shuttle | | 61 |
| 1.12.4 The determination of the ²³⁵ U enrichment of UF ₆ gas inside pipes at a centrifuge plant | | 62 |
| 1.13 Plutonium dating | | 63 |
| 1.14 Proposed neutron diagnostic systems for JET | | 64 |
| 1.14.1 Neutron yield measurements (time-resolved) | | 66 |
| 1.14.2 Neutron yield measurements (time-integrated) | | 66 |
| 1.14.3 The profile monitor | | 68 |
| 1.14.4 2.5 MeV spectrometers for deuterium plasmas | | 69 |
| 1.14.5 14 MeV spectrometers for deuterium-tritium plasmas | | 70 |
| 2. <u>CHEMICAL NUCLEAR DATA</u> | | 72 |
| 2.1 Introduction | | 72 |
| 2.2 Fission measurements | | 73 |

* For key see p. 36

| | <u>Page No.</u> |
|--|-----------------|
| 2.2.1 Development of a helium jet recoil transport system for VEC studies of short-lived nuclides | 73 |
| 2.2.2 Decay scheme studies on short-lived fission products | 73 |
| 2.2.3 Studies of ^{252}Cf fission products by means of a jet transport system | 73 |
| 2.2.4 Control of VEC beam line hardware and data acquisition with a PET/MOUSE microcomputer system | 74 |
| 2.2.5 Software for the acquisition and analysis of γ -spectral data in decay scheme studies on short-lived fission products | 74 |
| 2.2.6 γ -spectrum analysis using SAMP80 | 76 |
| 2.2.7 Heavy ion reactions on ^{93}Nb and ^{92}Mo | 76 |
| 2.2.8 Heavy ion - heavy element reactions | 77 |
| 2.2.9 Absolute determination of the energy of alpha particles emitted by ^{236}Pu | 77 |
| 2.3 Cross-section measurements | 77 |
| 2.3.1 Integral experiments to measure the partial capture cross-sections for the production of $^{242\text{m}}\text{Am}$ and ^{242}Cm from ^{241}Am , and ^{244}Cm from ^{243}Am , using ZEBRA | 77 |
| 2.3.2 PFR high power reaction rate experiment | 78 |
| 2.3.3 ^{235}U fission mass and counting comparison and standardisation | 78 |
| 2.4 Half-life measurements | 79 |
| 2.4.1 ^{235}Np decay data | 79 |
| 2.4.2 ^{237}Np half-life and I_{α} | 79 |
| 2.5 Fission product decay data | 79 |
| 2.5.1 Data Library Sub-committee | 79 |
| 2.5.2 CASCADE | 80 |
| 3. <u>REACTOR PHYSICS DIVISION, AEE WINFRITH</u> | 82 |
| 3.1 The UK Nuclear Data Library and allied topics | 82 |
| 3.2 Studies of the $^{93}\text{Nb}(n,n')^{93\text{m}}\text{Nb}$ reaction | 83 |

| | <u>Page No.</u> |
|--|-----------------|
| 4. <u>DIVISION OF RADIATION SCIENCE AND ACOUSTICS, NATIONAL PHYSICAL LABORATORY</u> | 84 |
| 4.1 International intercomparisons of neutron source strength | 84 |
| 4.2 International intercomparison of neutron fluence rate organised by BIPM | 84 |
| 4.3 International intercomparison of d+t neutron fluence and mean energy | 85 |
| 4.4 The $^{65}\text{Cu}(n,2n)$ cross-section at 14 MeV | 85 |
| 4.5 The indium cross-sections at 14 MeV | 86 |
| 4.6 Nuclear decay scheme measurements | 86 |
| 5. <u>BIRMINGHAM RADIATION CENTRE, UNIVERSITY OF BIRMINGHAM</u> | 88 |
| 5.1 Delayed neutron spectra | 88 |
| 5.2 Neutron spectra from (α,n) sources | 89 |
| 6. <u>DEPARTMENT OF PHYSICS, UNIVERSITY OF BIRMINGHAM</u> | 90 |
| 6.1 Measurements relating to tritium production in fusion breeder blankets | 90 |
| 7. <u>DEPARTMENT OF PHYSICS, UNIVERSITY OF ASTON IN BIRMINGHAM</u> | 94 |
| 7.1 The absolute measurement of (n,p) and (n,γ) cross-sections in the energy range 2 to 4.5 MeV | 94 |
| 7.2 The gamma rays associated with the inelastic scattering of 14 MeV neutrons in large samples of iron and concrete | 94 |
| 7.3 Measurements of $^{28}\text{Si}(n,p)^{28}\text{Al}$ and $^{64}\text{Zn}(n,2n)^{63}\text{Zn}$ excitation functions | 98 |
| 7.4 Application of a neutron monitoring antimony ring for the measurement of $^{56}\text{Fe}(n,p)^{56}\text{Mn}$ and $^{59}\text{Co}(n,\alpha)^{56}\text{Mn}$ cross-sections | 100 |
| 8. <u>DEPARTMENT OF PHYSICS, UNIVERSITY OF EDINBURGH</u> | 102 |
| 8.1 The polarisation and differential cross-section for elastic scattering of 3 MeV neutrons by heavy nuclei | 102 |
| 8.2 Polarisation of neutrons from the $^7\text{Li}(d,n)^8\text{Be}$ reaction | 103 |
| 9. <u>DEPARTMENT OF PHYSICS, UNIVERSITY OF LIVERPOOL</u> | 105 |
| 9.1 Nuclear structure data evaluation | 105 |

PREFACE

This report is prepared at the request of the United Kingdom Nuclear Data Committee and covers the period from January to December, 1982.

Nuclear data are presented by laboratory. There are contributions this year from the Harwell and Winfrith Laboratories of the UKAEA, the National Physical Laboratory, the Birmingham Radiation Centre, the University of Birmingham, the University of Aston in Birmingham, the University of Edinburgh, and the University of Liverpool.

This report includes work from various collaborations between Harwell, Winfrith, the Universities of Birmingham, Manchester and Guelph (Canada) and the Bureau International des Poids et Mesures, and between the National Physical Laboratory, the Institut für Radiumforschung und Kernphysik (Vienna) and the Institute of Atomic Energy (Beijing). Contributions on "Chemical Nuclear Data" are gathered by the Chemical Nuclear Data Committee and grouped under that heading.

Contributions to the report on nuclear data topics are welcome from all sources and we extend an invitation to researchers in other laboratories of industry, government, the universities and polytechnics to use this channel of communication.

Where the work is clearly relevant to requests in WRENDA 81/82 (INDC(SEC)-78/URSF) request numbers are given after the title of the contribution.

NUCLEAR DATA FORUM LECTURES

The sixteenth Nuclear Data Forum took place at the National Physical Laboratory on 13th December 1982 with 67 participants. The themes this year were neutron standards and reactor dosimetry. Two invited lectures were presented, one by Mr. E.J. Axton on the evaluation including covariances of the thermal neutron constants of $^{233,235}\text{U}$, $^{239,241}\text{Pu}$ and $\bar{\nu}$ (^{252}Cf), the other by Mr. J.L. Rowlands on neutron fluence and spectrum determination in fast reactors. Both these lectures are reproduced below. There were twelve contributed talks, six continuing the two themes mentioned above, talks on the ^{64}Cu decay scheme, the analysis of neutron activation data, tritium production in fusion breeder blankets and neutron interrogation by the die-away technique, and two reports on the Antwerp International Conference on Nuclear Data for Science and Technology and the Cambridge International Conference on the Neutron and its Applications to make the fiftieth anniversary of the discovery of the neutron, both in September 1982.

Evaluation of the thermal neutron constants of ^{233}U , ^{235}U , ^{239}Pu and ^{241}Pu and the fission neutron yield of ^{252}Cf *

E.J. Axton

Central Bureau for Nuclear Measurements, Geel, Belgium

Lecture given at the Nuclear Data Forum, NPL**, Dec. 1982

1. Introduction

The thermal neutron constants comprise the thermal neutron (2200 m s^{-1}) absorption and fission cross sections, $\bar{\nu}$ (total number of neutrons emitted per fission), and η (total number of neutrons emitted per neutron captured) for the nuclides ^{233}U , ^{235}U , ^{239}Pu , and ^{241}Pu . In addition $\bar{\nu}$ for ^{252}Cf is included because it is widely used as a standard for the measurement of $\bar{\nu}$ for neutron-induced fission of the other nuclides. The importance of these data stems from the role they play in the prediction of the neutron economy in nuclear power reactors. Following the general declassification and release of nuclear data on an international scale, data from various national sources were first compared at the first International Conference on Peaceful Uses of Atomic Energy in 1955, where satisfactory agreement was found. Since that era a continuous supply of new data has appeared, with new techniques and greater accuracy. This has prompted a continuous re-evaluation of the data over the years. Owing to the correlated nature of the measurements these evaluations necessarily take the form of simultaneous least-squares fits to all the data, together with updating older data in terms of newer values for standard cross sections, half-lives, etc.

Invariably such evaluations indicate disturbing discrepancies which have been attributed variously to measurements of $\bar{\nu}$, of η , of α (ratio of absorption to fission cross sections), and of $\bar{\nu}_p$ ratios, and to differences between measurements with monoenergetic neutrons and those in Maxwellian spectra.

*This is a summary of the work performed at CBNM during the period 1 January 1982 to 31 December 1982. The full report will be available shortly under the reference CBNM/PH/1/82.

**Lecture presented by T.B. Ryves

In the past, the more important correlated errors have been dealt with by treating them as independent variables to be fitted in the evaluation. However, if there are too many correlated errors the system runs out of degrees of freedom. The purpose of the present exercise is to investigate the effect of treating all correlated errors by the introduction of a full covariance matrix. Unfortunately, the time available was not sufficient to enable a study of all available data. Some older data had to be omitted because there was insufficient information to permit the construction of a covariance matrix. More importantly, it was necessary to exclude all measurements in Maxwellian neutron spectra.

Results for various subsets of data and comparisons with previous evaluations are presented.

2. The new evaluation

Since the 1975 (uncompleted) International Atomic Energy Agency multiparameter evaluation a considerable quantity of new data has become available, and older data has been updated. Although several evaluations of subsets of data have been published (for example \bar{v} for ^{252}Cf ^(1,2) and \bar{v}_p ratios⁽³⁾) no simultaneous fit to all the data has been made. At the beginning of 1982 it was thought worthwhile to undertake such an exercise with the special objective of including a full covariance matrix in the calculation. Since there was no guarantee of completion in the strictly limited available time of one man-year the programme was divided into stages with priorities 1-3 as follows:

- (1) all \bar{v}_p ratios
- (2) the addition of monoenergetic measurements of σ_a , σ_f , and η
- (3) the addition of measurements, made in thermal Maxwellian spectra, of $\bar{\sigma}_a$, $\bar{\sigma}_f$ ratios, $\bar{\sigma}_a/\bar{\sigma}_f$ ratios, $\bar{\eta}$ ratios, $\bar{\eta}\bar{\sigma}_a$ ratios, and $(\bar{\eta} - 1)\bar{\sigma}_a$ ratios.

In the event, stages (1) and (2) were completed but there was insufficient time available to undertake (3). Apart from shortage of time there was also a problem of space. The 1975 IAEA data set contains well over 200 measurements. It was necessary to find a way to reduce the size of the covariance matrix, which would otherwise be unmanageable with the computing power available.

When this work was well advanced, a paper was presented at the 1982

Antwerp Conference⁽⁴⁾, in which the last remaining discrepancy (the reconciliation of σ_f and $\bar{\sigma}_f$) appeared to have been removed following the re-interpretation of the precise Chalk River $\bar{\alpha}$ measurements by Beer et al.⁽⁵⁾, Durham et al.⁽⁶⁾ and Lounsbury et al.⁽⁷⁾ Stehn et al.⁽⁴⁾ used a least-squares fitting procedure similar to that of the IAEA to perform a simultaneous multiparameter fit using as input recent evaluations of subsets of data.

2.1 The Program

The program is similar to that used by the IAEA but with common errors dealt with in a covariance matrix instead of by including common errors as variables to be fitted or by adjusting the weights. Owing to the presence of ratios and other data combinations it is necessary to linearise the problem by assuming input values for the parameters to be fitted, and if necessary, to iterate the calculation. The linear model is

$$y = Ab + \epsilon$$

where y is a specified n -element observation vector, A is a specified n by p design matrix containing the differentials of each measurement with respect to the parameters to be fitted, b is a p -element regression vector to be determined (the solution) and ϵ is an unknown n -element noise vector with zero mean and covariance Z . The solution satisfies the normal equation

$$A^T Z^{-1} A b = A^T Z^{-1} y$$

and is

$$b = (A^T Z^{-1} A)^{-1} A^T Z^{-1} y$$

with covariance

$$v = (A^T Z^{-1} A)^{-1}$$

The residuals (Res) are given by $y - Ab$, and the statistical parameter χ is given by $\chi^2 = \text{Res}^T Z^{-1} \text{Res}$. The elements $y_{\text{obs } i}$ of y are the fractional differences between the measurements and their respective input values.

For a simple \bar{v} measurement

$$y_{\text{obs } i} = \frac{\bar{v}_m i}{\bar{v}_{\text{in } i}} - 1$$

where 'm' refers to measurement and 'in' refers to input. For a ratio R of \bar{v}_1/\bar{v}_2

$$y_{\text{obs } i} = \frac{R_{m i} \bar{v}_{2 \text{ in}}}{\bar{v}_{1 \text{ in}}} - 1$$

For a measurement of η

$$y_{\text{obs } i} = \frac{\eta_{m i} \sigma_{a \text{ in}}}{\bar{v}_{\text{in}} \sigma_{f \text{ in}}}$$

The fitted values are given by the input parameters multiplied by $(1 + b)$, with covariance V .

The programs were written in the IBM APL language and operated on the IBM computer at CBNM. For ease of programming relative uncertainties are used throughout.

2.2 Input Data

(a) \bar{v} for ^{252}Cf . The data are taken from the evaluation by Smith⁽¹⁾ with additional measurements by Smith⁽⁸⁾, Zhang and Liu⁽⁹⁾, Edwards, Findlay and Lees⁽¹⁰⁾, and Spiegel, Gilliam and Slater⁽¹¹⁾. For the boron pile, the evaluation by Ullo is used, and also the interpretation of the boron pile value in terms of the NPL manganese bath is included.

(b) \bar{v} ratios. Only the ratios considered by Boldeman and Fréhaut⁽³⁾ (for which foil thickness corrections are available) were used. In all cases the measured values are used uncorrected for, for example, mean fission energy differences, delayed γ 's, delayed neutrons and foil thickness corrections. The program then makes the appropriate corrections and formulates the covariance matrix accordingly. The liquid scintillator measurements are correlated through uncertainties in delayed neutrons and delayed γ corrections, uncertainties in foil thickness corrections (all based on Boldeman's γ -ray table), detector slope multiplied by uncertainties in mean energies, and uncertainty in detector slope multiplied by mean energy differences. The latter item is divided by an arbitrary factor of 10 for correlations between different authors. All manganese bath measurements are correlated by the uncertainty in the sulphur thermal cross section. All measurements dependent on the NPL manganese bath are correlated by the overall bath uncertainty. There are also a number of one-off correlations which are entered in the covariance matrix on an element by element basis. Examples of such are

(1) the high correlation between the two Gwin et al.⁽¹²⁾ ratios due to the uncertainty in the detector response to californium neutrons,

- (2) the correlation between the Spiegel et al.⁽¹¹⁾ and Bozorgmanesh⁽¹³⁾ measurements due to the common element in the calibrations of the neutron sources NBS I and NBS II,
- (3) correlations in the $\bar{\nu}_p$ ratios of Boldeman, of Hopkins and Diven, and of Mather due to uncertainties common to several ratios measured by the same authors,
- (4) the common uncertainty in the two interpretations of the boron pile.
- (c) Total and scattering cross sections. The input data are basically the same as those considered by Lemmel⁽¹⁴⁾. Only Smith's 1968 measurement for ^{241}Pu has been updated⁽⁸⁾. All data were corrected to the later value for the Avogadro constant (6.022045×10^{23} instead of 6.0248×10^{23}).
- (d) Fission cross sections. These are basically the same as in ref. 14. The input data are not entered as cross-section x half-life products as in ref. 14. They are corrected, where necessary, to standard reference cross sections. They are then entered as data with the appropriate assumed half-life and uncertainty. They are corrected by the program to the latest preferred half-life values and the covariance matrix adjusted accordingly.
- (e) η values. The Ullo and Goldsmith⁽¹⁵⁾ evaluation of the Smith et al.* and Macklin et al. measurements were used, and consequently there are significant correlations both between nuclides and between authors.

It was found that the total and scattering cross sections were not only uncorrelated with the other data, but also uncorrelated with each other. They were therefore fitted as a subset, and only the derived absorption cross sections and their covariance matrix were entered in the main program data set. Likewise, the fission cross sections could also be analysed as a subset, and only the output values and their covariance matrix were carried through to the main program. The input data for the main program therefore consisted of the output data from the two cross section analyses, plus the η , $\bar{\nu}$, and $\bar{\nu}_p$ ratio data. The inclusion or not of the sulphur thermal capture cross section as a parameter to be fitted has no effect on the output data provided that the covariance matrix is constructed correctly in each case. Mathematically the two problems are identical. If the sulphur cross section is included, an output value is obtained for it. With sulphur included there are 48 items of input data

*This measurement has since been replaced by that in ref. 8.

together with a 48^2 covariance matrix. This is close to the maximum possible (53^2) with store available with the APL package. The inclusion of the additional measurements in thermal Maxwellian spectra, of which there are at least forty, would therefore overload the system unless they were seen to be independent of the other data and therefore able to be analysed separately as a subset.

(f) Uncertainties. All uncertainties including those often called 'systematic' are estimated at the level of one standard deviation (68% confidence) and summed quadratically in accordance with the recommendations of the International Bureau of Weights and Measures. In the case of liquid scintillator measurements the uncertainties are entered net of any contributions from the corrections for delayed γ -rays, delayed neutrons, foil thickness, and mean fission spectrum energies. In the case of manganese bath measurements the uncertainty is entered net of the contribution from the uncertainty in the sulphur thermal absorption cross section. These uncertainties are added in the program, and the covariance matrix is adjusted accordingly.

3. Results

Figs. 1a and 1b compare the results of the present evaluation with the results of the evaluations of

- (1) Stehn, Divadeenam, and Holden⁽⁴⁾
- (2) Lemmel⁽¹⁴⁾ - monoenergetic 2200 m s^{-1} data only
- (3) Lemmel⁽¹⁴⁾ - all data
- (4) ENDF/B-V
- (5) Steen⁽¹⁶⁾

The ratios of the values of the set of fitted quantities $\bar{\nu}$, σ_f and σ_a and the derived quantities η and $1+\alpha$ from the present evaluation to the corresponding values from the five other evaluations are shown with the quantities from the present evaluation as numerators.

In order to test the compatibility of some subsets of data some more runs were carried out in which the absolute values of the set of fitted quantities were based on

- (6) manganese bath ^{252}Cf $\bar{\nu}$ data
- (7) liquid scintillator $\bar{\nu}$ data
- (8) η data

This evaluation \pm

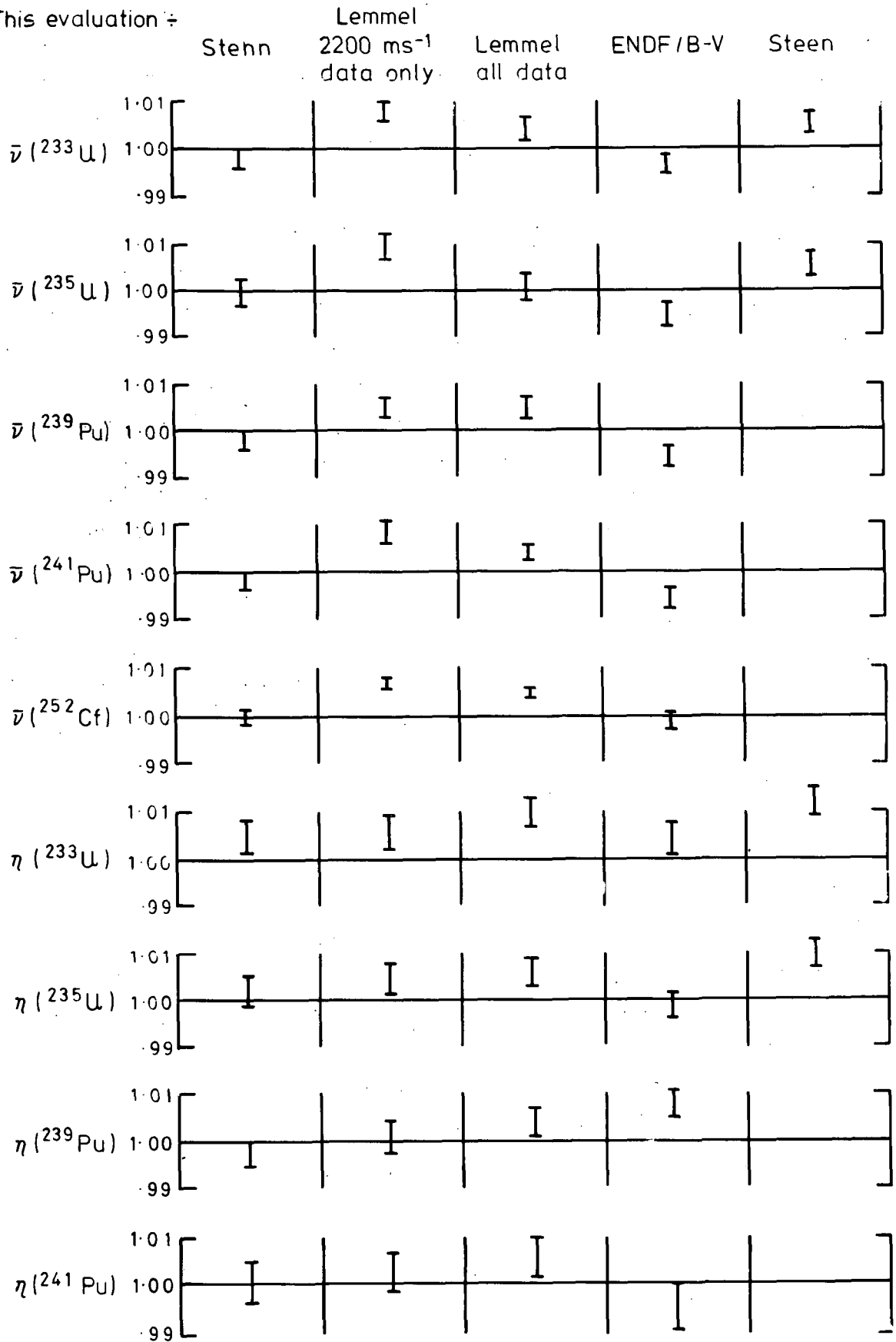


Fig. 1a Comparison of results of present evaluation with previous evaluations

This evaluation \div

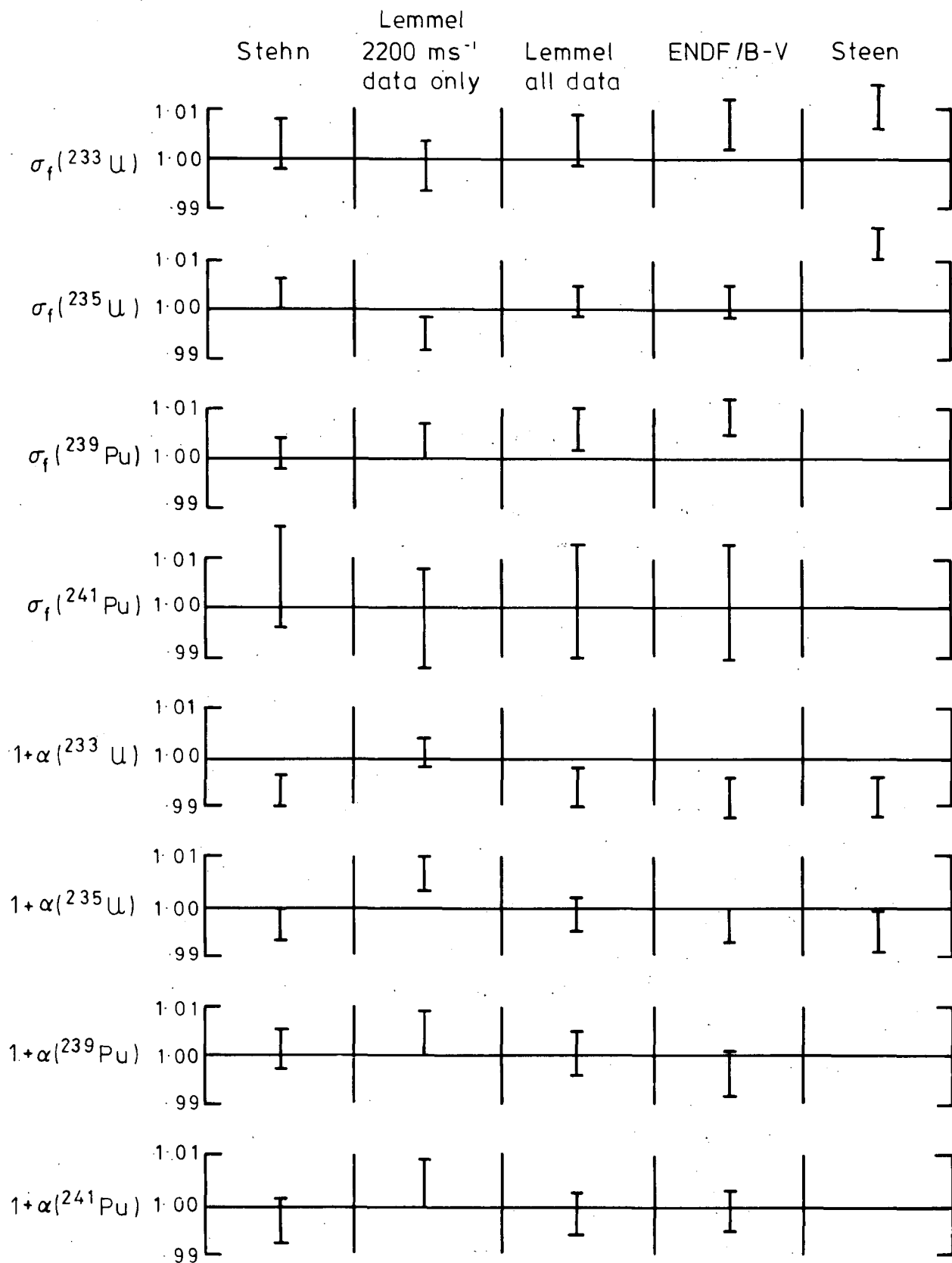


Fig. 1b Comparison of results of present evaluation with previous evaluations

- (9) all ^{252}Cf \bar{v} measurements but omitting η measurements - for this the fitted η values are imprecise, particularly for ^{233}U and ^{241}Pu , because of the large uncertainties in $1+\alpha$, which only improve when \bar{v} and η data both appear in the input data
- (10) all σ_f data omitted so that output σ_f values are determined by \bar{v} , η , and σ_a .

These results are compared in Fig. 2, in which the first column compares (6) with (7), the second column compares values derived from all data with (8), the third column compares values derived from all data with (9), the fourth column compares values derived from all data with (10), and the fifth column compares values derived from all data including covariances with values neglecting covariances.

4. Discussion of Results

The neglect of covariances has the effect of making the results look better than they really are ($\chi^2 = 31.54$ instead of 43.04 with 35 degrees of freedom). In most, but not all, cases the uncertainties of the output parameters are smaller, and the values are different. For example \bar{v} (^{252}Cf) reduces from 3.7661 ± 0.0054 to 3.7630 ± 0.0044 , σ_f (^{235}U) is raised from 584.7 ± 1.7 b to 585.5 ± 1.7 b, and \bar{v} (^{235}U) drops from 2.4274 ± 0.0048 to 2.4242 ± 0.0045 .

The conflict between measurements of \bar{v} (^{252}Cf) is illustrated in Fig. 2, which shows a difference of (0.475 ± 0.300) % between manganese bath and liquid scintillator results, which is significant. The independent value derived from η measurements only agrees better with the manganese bath result, but has a large uncertainty due to uncertainties in the measured values of $1+\alpha$. The latter uncertainties, particularly for ^{233}U and ^{241}Pu , are considerably reduced when η and \bar{v} data appear in the same fit.

The conflict between the manganese bath and the liquid scintillator measurements dates from the advent of the Spencer measurement which is one of the highest measurements and also has the highest claimed accuracy. It makes the largest single contribution to χ^2 . Smith has carried out a very careful study of manganese bath systematics which extended over several years. He was unable to detect a systematic error which would explain the conflict. His earlier proposal that the true value of the sulphur capture cross section σ_s might be significantly higher than the traditional value of 0.52 b is not supported by recent measurements. It is worth noting that

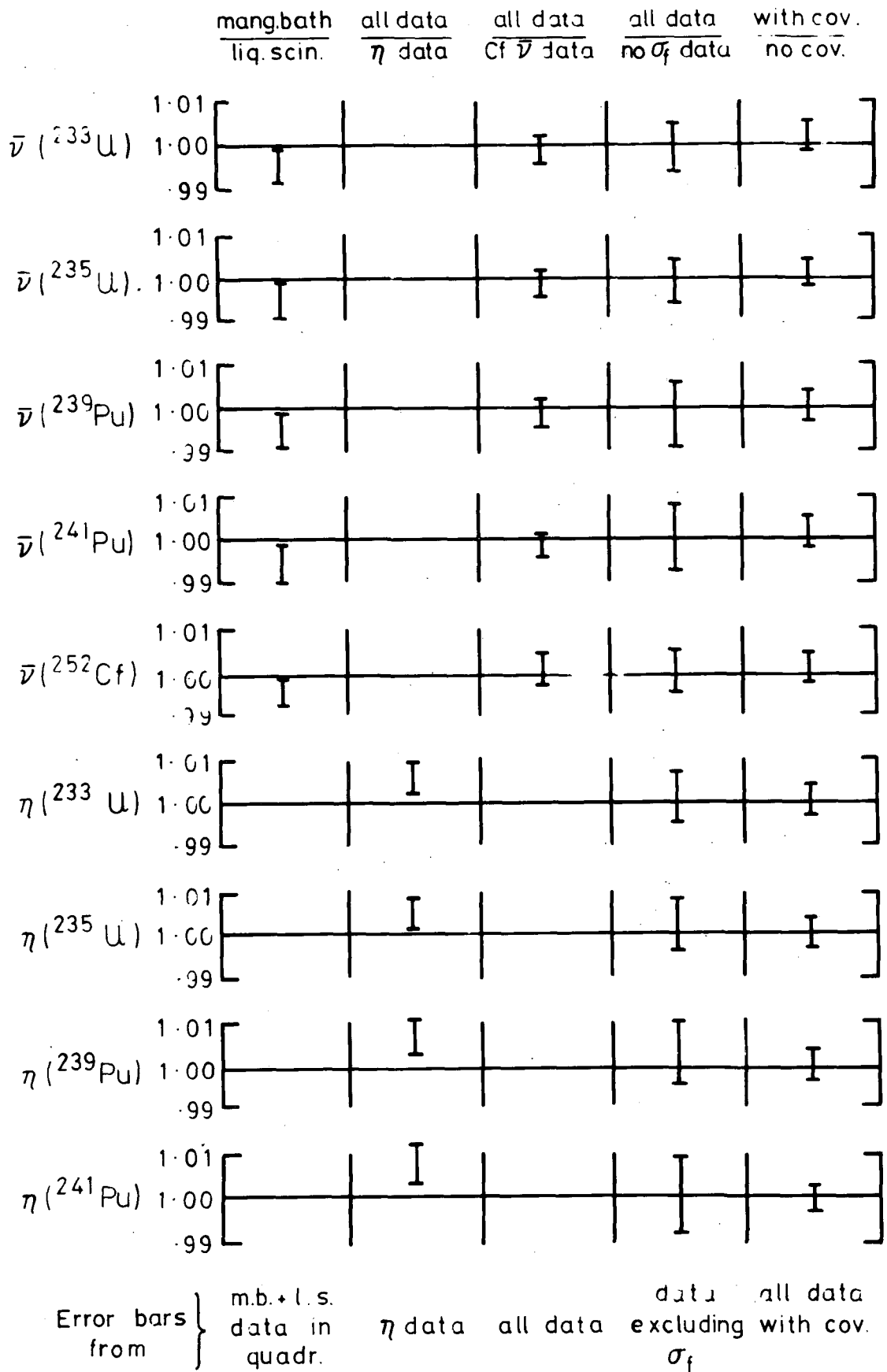


Fig. 2 Effect on results of present evaluation of restricting input data to different subsets and of neglecting covariances

the reduction of the uncertainty in σ_S from 0.03 to 0.015 b increases χ^2 from 38 to 43, with 34 degrees of freedom.

Could there be a systematic effect in the liquid scintillator measurements which has been overlooked? Although a very comprehensive account of the Spencer measurement has been published, it can do no harm to draw attention to some small effects which are not discussed in the report (but not necessarily ignored). Although perhaps individually negligible, they might collectively be significant if they work in the same direction.

(a) Delayed neutrons. The same delayed neutron corrections are applied to all $\bar{\nu}_p$ measurements irrespective of the length of the neutron detection gate. How good is the demarcation between prompt and delayed neutrons? Is it possible for a prompt neutron thermalised later to overlap a delayed neutron thermalised early?

(b) Photoneutron production.

- (1) At the time of the γ -flash the γ/n ratio is very high, and the γ 's are not confined to the neutron collimator. Photoneutrons can be produced by the (γ,n) reaction on the deuterium content of the scintillator, and also in (γ,n) reactions on materials external to the tank such as shields, filters and the neutron collimator. Such photoneutrons are time related to the γ -flash. At 82 m from the target this effect could well be negligible.
- (2) In the neutron capture process several γ 's per neutron are produced which are candidates for the ${}^2\text{H}(\gamma,n)$ reaction in the scintillator. These photoneutrons are time-related to the neutron capture.
- (3) Each fission produces on average 10 fission products, most of which emit γ -rays which are further candidates for the ${}^2\text{H}(\gamma,n)$ reaction. The photoneutron production would not necessarily be time related to the neutron gate.
- (4) Prompt γ 's from fission could produce photoneutrons in the ${}^2\text{H}(\gamma,n)$ reaction which would be indistinguishable from fission neutrons.

(c) Neutron collimation. Is it possible that neutrons scattered by the final (82 m) stage of the collimator can enter the tank other than via the through-tube?

(d) Is the light collection efficiency independent of the position of the neutron when it is captured?

A study of Fig. 2 indicates that, as observed by Smith⁽⁸⁾, there is no significant conflict between η and $\bar{\nu}$. For ^{252}Cf $\bar{\nu}$ is 3.7661 ± 0.0054 from all data, and 3.7665 ± 0.0056 when η measurements are omitted.

The differences between these (all-data) results and those of Lemmel⁽¹⁴⁾ which exclude Maxwellian spectra based results are significant, but these differences are undoubtedly due to improvements in data since 1975. They are not attributed to differences in computational techniques because the more important correlations were treated very adequately in the IAEA exercise.

Perhaps the comparison with the result of Stehn et al.⁽⁴⁾ is more interesting because Stehn uses most, but not all, of the new information which has emerged since 1975. The present results for $\bar{\nu}(^{252}\text{Cf})$ are the same as Stehn, but with a 13% larger uncertainty. For the fissile nuclides values of $\bar{\nu}$ are between 0.1% and 0.2% lower, with uncertainties 13% to 20% higher, except for ^{241}Pu where the uncertainty is actually lower. The present values of σ_f are higher than Stehn except for ^{241}Pu which agrees, e.g. for ^{235}U σ_f is $(0.314 \pm 0.348)\%$ higher. For ^{235}U η is $(0.222 \pm 0.301)\%$ higher, but combines with $1+\alpha$, which is $(0.310 \pm 0.319)\%$ lower, to produce $\bar{\nu}$ which is $(0.106 \pm 0.256)\%$ lower. There is only one instance where the difference exceeds the uncertainty, namely $\eta(^{233}\text{U})$ which is $(0.529 \pm 0.326)\%$ lower. The Stehn et al conference report⁽⁴⁾ does not give in detail the input data used. Not all the correlations considered by Lemmel⁽¹⁴⁾ were included. Some of the differences could perhaps be attributed to neglect of correlations (e.g. the systematically higher uncertainties). However, the major cause of differences is probably the fact that the Maxwellian spectra based data block is missing from the present data set.

5. Conclusions

For the first time a multiparameter fit to the thermal constants of the fissile nuclides has been performed with a full covariance matrix for the input data. The proper treatment of correlations can improve or worsen the appearance of the data set, depending on the nature of the problem. In this case it produces higher uncertainties in the fitted parameters, and a larger χ^2 . Neglect of correlations in this case produces slightly different values and makes the data look less discrepant than they really

are. It is unfortunate that there was insufficient time available to include at least the more important Maxwellian spectra based data.

In 1975 Lemmel⁽¹⁴⁾ observed a discrepancy between the 2200 m s^{-1} data and the Maxwellian data which could be attributed to α or g_f and g_a values on the assumption that \bar{v} and η measurements are reliable. He was inclined to suspect the g values, but he observed later that uncertainties in the low energy (0.005 - 0.02 eV) cross section shapes and in the g -factors derived from them could not explain the full amount of the discrepancies. Of equal, if not greater, importance is the actual shape of the reactor spectrum in this important energy range. The reactor spectrum is assumed to be a Maxwellian shape characterised by a certain temperature which is above the temperature of the moderator due to preferential absorption of low energy neutrons. However, in the energy range of interest there must be important shielding and flux depression effects which could distort the spectrum from the true Maxwellian shape. The spectrum is not easy to measure in that energy range. According to Stehn et al.⁽⁴⁾ the problem has been resolved by the Beer⁽⁵⁾ re-evaluation of the Chalk River α data. There are no details given. Although seven years old, the Beer reference does not seem to have received very much publicity, and it has proved impossible to date to obtain a copy. Thus it is not profitable to discuss the problem further. Even without the Maxwellian data, a comparison of this work with that of Stehn et al. reveals that they are in agreement within the uncertainties of the comparison in all cases except η for ^{233}U . The uncertainties are consistently higher, due in part to the inclusion of correlations.

Among the most important information to emerge from this work is probably the correlation matrix of fitted parameters, which should always be used if the parameters themselves are propagated into reactor calculations.

Acknowledgements

It is a pleasure to acknowledge the continuing encouragement of Dr. H.D. Lemmel throughout the year, and his assistance in obtaining copies of the more obscure references. Dr. J.R. Smith kindly provided an advance draft of his recent work, and Dr. R. Werz gave valuable guidance on the use of the APL computer language in least squares problems.

- (1) J.R. Smith, Electric Power Research Institute report EPRI-NP-1258 (1979)
- (2) J.W. Boldeman, NBS Special Publication 493 (National Bureau of Standards, 1977), p.182.
- (3) J.W. Boldeman and J. Fréhant, Nucl. Sci. Engng. 76 (1980) 49.
- (4) J.R. Stehn, M. Divadeenam and M. Holden, Int. Conf. Nucl. Data. Sci. Technol., Antwerp, Sept. 1982.
- (5) M. Beer et al., Electric Power Research Institute report EPRI-NP-163 (1975).
- (6) R.W. Durham et al., Proc. Conf. Nucl. Data Reactors, Paris, 1966, vol.2 (IAEA, Vienna, 1967), p.17.
- (7) M. Lounsbury, R.W. Durham and G.C. Hanna, Second Int. Conf. Nucl. Data Reactors, Helsinki, vol.1 (IAEA, Vienna, 1970), p.287.
- (8) J.R. Smith, private communication (1982).
- (9) H. Zhang and Z. Liu, Chinese J. Nucl. Phys. 2 (1980), 29, and private communication (1981).
- (10) G. Edwards, D.J.S. Findlay and E.W. Lees, Ann. Nucl. Energy 9 (1982) 127.
- (11) V. Spiegel, D.M. Gilliam and W.E. Slater, Proc. $\bar{\nu}$ Workshop, Sheraton-Washington Hotel, Nov. 1980, ed. A.D. Carlson (NBS, 1981).
- (12) R. Gwin et al., Oak Ridge National Laboratory report ORNL/TM 6246 (1978).
- (13) H. Bozargmanesh, Absolute measurement of the number of neutrons per spontaneous fission of ^{252}Cf , Ph.D. dissertation, Univ. of Michigan (1977).
- (14) H.D. Lemmel, Proc. Conf. Neutron Cross-sections and Technol., Washington, D.C., 1975, vol. 1 (NBS Special Publication 425, National Bureau of Standards, 1975) p.286.
- (15) J.J. Ullo and M. Goldsmith, Nucl. Sci. Engng. 60 (1976) 239.
- (16) N.M. Steen, Westinghouse Atomic Power Division report WAPD-RM-1052.

Neutron fluence and spectrum determination in fast reactors

J.L. Rowlands, AEE Winfrith

Lecture given at the Nuclear Data Forum, NPL, Dec. 1982

1. Introduction

One of the purposes of the Prototype Fast Reactor (PFR) at Dounreay is to determine the effects of irradiation on fuel and structural materials (such as the fuel cladding and the hexagonal boxes holding the fuel pins). The target burn up for the fuel is about 10% of the uranium and plutonium nuclei, i.e. 10% of these nuclei fission and are each replaced by two fission product nuclei, some of which are gaseous. For every fission reaction there are many neutron-nucleus scattering reactions. Each structural material atom is displaced from its lattice position about 100 times during the residence time of a subassembly. These displacements cause swelling and the amount of swelling is dependent on the temperature and on the presence of helium nuclei produced by (n,α) reactions. The swelling on the two sides of a subassembly can be different, because of differences in the flux, and consequently bowing occurs. This swelling and bowing could cause subassemblies to become stuck in the reactor. The fuel pins also swell and there is a potential for coolant channels to become blocked. Materials can also lose their strength or become brittle through irradiation effects. Structural material atomic displacement might well be the factor limiting fuel endurance and there is an economic incentive to increase the residence times of subassemblies and control rods.

The atomic displacement rate per fission in a subassembly depends on the fuel enrichment and on the neutron spectrum. Consequently it is greater in a larger fast reactor having a lower fuel enrichment. It will therefore be greater in a commercial sized fast reactor than in the Dounreay PFR (unless the commercial sized reactor design is changed to specify a heterogeneous core containing zones of breeder material and fuel having a higher enrichment). In order to use the information obtained from PFR in the design of larger fast reactors account must be taken of differences in neutron spectrum and in flux gradient across subassemblies (which determines the bowing) between PFR and the commercial design.

Measurements are made in PFR not only on fuel pins and subassemblies but also on samples of different structural materials. These are

irradiated in special rigs loaded into demountable subassemblies (DMSA). The objective of the irradiation programme is to correlate the observed irradiation damage effects with the irradiation conditions. These irradiation conditions are characterised by the total neutron fluence and the neutron energy spectrum.

In addition to the materials endurance irradiation experiments there are programs of integral nuclear data measurements being carried out in PFR. These are measurements of spectrum averaged capture and fission cross-sections for actinide isotopes.

The questions I would like to discuss are:

how accurately can we calculate the neutron fluence and spectrum? and what measurements are most suitable for providing a normalisation or adjustment to calculations of fluence and spectrum?

These questions must be considered relative to the accuracy requirements. For atomic displacements the requirements are:

±10% for relative calculations of the number of atomic displacements per atom of the material,

±1% for the ratio of the atomic displacements on two sides of a subassembly or control rod (for calculating bowing), and

±10% for relative calculations of helium production rates.

The number of atomic displacements caused in a nuclear reaction with a neutron of energy E is characterised by the atomic displacement cross-section. The displacement rate depends on the type of alloy in which the nucleus is present (although this dependence is small and is usually neglected). For scattering reactions in structural materials the cross-section has a threshold at about 1 keV and increases approximately in proportion to neutron energy. Capture reactions at lower energies also contribute because of the nuclear recoil accompanying gamma emission.

The approach adopted in the analysis of irradiation experiments is to correlate the observed irradiation damage effects with the calculated number of atomic displacements, the temperature and possibly also the helium production. A consistent method for the calculation of these characteristics is required (with a high relative accuracy rather than absolute accuracy), and so international standard atomic displacement cross sections have been adopted. Standard dosimetry reaction data have also been adopted internationally so that these calculations can be related to dosimetry reaction measurements in a consistent way.

For the interpretation of the programmes of integral nuclear cross section measurements a good characterisation of the spectrum is desirable, so that the uncertainty in a calculated cross section due to uncertainties in the spectrum is small. For a non-threshold reaction it should be less than about $\pm 3\%$. For a threshold reaction the requirement is that it should be correlated with other threshold reactions, such as ^{238}U fission to an accuracy of about $\pm 3\%$. (The uncertainty in the estimation of the high energy component of the spectrum ($E > 1 \text{ MeV}$) might be larger than this.)

There is no continuous monitoring of the in-core flux in PFR. Three ion-chambers situated outside the radial shield, together with the thermocouples situated in the coolant above each core subassembly, provide the only monitors of the flux and power. These monitors are calibrated by temperature and flow measurements in the secondary coolant circuit. This enables total reactor power to be monitored to $\pm 5\%$ (1 s.d.). Reaction rates in individual components must be derived by calculation. Dosimetry monitors can be incorporated in a few selected components. These monitors are then recovered for analysis following an irradiation. Confirmation of calculated reaction rates can also be obtained by analysing the activity induced in components, and, in particular, by measuring the burn-up of fuel pins (including special fuel samples having an accurately known initial composition).

2. Spectrum measurements in zero power fast reactor facilities

Spectra have been measured in the ZEBRA zero power fast reactor critical facility at Winfrith using a variety of techniques. The techniques used and their approximate energy ranges are as follows:

| <u>technique</u> | <u>energy range</u> | |
|---|---------------------|---------|
| time of flight (200 m) | 200 eV | 500 keV |
| proton recoil counter in-core | 5 keV | 1.2 MeV |
| proton recoil counter in-beam | 300 keV | 3 MeV |
| ^6Li film coated semiconductor counter | 500 keV | 5 MeV |
| double scintillator in-beam | 300 keV | 5 MeV |

The accuracies achieved are approximately as follows:

| | | |
|-----|---------------|--------------------|
| TOF | $\pm 5\%$ | 10 - 100 keV |
| | $\pm 10\%$ at | 500 eV and 500 keV |
| PRC | $\pm 5\%$ | 50 keV - 1 MeV |
| | $\pm 10\%$ at | 10 keV |

MeV energies (relative to 100 keV) $\pm 10\%$

Reaction rate ratio measurements have also been made and these provide a measure of broad characteristics of spectra.

Spectrum measurements have also been made in other fast reactor critical facilities. The cross-sections in the FGL5 library have been adjusted to fit measurements made in critical facilities, including the broad shapes of the measured spectra and reaction rate ratios.

3. Accuracy of total fluence prediction in core components

A reaction rate which can provide a measure of the total integrated flux is the ^{239}Pu fission rate. This fission cross-section is fairly flat over a wide range of the neutron spectrum. Since ^{239}Pu fission is the predominant source of energy in a fast reactor the average ^{239}Pu fission rate can be related to the total power output. The accuracy with which the ^{239}Pu fission rate in a region of the reactor can be related to the reactor power depends on the accuracy to which the following are known:

- the energy released in fission,
- the energy released in other reactions per fission (in particular ^{238}U capture and other capture reactions),
- fissions in other substances (^{238}U , ^{240}Pu , ^{241}Pu) per fission in ^{239}Pu ,
- the ^{239}Pu fission rate distribution in the reactor (average rates in reactor zones, detailed variation), and
- variation of the ^{239}Pu composition of the core and breeder regions with burn-up.

The accuracy obtained using transport theory methods and detailed geometrical representations is higher than that obtained using the more approximate diffusion theory methods (which use average composition for reactor regions) which are used for standard PFR flux calculations. The more accurate transport theory methods must be used when accurate reaction rates are required.

The ZEBRA facility has been used to investigate relative reaction rates and reaction rate distributions in both core and breeder regions and in both uniform cores and cores with different patterns of control rods inserted. Studies were made in ZEBRA Assembly 13 (a core having the size of PFR) of reaction rates in breeder regions simulating a fresh uranium oxide fuelled radial breeder and a radial breeder in which plutonium has been built up by irradiation. The analysis showed that when accurate calculation methods are used the power in the breeders (relative to the

core) can be estimated to $\pm 3\%$ although when the standard diffusion theory methods are used the discrepancy can be $\sim 10\%$. The power in the outer core relative to the inner core is predicted to within about $\pm 1\%$. In the larger ZEBRA Assembly BZB the ^{239}Pu fission rate distribution in the core was measured for nine different patterns of control rod insertion. Some very large changes in the fission rate distribution resulted ($\sim 30\%$). The standard deviation of the difference between the measured and calculated fission distribution, normalised to total core fission rate, was less than $\pm 1\%$.

Studies of reaction rate distributions close to control rods show that standard diffusion theory underestimates the flux dip into the absorber rods, with the 10% dip in the ^{239}Pu fission rate being underestimated by about 10% of the dip i.e. 1% overall. The underestimate is larger, however, for high energy reactions which are more characteristic of irradiation damage, with the gradient being underestimated by about 20%.

Measurements of the isotopic composition of PFR fuel pins following irradiation provide a test of the accuracy of prediction of fission rates and other reaction rates. These measurements are not as accurate as measurements on isotopically pure samples but the results obtained to date confirm predictions to within about $\pm 3\%$.

We must distinguish between the accuracy which can be obtained using the most sophisticated calculation methods for simple geometries and compositions, and the accuracy which is provided by the standard PFR calculation methods which use the more approximate diffusion theory and average compositions over subassembly regions. The diffusion theory methods are not so accurate for calculations of flux in non-fuelled regions such as the demountable subassembly experiments and control rods. The high energy flux calculated using these methods might be in error by 10% to 20%. The PFR is too complex to represent in detailed neutron flux calculations, so simplifications are made in the geometrical representation, such as homogenising the fuel pin compositions of subassemblies and the experiments loaded into demountable subassemblies. Control rod movement is not treated explicitly in calculations at present, and this could affect the accuracy of both the neutron fluence (or integrated flux) and the flux spectrum prediction for DMSA experiments.

4. Spectrum variation in PFR

The spectrum variation can be characterised by the variation in spectrum averaged cross-sections or cross-section ratios. The calculated values of cross-sections at points in the inner core, outer core, radial breeder, axial breeder and central channel in PFR are given in Table 1, and the values of the ratios to ^{239}Pu fission, normalised to the inner core value are given in Table 2. The ^{239}Pu fission cross-section increases by about a factor of 3 between the core and the edge of the breeder region whereas the ^{238}U fission cross-section, which is a measure of the fraction of the neutron flux above about 1 MeV, decreases by about a factor of 10. The variation in the iron atomic displacement cross-section (denoted by Fe(DPA)) is smaller than the variation in the ^{238}U fission cross-section, decreasing by about a factor of 3. The ^{240}Pu fission cross-section varies less rapidly. The increase in the $^{10}\text{B}(n,\alpha)$ cross-section is about a factor of 5. The variation of the ratios to ^{239}Pu fission are larger for the threshold reactions and for the iron displacement cross-section. The $^{238}\text{U}/^{239}\text{Pu}$ fission ratio varies by about a factor of 100 into the radial reflector, while the Fe(DPA)/ $^{239}\text{Pu}(n,f)$ ratio varies by about a factor of 10. Again we see that the $^{240}\text{Pu}/^{239}\text{Pu}$ fission ratio variation is more similar to the variation of the Fe(DPA)/ $^{239}\text{Pu}(n,f)$ ratio.

Table 1
Spectrum averaged cross-sections in regions of PFR

| | $^{239}\text{Pu}(n,f)$ | $^{238}\text{U}(n,f)$ | $^{240}\text{Pu}(n,f)$ | $^{10}\text{B}(n,\alpha)$ | Fe(DPA)* |
|------------------|------------------------|-----------------------|------------------------|---------------------------|----------|
| Inner core | 1.80 b | 0.052 b | 0.401 b | 2.58 b | 269 b |
| Outer core | 1.80 | 0.057 | 0.418 | 2.56 | 280 |
| Radial breeder | 4.55 | 0.0090 | 0.228 | 9.81 | 127 |
| Axial breeder | 2.90 | 0.0144 | 0.221 | 6.29 | 135 |
| Radial reflector | 6.42 | 0.0028 | 0.205 | 14.55 | 90 |
| Central channel | 1.91 | 0.047 | 0.378 | 3.00 | 252 |

*Fe (DPA) denotes the iron atomic displacement cross-section

Table 2
Variation of spectrum averaged cross-sections across a fast reactor:
ratios to $^{239}\text{Pu}(n,f)$ normalised to unity in the inner core

| | $^{238}\text{U}(n,f)$ | $^{240}\text{Pu}(n,f)$ | $^{10}\text{B}(n,\alpha)$ | Fe(DPA) |
|------------------|-----------------------|------------------------|---------------------------|---------|
| Outer core | 1.08 | 1.04 | 0.99 | 1.04 |
| Radial breeder | 0.07 | 0.23 | 1.50 | 0.19 |
| Axial breeder | 0.17 | 0.34 | 1.51 | 0.31 |
| Radial reflector | 0.01 | 0.14 | 1.58 | 0.09 |
| Central channel | 0.85 | 0.89 | 1.09 | 0.88 |

An indication of the accuracy to which this spectrum variation can be predicted can be obtained by seeing how well the $^{238}\text{U}/^{239}\text{Pu}$ fission ratio variation measured in a ZEBRA assembly is predicted. This is shown in Table 3. The fission ratio decreases by about a factor of 8 in going through the radial breeder in this assembly and this variation is predicted to within about 10%. This agreement is perhaps fortuitous because the adjustments made to the FGL5 library were not chosen to reproduce the flux attenuation through breeder regions. Anisotropic scattering is not treated in these calculations and this effect might be important in this case. The agreement gives some confidence that the variation in the iron damage cross-section can be predicted to within the required accuracy of $\pm 10\%$ in fast reactor core and breeder regions.

The variation in (n,α) reactions, with thresholds above about 3 MeV, might not be so accurately predicted in the breeder regions. However, for regions within the core, including control rods and demountable subassemblies, this accuracy can be achieved if the fine structure of the geometry is modelled in detail and transport theory methods are used. Absolute measurements of the helium production in different materials are required, however, to provide normalisations for the calculations of the relative reaction rates at different positions.

Table 3
Comparison of measured and calculated radial variations of ^{238}U $(n,f)/^{239}\text{Pu}(n,f)$ across a fast reactor assembly (ZEBRA Assembly 13) normalised to the inner core average

| | R (cm) | $\frac{^{238}\text{U}(n,f)}{^{239}\text{Pu}(n,f)}$ | C/E | Uncertainty |
|----------------|--------|--|-------|-------------|
| Outer core | 65.0 | 1.14 | 0.99 | $\pm 1\%$ |
| | 70.6 | 1.10 | 0.989 | $\pm 1\%$ |
| Radial breeder | 81.4 | 0.557 | 1.01 | $\pm 3\%$ |
| | 92.1 | 0.227 | 0.94 | $\pm 5\%$ |
| | 103.1 | 0.162 | 0.90 | $\pm 5\%$ |
| | 108.5 | 0.129 | 0.91 | $\pm 5\%$ |

R denotes the distance from the core centre.

C/E denotes the ratio of calculated to measured value.

5. Dosimetry measurement requirements

Although calculation methods and associated nuclear data libraries have the potential to achieve the required accuracies, the approximations made in the standard methods' implementations for PFR, combined with the

complexity involved in following the power history in detail and modelling the effects of control rod movements, make it desirable to monitor the fluence and characteristics of the spectrum by dosimetry measurements.

The requirements are for reactions appropriate for the following applications:

- a total fluence monitor (e.g. ^{239}Pu fission),
- a reaction with a similar spectral dependence to the iron atomic displacement cross-section, and
- a reaction with a threshold at MeV energies which can be related to the helium producing threshold reactions.

The required characteristics of the dosimetry reaction are:

- an induced activity with a half-life longer than a few years to provide an integration over an irradiation period of about 1 year,
- a readily measurable induced activity (preferably by gamma-ray spectrometry),
- a cross-section shape which is sufficiently accurately known and which is related to the spectral characteristic to be measured,
- absence of conflicting reactions in the dosimetry material (i.e. reactions leading to the same activation product or a similar activity),
- a negligibly small (or accurately known) absorption cross-section for the activation product, and
- a material suitable for irradiation in a fast reactor environment.

The reaction $^{239}\text{Pu}(n,f)$ is proposed as the total fluence monitor (the activity of a suitable long lived fission product such as ^{137}Cs is measured). The plutonium is alloyed with Pd to provide stability. The fractional burn-up of ^{239}Pu is high in a standard subassembly irradiation period and fission in ^{240}Pu (formed by capture in ^{239}Pu) also contributes to the fission product production. Capture reactions do not provide useful additional spectral information because they are more sensitive to lower energies than the $^{239}\text{Pu}(n,f)$ reaction. Threshold fission reactions, such as $^{232}\text{Th}(n,f)$, $^{237}\text{Np}(n,f)$, $^{238}\text{U}(n,f)$ and $^{240}\text{Pu}(n,f)$ are sensitive to the spectrum at MeV and high keV energies but fission in the capture products (^{233}U , ^{239}Pu and ^{241}Pu) complicates the interpretation of these measurements. In a long irradiation most of the fissions occur in these capture products (see Table 4).

Table 4

Fissile material dosimeters - percentage of fissions in different isotopes following a long irradiation*

| ^{235}U (93%) | | ^{237}Np (100%)** | | ^{239}Pu (95%) | |
|------------------------|-------|----------------------------|-------|-------------------------|-------|
| ^{235}U | 97.5% | ^{237}Np | 36.9% | ^{239}Pu | 93.1% |
| ^{234}U | 0.3 | ^{238}Np | 0.7 | ^{240}Pu | 4.0 |
| ^{236}U | 0.7 | ^{238}Pu | 55.8 | ^{241}Pu | 2.7 |
| ^{238}U | 0.3 | ^{239}Pu | 6.3 | | |
| ^{237}Np | 0.2 | | | | |
| ^{238}Pu | 0.2 | | | | |
| ^{239}Pu | 0.6 | | | | |

*Fluence $6.57 \times 10^{23} \text{ n cm}^{-2}$

**Uncertainties in capture reaction rates affect the accuracy of interpretation for ^{237}Np and other threshold fission dosimeters

Reactions having an appropriate threshold energy, and resulting in an activity which has a suitable half-life and is easily detectable, are very few. Threshold reactions which result in an activity with a half-life longer than about 1 year are:

| <u>dosimetry reaction</u> | <u>half-life</u> | <u>threshold energy (MeV)</u> | |
|--|------------------|-------------------------------|------------------|
| | | <u>Q</u> | <u>effective</u> |
| $^{54}\text{Fe}(n,p)^{54}\text{Mn}$ | 312.5 days | -0.09 | ~4.4 |
| $^{60}\text{Ni}(n,p)^{60}\text{Co}$ | 5.271 years | 2.08 | ~6.8 |
| $^{93}\text{Nb}(n,n')^{93\text{m}}\text{Nb}$ | ~15.9 years | 0.03 | ~0.3 |

The $^{93}\text{Nb}(n,n')^{93\text{m}}\text{Nb}$ reaction has a sensitivity more closely related to the iron atomic displacement cross-section but this reaction cross-section is not well known. Measurements are currently in progress using the Birmingham Radiation Centre Dynamitron (see sect. 1.7 below). Integral measurements of the $^{93}\text{Nb}(n,n')^{93\text{m}}\text{Nb}$ reaction relative to $^{239}\text{Pu}(n,f)$ have been made in the AEE Winfrith ZEBRA reactor to an accuracy of $\pm 1\%$ random and $\pm 2\%$ systematic (see sect. 3.2 below). These measurements are consistent to within about 5% with the 1980 evaluation of Strohmaier. Integral measurements in a range of spectra could provide an independent test of this evaluation and could provide data suitable for normalising the cross-section or adjusting its shape.

If it is known that the spectrum in a region remains constant during the irradiation then it is not so essential for the active product to have a long half-life. A short-lived activity, which gives information about the spectrum at the end of the irradiation, is acceptable. This is not

appropriate for the DMSA irradiations in PFR because control rod movement could affect the spectrum.

Table 5 shows the variation with spectrum of the ratio of different reactions to the calculated iron atomic displacement reaction. The spectra are those for different regions of PFR. It will be seen that the $^{240}\text{Pu}(n,f)$ reaction is most closely correlated with the Fe(DPA) reaction. The ratio of the $^{93}\text{Nb}(n,n')^{93m}\text{Nb}$ reaction to the Fe(DPA) reaction varies by about 20% through the core and breeder regions and by up to about a factor of 2 through the inner shielding. However, we also see that the atomic displacement cross-section in nickel, another structural material, has a spectral dependence which is a little different from that of iron, the variation from the core to the radial breeder differing by 10%.

Table 5

Variation with position of possible dosimetry reaction rates relative to Fe(DPA) normalised to unity in the inner core

| | Outer core | Radial breeder | Steel reflector | Diagrid |
|---|------------------------------|------------------------------|------------------------------|------------------------------|
| Thermal fission $^{239}\text{Pu}(n,f)^*$ | 0.92 | 2.11 | 2.29 | 12.51 |
| Threshold fission $^{234}\text{U}(n,f)$ $^{238}\text{U}(n,f)$ $^{237}\text{Np}(n,f)$ $^{240}\text{Pu}(n,f)$ | 1.02 1.07 1.01 1.01 | 0.89 0.64 0.93 1.01 | 0.80 0.37 0.81 0.92 | 0.57 0.47 1.49 1.44 |
| Threshold activation $^{54}\text{Fe}(n,p)^*$ $^{93}\text{Nb}(n,n')^{93m}\text{Nb}^*$ | 1.08 1.02 | 0.58 0.84 | 0.36 0.72 | 0.11 0.51 |
| Other atomic displacement rates Ni(DPA) | 0.98 | 1.10 | 1.12 | 1.31 |

*Proposed PFR dosimetry reactions

6. Dosimetry by measuring the activity of components irradiated in PFR

The activities which have been induced in control rod guide tubes and absorber wrapper tubes have been measured following removal of these components from PFR. The reactions measured are:

| | <u>half-life</u> | <u>effective threshold</u> |
|--|------------------|----------------------------|
| $^{54}\text{Fe}(n,p)^{54}\text{Mn}$ | 312.5 days | 4.4 MeV |
| $^{58}\text{Ni}(n,p)^{58}\text{Co}$ | 70.85 days | 4.3 MeV |
| $^{58}\text{Ni}(n,p)^{57}\text{Co}$ | 21.1 secs | |
| $^{60}\text{Ni}(n,p)^{60}\text{Co}$ | 5.271 years | 6.8 MeV |
| $^{59}\text{Co}(n,\gamma)^{60}\text{Co}$ | 5.271 years | (thermal) |

The random uncertainty on the measurements is $\pm 0.5\%$ and the systematic uncertainty $\pm 2\%$ to 3% . These measurements provide a check of the calculated values of reaction rate gradients across control rods. However, discrepancies in the prediction of ^{58}Co could indicate that burn-up of the ^{58}Co produced is not negligible. Data are required for ^{58}Co absorption reaction cross-sections for the interpretation of these measurements.

7. Dosimetry in zero power critical facilities

A much wider range of reactions can be used in zero power reactors because the dosimetry samples can be removed quickly and the activity measured within a very short time of the completion of the irradiation. Two stage reactions and burn-up of activation products are not significant processes.

In order to provide a measurement of the flux spectrum shape at energies which determine the Doppler effect (below about 10 keV) resonance reactions have been used. For example, relative measurements of the $^{55}\text{Mn}(n,\gamma)^{56}\text{Mn}$ reaction (which has a prominent resonance at 237 eV), when combined with measurements of $^{181}\text{Ta}(n,\gamma)^{182}\text{Ta}$ and $^{197}\text{Au}(n,\gamma)^{198}\text{Au}$ in cores with and without sodium, provides a measurement of the change in spectrum at Doppler energies resulting from removal of sodium. A way of enhancing the resonance contribution is to use sandwich foils of the material and to calculate the differences between the activities induced in foils in different layers.

An indication of the accuracy of calculations of the high energy component of fast reactor spectra can be obtained from the comparison with reaction rate ratio measurements made in ZEBRA and in standard spectra (Table 6).

Table 6

Ratio of calculated to measured values of dosimetry reactions

| | ZEBRA 14 core | ZEBRA BZD/3 core | Fission spectra | |
|--|------------------|---------------------|------------------|-------------------|
| | | | ^{235}U | ^{252}Cf |
| $^{54}\text{Fe}(n,p)^{54}\text{Mn}$ | 0.90 | 0.95 | 1.02 | 1.03 |
| $^{58}\text{Fe}(n,\gamma)^{59}\text{Fe}$ | 0.99 | 1.01 | - | - |
| $^{58}\text{Ni}(n,p)^{58}\text{Co}$ | 0.88 | 0.92 | 0.97 | 0.99 |
| $^{60}\text{Ni}(n,p)^{60}\text{Co}$ | 0.96 | 0.90 | - | - |

Calculated using ENDF/B-V dosimetry cross-sections. Reactor spectra calculated using FGL5. Fission spectra from ENDF/B-V. Typical accuracy of ZEBRA measurements $\pm 5\%$. Typical accuracy of fission spectrum averages: ^{235}U $\pm 5\%$ to 7% , ^{252}Cf $\pm 2\%$ to 3% .

8. Conclusions

(a) Fast reactor core dosimetry requirements

The objective is to achieve longer irradiations by improving knowledge of the relationship between irradiation damage and irradiation conditions and by improving the accuracy of prediction of the irradiation conditions in a fast reactor core. This requires a more accurate correlation of irradiation damage effects with neutron fluence and selected spectral parameters. Use is made of data from both UK and abroad. Hence standard parameters are used for characterising the irradiation conditions (e.g. the NRT damage cross-sections and the International Dosimetry File). This should result in a more accurate definition of irradiation limits for materials.

A more accurate knowledge of irradiation conditions during reactor operation would enable operation to be planned to achieve the highest possible irradiations. This requires a correlation of dosimetry measurements with reactor instrumentation and the development of calculation methods so that these, when combined with the reactor instrumentation measurements, enable the irradiation conditions to be predicted accurately.

(b) Dosimetry measurement requirements

The present uncertainty in relating total neutron fluence to the PFR reactor monitoring system is about $\pm 5\%$ for core fuel and it is more uncertain in experimental channels, breeder regions and shields. Dosimetry reaction monitors are required when there are higher accuracy targets, and the reaction $^{239}\text{Pu}(n,f)$ has been chosen to monitor total fluence in these situations. Spectrum dependent parameters can be predicted for simple geometry fast reactor compositions to a relative accuracy which is typically about $\pm 3\%$ for threshold reactions in core regions and about $\pm 10\%$ in outer regions of breeders. (This is relative to a reference threshold reaction.) An absolute normalisation is required for some reactions (e.g. (n,α) helium formation).

The complexity of the geometry of PFR (particularly the experimental channels such as the demountable subassemblies) leads to the requirement for spectral monitors. The $^{93}\text{Nb}(n,n')^{93\text{m}}\text{Nb}$ reaction appears to be the most suitable for monitoring the spectral characteristic most closely related to the atomic displacement cross-section. However there is a need for more differential measurements for this cross-section. The development of an atomic displacement monitor is a desirable aim. Measurements or calculations of the absorption cross-sections of some activation products are also needed for the interpretation of material activation measurements.

CINDA-TYPE LISTING

| Element S A | Quantity | Type | Energy (eV) | | UKNDC (83)P109 (Apr.83) page no. | Lab | Comments |
|----------------|----------------|-----------|-------------|-------|---|--------------|--|
| | | | min | max | | | |
| Al 27 | (n,p) | expt,prog | 2.0+6 | 4.5+6 | 94 | BIR Hussain+ | absol xsec |
| Al 27 | (n, α) | " " | 1.4+7 | | 48 | HAR Cookson+ | α ang dist |
| Si 28 | (n,p) | " " | 1.3+7 | 1.5+7 | 98 | BIR Jarjis | figs |
| Ti 47 | (n,p) | " " | 2.0+6 | 4.5+6 | 94 | BIR Hussain+ | absol xsec |
| V nat | (n, α) | " " | 1.4+7 | | 48 | HAR Cookson+ | α ang dist |
| Cr nat | (n, α) | " " | 1.4+7 | | 48 | HAR Cookson+ | α ang dist |
| Fe nat | γ spec | " " | 1.4+7 | | 94 | BIR Cox+ | from n interaction |
| Fe nat | (n, α) | " " | 1.4+7 | | 48 | HAR Cookson+ | α ang dist |
| Fe 56 | res param | " " | 1.1+3 | | 37 | HAR Syme+ | reanalysed trans data |
| Fe 56 | (n,p) | " " | 1.3+7 | 1.5+7 | 100 | BIR Jarjis | figs |
| Co 59 | (n, α) | " " | 1.3+7 | 1.5+7 | 100 | BIR Jarjis | figs |
| Ni nat | (n, α) | " " | 1.4+7 | | 48 | HAR Cookson+ | α ang dist |
| Ni 58 | (n,p) | " " | 2.0+6 | 4.5+6 | 94 | BIR Hussain+ | absol xsec |
| Zn 64 | (n,p) | " " | 2.0+6 | 4.5+6 | 94 | BIR Hussain+ | absol xsec |
| Zn 64 | (n,2n) | " " | 1.3+7 | 1.5+7 | 98 | BIR Jarjis | figs |
| Cu 65 | (n,2n) | eval,prog | 1.4+7 | | 85 | NPL Winkler+ | includes latest data |
| Nb 93 | inelastic | expt,prog | 3.0+6 | 6.0+6 | 48 | HAR Gayther+ | ^{93m} Nb activ at BIR |
| Nb 93 | inelastic | " " | fast | | 83 | WIN Taylor+ | |
| In nat | abs | " " | 1.4+7 | | 86 | NPL Ryves+ | all activ prods measd |
| In 115 | (n, γ) | " " | 1.4+5 | 5.7+5 | 84 | NPL Hunt+ | internat intercomp, meas in prog |
| In 115 | (n, γ) | " " | 2.0+6 | 4.5+6 | 94 | BIR Hussain+ | absol xsec |
| In 115 | inelastic | " " | 2.5+6 | 1.4+7 | 84 | NPL Hunt+ | internat intercomp, meas complete, anal in prog |
| W nat | elastic | " " | 3.0+6 | | 102 | EDG Annand+ | polar + diff elas scatt |
| Au 197 | (n, γ) | " " | 2.0+6 | 4.5+6 | 94 | BIR Hussain+ | absol xsec |
| Hg nat | elastic | " " | 3.0+6 | | 102 | EDG Annand+ | polar + diff elas scatt |
| Tl nat | elastic | " " | 3.0+6 | | 102 | EDG Annand+ | polar + diff elas scatt |
| Pb nat | elastic | " " | 3.0+6 | | 102 | EDG Annand+ | polar + diff elas scatt |
| Bi nat | elastic | " " | 3.0+6 | | 102 | EDG Annand+ | polar + diff elas scatt |

| Element S A | Quantity | Type | Energy (eV) | | UKNDC (83)P109 (Apr.83) page no. | Lab | Comments |
|----------------|----------------|-----------|-------------|-------|---|-----------------|---|
| | | | min | max | | | |
| U nat | elastic | expt,prog | 3.0+6 | | 102 | EDG Ammand+ | polar + diff elas scatt |
| U 233 | abs | eval,prog | 2.5-2 | | 8 | NPL Axton | simul eval therm consts ²³³ U, ²³⁵ U, ²³⁹ Pu, ²⁴¹ Pu and $\bar{\nu}$ (²⁵² Cf) |
| U 233 | fission | " " | 2.5-2 | | 8 | NPL Axton | " " " |
| U 233 | eta | " " | 2.5-2 | | 8 | NPL Axton | " " " |
| U 233 | nu | " " | 2.5-2 | | 8 | NPL Axton | " " " |
| U 235 | abs | " " | 2.5-2 | | 8 | NPL Axton | " " " |
| U 235 | fission | " " | 2.5-2 | | 8 | NPL Axton | " " " |
| U 235 | fission | expt,prog | 2.5+6 | 1.4+7 | 84 | NPL Hunt+ | internat intercomp, meas complete, anal in prog |
| U 235 | eta | eval,prog | 2.5-2 | | 8 | NPL Axton | simul eval therm consts ²³³ U, ²³⁵ U, ²³⁹ Pu, ²⁴¹ Pu and $\bar{\nu}$ (²⁵² Cf) |
| U 235 | nu | " " | 2.5-2 | | 8 | NPL Axton | " " " |
| U 235 | delayed n | expt,prog | fast | | 88 | BIR Owen+ | delayed n spec |
| U 238 | (n, γ) | " " | 1.0+3 | 4.0+4 | 38 | HAR Bee | simul anal av trans and capt |
| U 238 | total | " " | 1.0+3 | 4.0+4 | 38 | HAR Bee | simul anal av trans and capt |
| Np 235 | half life | " " | | | 79 | HAR Whittaker+ | prelim val 385 \pm 4 d |
| Pu 239 | abs | eval,prog | 2.5-2 | | 8 | NPL Axton | simul eval therm consts ²³³ U, ²³⁵ U, ²³⁹ Pu, ²⁴¹ Pu, and $\bar{\nu}$ (²⁵² Cf) |
| Pu 239 | fission | " " | 2.5-2 | | 8 | NPL Axton | " " " |
| Pu 239 | eta | " " | 2.5-2 | | 8 | NPL Axton | " " " |
| Pu 239 | nu | " " | 2.5-2 | | 8 | NPL Axton | " " " |
| Pu 241 | abs | " " | 2.5-2 | | 8 | NPL Axton | " " " |
| Pu 241 | fission | " " | 2.5-2 | | 8 | NPL Axton | " " " |
| Pu 241 | eta | " " | 2.5-2 | | 8 | NPL Axton | " " " |
| Pu 241 | nu | " " | 2.5-2 | | 8 | NPL Axton | " " " |
| Am 241 | (n, γ) | expt,prog | fast | | 77 | HAR Glover+ | sig to ^{242m} Am, ²⁴² Cm |
| Am 243 | (n, γ) | " " | fast | | 77 | HAR Glover+ | sig to ²⁴⁴ Cm |
| Am 243 | eval | eval,prog | | | 49 | HAR Patrick+ | eval and prod of data files |
| Cf 252 | ni | " " | spont | | 8 | NPL Axton | simul eval therm consts ²³³ U, ²³⁵ U, ²³⁹ Pu, ²⁴¹ Pu and $\bar{\nu}$ (²⁵² Cf) |
| Cf 252 | fiss prod | expt,prog | | | 73 | HAR Cuninghame+ | meas decay sch short lived fiss prods |

1. NUCLEAR PHYSICS DIVISION, AERE, HARWELL

(Division head: Dr. J.E. Lynn)

Introduction

Nuclear data measurements in Nuclear Physics Division are diverse and are performed on a variety of sources. Individual research items are labelled with a single letter indicating on which accelerator the experiments were performed. These labels are as follows:

| | |
|--|---|
| Cockcroft-Walton Generator | A |
| 3 MV pulsed Van de Graaff Generator IBIS | B |
| 6 MV Van de Graaff Generator | C |
| 14 MeV Tandem Generator | D |
| Electron Linac | E |
| Variable Energy Cyclotron | G |
| Synchrocyclotron (now defunct) | H |
| 500 kV Van de Graaff | I |

In the contents pages there is a reference to the accelerator on which a measurement was made.

The material for this contribution is taken from the chapter on Nuclear Data and Technology for Nuclear Power in the 1982 Nuclear Physics Division Progress Report AERE PR/NP 30.

1.1E The new machine for the electron linac laboratory (J.E. Lynn, M.S. Coates, B.P. Clear, J. Down, R.A.J. Riddle and P.W. Swinden)

Commissioning work on both the Fast Neutron and Low Energy electron beam lines was completed as expected and experimental operation has started (see sect. 1.4 below). The contracted beam time for the joint Harwell/SERC Neutron Beams Project has been provided in the Condensed Matter Cell at powers up to 45 kW, although the modifications to the existing beam scraper system which are needed before this power level is used routinely (see UKNDC(82)P105, p.24) will not be installed for several months. A serious fault on the first accelerator section interrupted machine operation for several weeks during the middle part of 1982 and resulted in delays to the remainder of the commissioning programme. In particular the Neutron Booster target is not now expected to be operational before the middle of 1983 and the Litton klystron, which has been delivered, will not be installed and tested until about the same time.

The accelerator fault referred to above showed up as a failure of the first section to transmit RF pulse power properly with the result that electrons could not be accelerated for injection into the other linac sections. Detailed examination and testing of the section failed to reveal conclusively the basic nature of the problem. The investigation was complicated by the fact that the fault disappeared at low RF power levels, which thus limited the usefulness of the RF bench tests which could be carried out with the section removed from the machine. Eventually the section was returned to the manufacturer who as a last resort recommended careful chemical cleaning of the section which was recognised to be unusually dirty. This process was carried out and the section reassembled into the linac. In the event full performance has been regained although there are still incipient signs that the problem has not completely disappeared. A design study for another accelerator section is at present underway.

1.2H Resonance analysis of transmission data for the 1.15 keV ^{56}Fe resonance (D.B. Syme and A.D. Gadd)
(WRENDA 513)

Two recent measurements of the neutron width of the important resonance at 1.15 keV in ^{56}Fe ^(1,2) have found values near 80 meV, in strong disagreement with the value of 50 meV agreed by several earlier measurements⁽³⁾. The discrepancy is many times the quoted errors. To help

resolve this discrepancy, we have begun an analysis of five sets of high resolution transmission data taken on the Harwell synchrocyclotron (UKNDC(79)P94, p.43). These include runs with separated $^{56}\text{Fe}_2\text{O}_3$ and natural iron and all except one have permanent filters to indicate the background.

Simultaneous fits to these 5 data sets using the R-matrix shape analysis code REFIT have given Γ_n values between 41 and 47 meV. Before a final value and error can be given it is necessary to establish the sensitivity to the line shape assumed for the detector resolution function. This line shape is being calculated in detail but these calculations are not yet complete (see sect. 1.5 below). However the present preliminary values clearly support the lower value of Γ_n .

-
- (1) G. Rohr, NEANDC/NEACRP Specialists' Meeting on Fast Neutron Capture Cross Sections, Argonne, April 1982.
 - (2) R.L. Macklin, private communication (1982), paper accepted for publication in Nucl. Sci. Engng.
 - (3) For references, see M.S. Coates et al., 'Can we do more to achieve accurate nuclear data?', Proc. Int. Conf. Nucl. Data Sci. Technol. Antwerp, September 1982, in publication

1.3 Average neutron transmission and thin sample capture of ^{238}U in the 1 to 40 keV energy range (N.J. Bee (Imperial College))

The analysis of ^{238}U transmission measurements in the unresolved energy range described previously (UKNDC(82)P105, p.26) has been extended to include capture cross-section data. Reasonable fits to the data can be obtained with a constant p-wave strength function of 1.6×10^{-4} and values of the s-wave strength function of between 0.4 and 1×10^{-4} on the assumptions that the $J = 1/2$ and $3/2$ level spacings are 20 and 10 eV respectively and that Γ_γ is 23.5 meV for all resonances. The effective s-wave scattering radius is found to be 9.8 ± 0.1 fm which is higher than the value of 9.44 ± 0.25 fm found in the resolved region⁽¹⁾. The value of the s-wave strength function is found to be below 0.7×10^{-4} above 10 keV which is lower than the values normally assumed⁽²⁾. However, above 10 keV there are systematic errors in the transmission measurements, attributed to background effects, which make accurate analyses impossible. It is concluded that more accurate thin sample transmission and capture data are required particularly above 10 keV.

- (1) D.K. Olsen, G. de Saussure, R.B. Perez, E.G. Silver, F.C. Difilippo, R.W. Ingle and H. Weaver. Nucl. Sci. Engng. 62 (1977) 479.
- (2) M.G. Sowerby and N.J. Bee. Proc. IAEA Consultants Meeting on U and Pu Resonance Parameters, INDC(NDS)-129/GJ (1981) p.136.

1.4E Measurements of the performance of the Fast Neutron target of HELIOS
(D.B. Syme, G.D. James and A.D. Gadd)

The main characteristics of the pulsed neutron beam from the Fast Neutron target of the electron linear accelerator HELIOS have been measured by a set of neutron time-of-flight experiments sharing the 150 m neutron beam line. Information was obtained simultaneously on the flux shape and intensity, the background levels and the resolution function. Measurements were made with and without a 25 mm thick polythene moderator adjacent to the neutron source. The experiments and their results are given below.

The main finding is that the target characteristics have been confirmed to be within design specifications and satisfactory for provision of the intense pulsed neutron beams required for high resolution neutron time-of-flight measurements over the energy ranges relevant to fast reactors and fusion reactors.

Experiments

- (1) Flux shape and intensity above 1 keV.

These were measured by a $^{235}\text{U}_3\text{O}_8$ -loaded parallel-plate ionisation chamber*, 50 m from the source, using time-of-flight techniques.

- (2) Fast neutron flux shape and intensity and gamma-ray flux and intensity.

These were measured using time-of-flight methods on a 150 m path with a NE213 liquid scintillator detector providing pulse shape discrimination of neutrons and gamma-rays.

- (3) Backgrounds in the fast neutron spectrum.

"Notch" filters were used to indicate background events at specific neutron energies in spectra observed as in (2) above.

- (4) Contribution of the electron pulse to the resolution function.

The time distribution of the prompt gamma-ray pulse from the target was sampled by a 1 cm^3 plastic scintillator at 56 m.

*Constructed by the Radiation Protection Group of I. & A.P. Division (Dr. J. Leake), using foils supplied by the Stable Isotope Unit of Chemistry Division (Mrs. K.M. Glover).

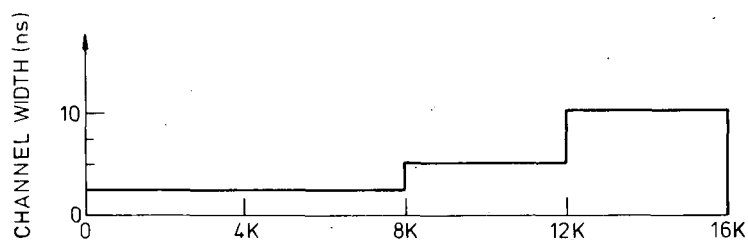
- (5) Resolution function for neutrons of a given energy.

This was measured through observation of the time distribution of neutron capture events in a narrow resonance in (e.g.) an iron sample 8 m from the source. A Moxon-Rae detector was used to register the capture gamma-rays.

Results

- (1) The intensity of the fast neutron flux (per incident electron) was confirmed to be as expected from both experiments (1) and (2).
- (2) The shape of the fast neutron flux was also confirmed. This is shown schematically in Fig. 1.1 in the form of a typical raw time-of-flight spectrum as observed with, e.g. the $^{235}\text{U}_3\text{O}_8$ ionisation chamber. The fast flux extends from energies above 20 MeV down to about 10 keV with a peak at ~ 1 MeV. The spectrum below 100 keV arises from fast neutron moderation in the water cooling between the target plates and is nearly constant as expected for a slowing down spectrum and a detector with a $1/v$ response. This part of the flux usefully covers the fast reactor resonance region (down to 100 eV).
- (3) The insertion of the 25 mm polythene moderator lowers the fast flux and does not enhance the moderated component until below 300 eV (not shown). The Neutron Booster target is already optimised for such low energy work and the Fast Neutron target is designed to cover the higher energies without a separate moderator.
- (4) The insertion of the moderator shifts and narrows the resolution function observed for neutrons but the improved resolution does not maintain the conventional figure of merit, $F = \text{Flux}/(\text{resolution width})^2$, above 0.3 keV. At 1.15 keV F falls by a factor 1.5 when a moderator is inserted. This confirms that the Fast Neutron target is best used without additional moderation. The resolution functions measured using the well known resonance at 1.15 keV in ^{56}Fe are shown in Fig. 1.2. The calculated Doppler-broadened lineshape for the resonance is also shown. The electron pulse width is narrow by comparison. The observed lineshape is clearly dominated by the asymmetric component due to neutron scattering (moderation) in the target itself. A good knowledge of the lineshape is required for proper resonance shape analysis of neutron reaction data. The FWHM of the resolution

(1) CHANNEL STRUCTURE



(2) PRACTICAL SPECTRA

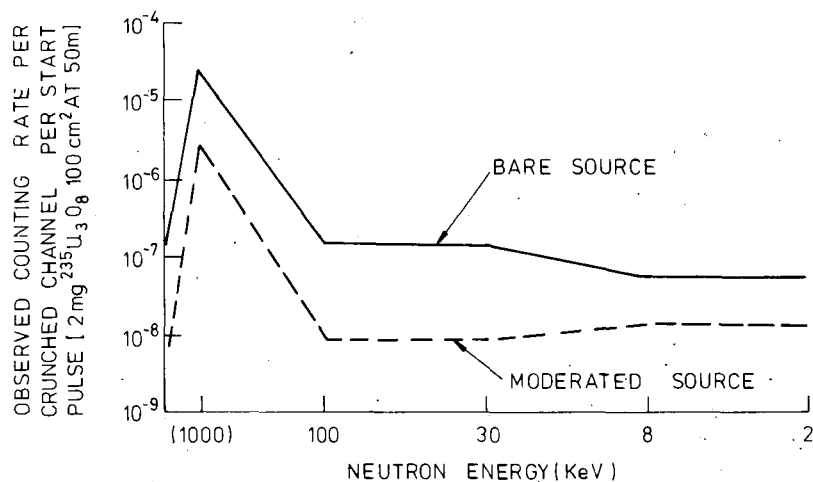


Fig. 1.1 Neutron time-of flight spectra from the Fast Neutron target of HELIOS, with and without adjacent moderator. Spectra taken on a 50 m path with the channel structure of (1) are shown schematically in (2). The detector was a double-sided parallel-plate ionisation chamber with a $^{235}\text{U}_3\text{O}_8$ deposit of total thickness 2 mg cm^{-2} and 12.5 cm diameter. The main features of the spectra are the intense fast neutron burst above 100 keV and the semi-moderated tail to lower energies.

function of the bare target has been predicted to be $\sim 70 \text{ ns}^{(1)}$ and measured here as $77 \pm 5 \text{ ns}$ at 1.15 keV. It is intended to extend the energy range of these measurements and repeat the calculations in more detail.

- (5) The shape of the narrow electron pulse is satisfactory, with no appreciable long tail. An example is given in Fig. 1.3.

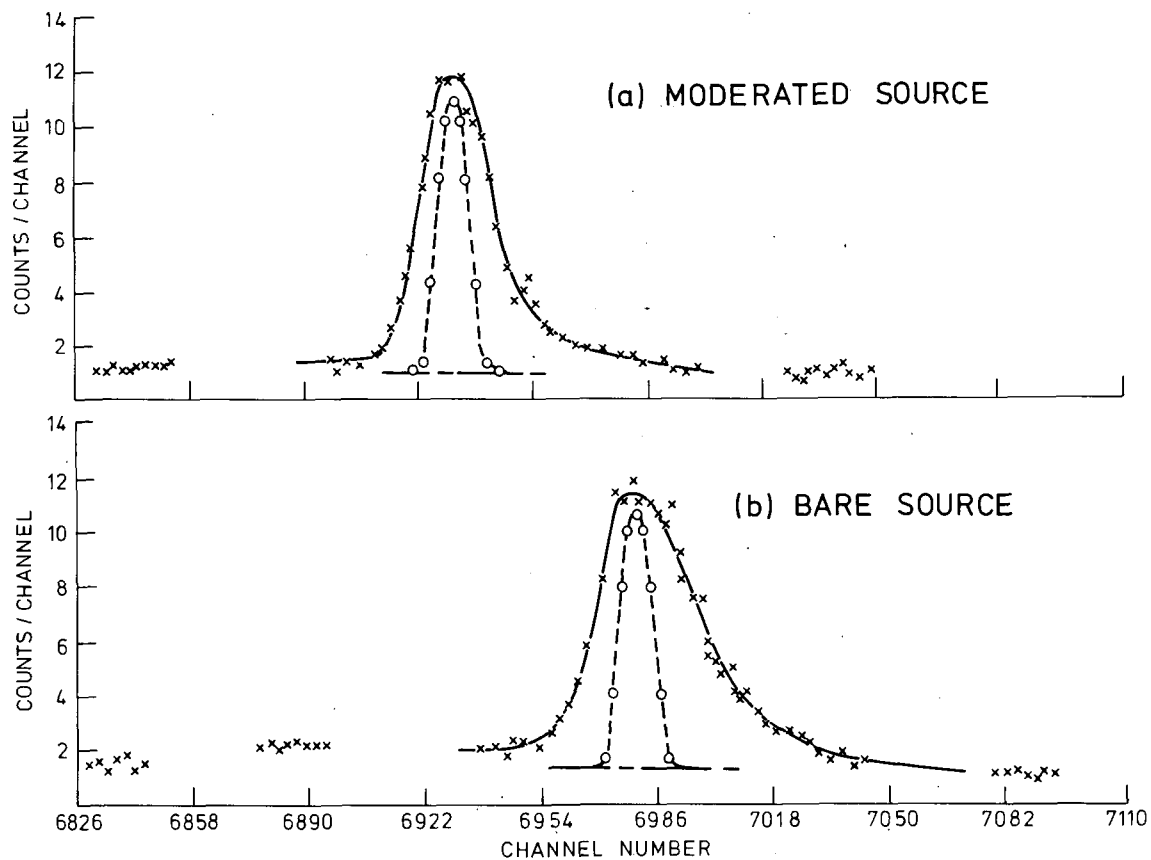


Fig. 1.2 Time distribution of neutron capture gamma-rays observed from the 1.15 keV resonance in ^{56}Fe : (a) from the target with adjacent moderator of 25 mm polythene viewed in transmission; (b) from the target alone. The conditions were chosen to make the asymmetric contribution from the target (and moderator) dominate over the Doppler-broadened lineshape for the resonance (dotted line).

- (6) Backgrounds are low in the fast neutron flux above 100 keV. A notch filter of SiO_2 was used to indicate neutronic signal to backgrounds and gave values of 1%, 2% and $1\frac{1}{2}\%$ respectively at 1 MeV, 0.44 MeV and 0.2 MeV. Gamma-ray backgrounds in the NE213 detector were separately but simultaneously observed to be less than 2% of the neutron counting rate for energies well above the detector bias (100 keV).

(1) G. Constantine, private communication to M.S. Coates

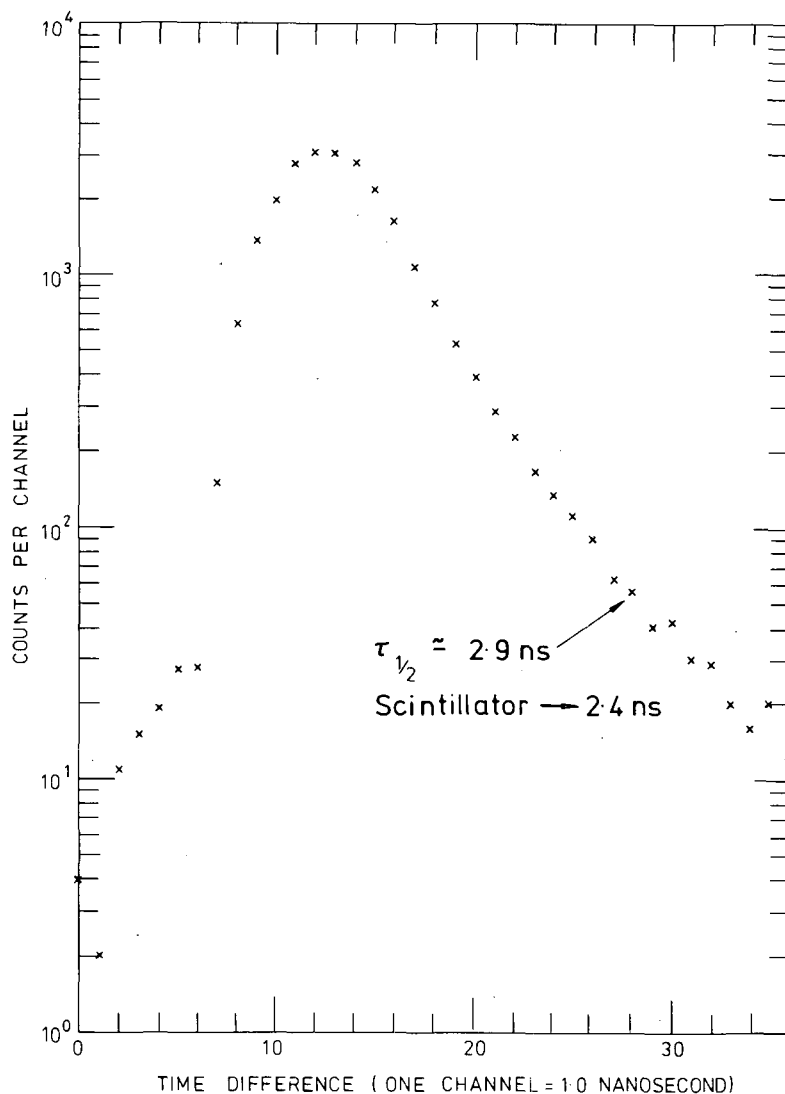


Fig. 1.3 Time distribution of the prompt gamma-ray burst from the Fast Neutron target of HELIOS. Not corrected for the decay time of the plastic scintillator used. In this case the electron pulse was set to be 7 ns FWHM.

1.5 Background and resolution functions in neutron time-of-flight spectrometers (D.B. Syme and A.D. Gadd)

Systematic discrepancies between different measurements of neutron resonance parameters arise largely because of inadequate knowledge of the background and resolution functions for neutron time-of-flight spectrometers. Several bodies of work designed to better characterise these functions were described in UKNDC(82)P105, p.28. A paper on the contribution to these functions of neutron scattering in the source room was presented at the September Antwerp Conference⁽¹⁾. Work has begun on Monte Carlo calculations of the contribution of detector room scattering to the background and resolution functions. This is described in the next two

sections. The first measurements have been made of the resolution function of the neutron time-of-flight spectrometer based on the Fast Neutron target of the electron linear accelerator HELIOS. These are reported in sect.

1.4.

1.5.1 Response functions of detectors in shields to pulsed neutron beams
(D.B. Syme)

In a search for significant sources of background it is interesting to calculate the return to the detector from surrounding shielding, etc. of neutrons originally scattered out of the incident beam by the detector itself. The range of sizes of detector shields makes it likely that backgrounds observable by notch filters can be generated in this way. Most pulsed white sources have an energy spectrum composed of an intense high energy evaporation component centred around 1 MeV and a moderated ($1/E$) tail of considerably lower intensity extending to lower energies. The high energy component will preferentially scatter out of the detector and may be returned from the shield, delayed and at lower energy. Returned neutrons are likely to be captured with increased efficiency in a detector with a $1/v$ response and may constitute a significant background effect. This has been confirmed, e.g. by Gayther, who improved the signal-to-background of low energy capture measurements by insertion of a helium filter which preferentially removed high energy neutrons near the 1.15 MeV resonance⁽²⁾.

We have made some preliminary Monte Carlo simulations using the code MORSE⁽³⁾. Part of the neutron flux scattered out from a parallel beam by a detector is reflected by surrounding shielding towards the detector. The returning flux was examined with the detector at the centre of cubical shields of lead and borated resin. Examples with a 10 cm diameter and 1.27 cm thick ^6Li glass detector are given in Fig. 1.4. The early peak is the outgoing flux and is the same for all the enclosure sizes shown. The returned flux is the remainder and is separated from the outgoing flux by the expected times for cubical shields of 1 and 2 m inside dimensions. The outgoing and incoming fluxes overlap for the small shield (20 cm inside cube) partially because of the position of the notional point detector for flux estimation. The integrated returned flux has the expected inverse square variation with enclosure size. This has been confirmed experimentally with capture detectors by Moxon⁽⁴⁾. The time delays of the returned flux will make at least some of it observable with notch filters, depending also on the flight path length.

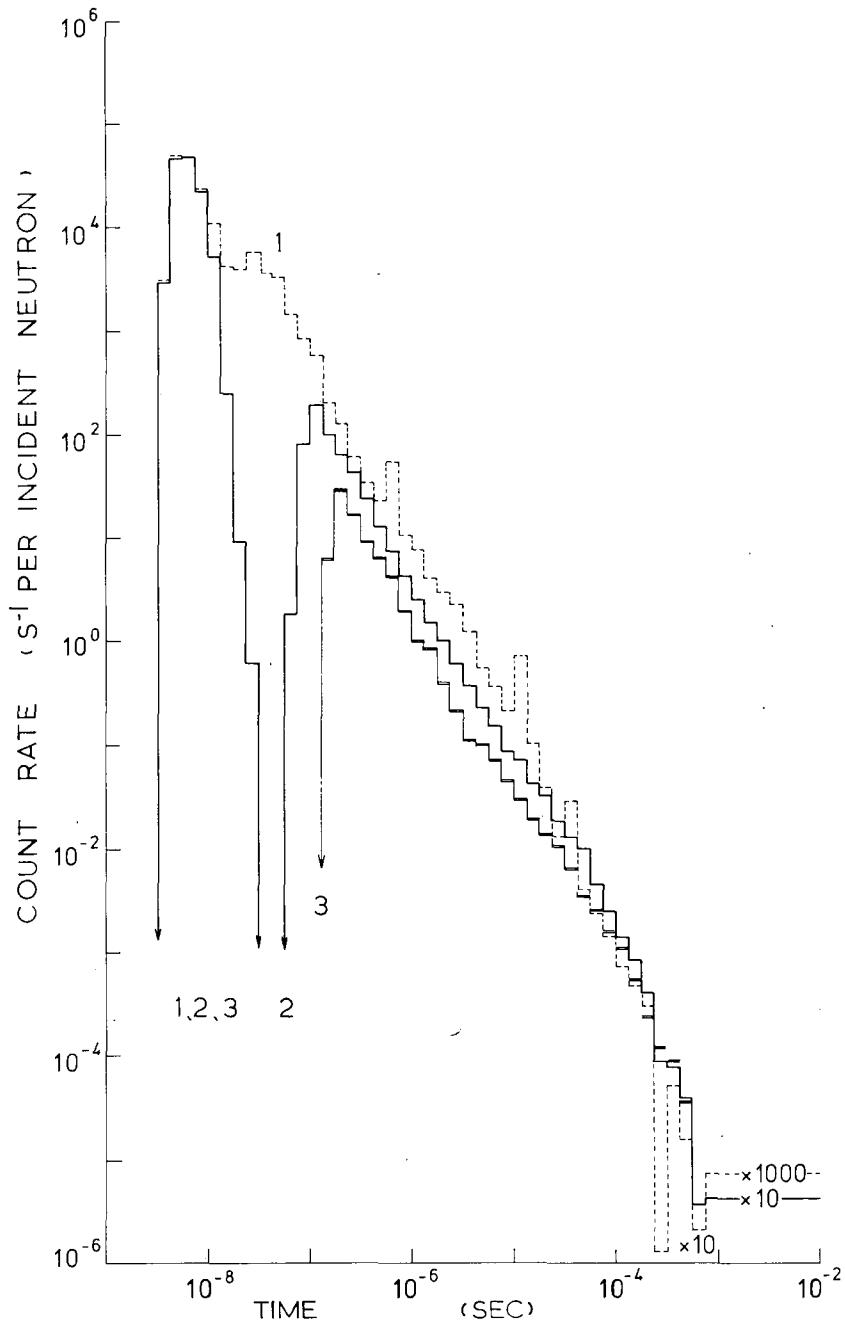


Fig. 1.4 Calculated neutron fluxes caused by scattering of a 1 MeV parallel beam by a 10 cm diameter, 1.27 cm thick ^6Li glass detector at the centre of shields of various sizes. The shields 1, 2, 3 are of 10 cm lead followed by 30 cm of borated resin in the form of cubes of inner dimensions of 0.2, 1.0 and 2.0 metres respectively. The neutron fluxes are those passing through a notional point detector 5 cm outside the edge of the ^6Li glass detector.

A more complete calculation requires proper account to be taken of the probability of interaction in the detector for each returned neutron. It is difficult to register a significant number of returned neutron events in a straightforward Monte Carlo simulation because of the combination of low probability scatters involved and it has been necessary to develop an estimator technique (like the point estimator one used for flux estimation) which overcomes these difficulties. This is described in sect. 1.5.2 below. The results in fact look very similar to those of Fig. 1.4 and so are not reproduced here.

Spectra of the kind shown are being accumulated for a range of incident neutron energies. The total returned flux detected at a given time depends on the incident flux shape and intensity at all earlier times. For a given detector and shielding arrangement the intensity and time dependence of the total returned flux will be compared with the incident flux to determine resolution and background parameters. This work is continuing.

1.5.2 Region of interest estimator (R.B. Thom and D.B. Syme)

It is commonly required in the Monte Carlo treatment of a problem to calculate a particle reaction rate in a small detector volume. In a straightforward crude simulation few particles will actually enter the scoring volume, giving rise to a poorly determined reaction rate. For this reason standard "variance reduction" techniques are available to ensure that as many particles as possible contribute to the final result.

Two of the most commonly used techniques are, firstly, the splitting and rouletting (SR) of particles to improve the flow of particles to the volume of interest and secondly the point flux estimator (PE) where at each collision one computes the component of the particle's weight which is scattered in the direction of a point (the "point detector") defined in the volume of interest. Allowance is made for weight attenuation between the scattering position and the point detector. Under favourable conditions both of these techniques can give satisfactory results. In the case where the average reaction rate for more than one small volume is required an alternative method, called here the region of interest estimator (ROI), has been investigated.

In this approach the detector volume (or volumes) is considered to be enclosed in a spherical surface, the "region of interest". At each collision during a particle history, one calculates that component of

particle weight scattered into the solid angle subtended by the sphere at the collision point. This weight is treated as a pseudo-particle, and is transferred without further interaction but with the necessary attenuation to a point on the surface of the sphere. Upon completion of the current (real) particle history, the pseudo-particles residing on the surface of the sphere are treated as normal particles and continue their individual histories into the region of interest. A normal particle is allowed to enter the region of interest but does not score in the detector volume.

A subroutine ROIEST has been written based on the above approach and used in the Monte Carlo code MORSE⁽³⁾. A test case has been run where the particle flux scattered into a small volume was measured simultaneously with the PE and ROI estimators. The results are very encouraging with both sets of data agreeing within statistical error. Under these conditions, which favoured the point estimator, the variances of the ROI were only slightly inferior. The advantage of the ROI estimator is that it properly treats interactions over a finite detector volume, without demanding an impractically large number of real scatters into that volume. It therefore makes possible the solution of problems like those of sect. 1.5.1 above.

-
- (1) D.B. Syme, B. Thom and A.D. Gadd, 'Background and resolution functions in neutron time-of-flight spectrometers', Proc. Int. Conf. Nucl. Data Sci. Technol. Antwerp, September 1982, to be published.
 - (2) D.B. Gayther, NEANDC Topical Conf. Neutron Capture Cross-section Measurements, Harwell, 1975, ed. G.D. James, report AERE-R 8082, 4 (1975).
 - (3) M.B. Emmett, the MORSE Monte Carlo Radiation Transport Code System, ORNL-4972 (1975), also RSIC CCC-203 (1978).
 - (4) M.C. Moxon, private communication.

1.6 Fission chambers for the intercomparison of fast neutron flux density measurements (D.B. Gayther)

Various difficulties have caused the schedule for the intercomparison described in the previous progress report (UKNDC(82)P105, p.36) to be revised. At this stage nine laboratories are expected to participate with the first measurement starting in February 1983 and the remainder taking place throughout 1983 and the early part of 1984.

1.7 The $^{93}\text{Nb}(n,n')^{93\text{m}}\text{Nb}$ reaction (D.B. Gayther and C.A. Uttley, K. Randle (University of Birmingham), W.H. Taylor and M.F. Murphy (A.E.E. Winfrith))
(WRENDA 718)

The measurement at a mean neutron energy of 3.15 MeV outlined in UKNDC(82)P105, p.35 has been repeated with a neutron output from the titanium deuteride target a factor of three higher than that obtained previously. Values of the average neutron flux through the niobium foil determined from the counts in the ^{238}U fission chamber, the ^{140}La activity in a ^{235}U foil and the ^{58}Co activity in a nickel foil were in good agreement at about $6 \times 10^7 \text{ n cm}^{-2} \text{ s}^{-1}$.

Additional measurements have also been carried out at neutron energies near 4, 5 and 6 MeV using atomic deuteron beams of 1, 2 and 2.65 MeV on titanium deuteride targets and limiting the beam power dissipated over a target area of about 0.8 cm^2 to about 600 watts. The mean neutron fluxes at the niobium foil obtained in these runs were 7.6×10^7 , 4.8×10^8 and $3.8 \times 10^8 \text{ n cm}^{-2} \text{ s}^{-1}$ respectively. These give adequate niobium K X-ray counting rates for irradiations of ~10 hrs duration to achieve the target accuracy ($\pm 5\%$) in the $^{93}\text{Nb}(n,n')^{93\text{m}}\text{Nb}$ cross-section determination.

Further measurements on the Birmingham Dynamitron are planned in the important neutron energy region below 2 MeV.

1.8A (n, α) cross-sections (J.A. Cookson and M.A. Langton*)
(WRENDA 367-8, 493-8, 569-75)

This programme of measurements of alpha particle angular distributions from (n, α) reactions at a neutron energy of about 14.5 MeV on natural targets of Al, V, Cr, Fe and Ni is almost complete. Only Cr measurements have yet to be made and the processing of the other data is well advanced.

1.9 Suggested improvements to the procedures used in making accurate nuclear data measurements (M.S. Coates, D.B. Gayther, G.D. James, M.C. Moxon, B.H. Patrick, M.G. Sowerby and D.B. Syme)

Despite many years of effort it is rare to find a set of different neutron measurements on a given parameter which are consistent within the errors assigned to the individual determinations. These discrepancies are of course signals of the presence of systematic errors and as such show that major obstacles must be overcome before the accuracy goals asked for in request lists can be met. We have given our views on this situation in an invited paper entitled "Can we do more to achieve accurate nuclear

* Physics Department, University of Birmingham

data?" which was presented to the International Conference on Nuclear Data for Science and Technology, Antwerp, 6-10 September 1982. The abstract of the paper is as follows:

We ask whether more effective methods can be used to reduce the discrepancies which often persist between individual measurements of neutron nuclear data. With this in mind we trace the historical development of a few selected measurements to see what lessons can be learned from the past. Several common sources of systematic error are noted. These have been qualitatively recognised for many years but have nevertheless continued to be the most likely causes of discrepancies. Experimenters have just not been sufficiently thorough in demonstrating an adequate treatment of these systematic effects. We suggest several improved procedures for future measurements.

1.10 Evaluation of neutron nuclear data

1.10.1 Nuclear data files (B.H. Patrick and E.M. Bowey)

To gain experience in the production of ENDF/B format files and to enable UKNDL and ENDF/B processing codes to be compared, it was decided to construct an ENDF/B version of our recent ^{243}Am evaluation which is contained in the U.K. Nuclear Data Library as DFN 1010. No format translating codes were used in this exercise, and rather than simply producing a pointwise ENDF/B file, resolved and unresolved resonance parameters were included. Although the aim was to produce an ENDF/B version which would lead to exactly the same pointwise values as given in the UKNDL version, it was found that small differences inevitably occurred due to the different formats employed by the two libraries. The ENDF/B version has been produced in formats IV and V, both with MAT number 9530 and these have been sent to the NEA Data Bank, and to the Nuclear Data Section of the IAEA as part of a contribution to the Co-ordinated Research Programme on the Intercomparison of Evaluations of Actinide Neutron Nuclear Data.

The UKNDL and ENDF/B versions of the evaluation will be used in appropriate group constant producing codes to check that there is satisfactory agreement in the outputs.

1.10.2 Nuclear data codes (E.M. Bowey and B.H. Patrick)

Further tests have been carried out on programs used for processing evaluated data files. These tests have used the UKNDL and ENDF/B versions of the ^{243}Am evaluation described above and in addition to the codes

mentioned in last year's report (UKNDC(82)P105, p.33), the Bologna code CRESO and the Los Alamos code NJOY have been included.

The tests have shown that all the calculations at 0 K agree well within the allowed errors at all tested energies (<250 eV). However, when the cross-sections were Doppler broadened to 300 K, some significant differences were observed. These problems have been discussed with some of the authors and, as a result, alterations will be made to at least some of the codes. When the revised versions are received, further tests will be carried out and it is hoped to issue a complete report in due course.

1.10.3 Joint Programme on Neutron Data Evaluation (M.G. Sowerby)

The U.K. is participating in the Joint Programme on Neutron Data Evaluation organised under the auspices of the NEA. The first version of the Joint Evaluated File (JEF-1) is nearly complete but this does not include error files. A note has been written which explains the ENDF/B-V format for covariance files in cross-sections and recommends how these should be used in evaluations for JEF.

The U.K. has the responsibility in co-operation with France for producing a new evaluation of ^{238}U for the next version of JEF. Some work on data in the resolved and unresolved resonance regions has started.

1.10.4 The status of FISPIN on the Harwell computer (D.A.J. Endacott)

1.10.4.1 FISPIN Coding

During the year a new version of the coding has been implemented on the Harwell Computer, and is labelled version 5.2. It differs from the previous version (5.1) as follows:

- (1) improved convergence
- (2) extra facilities added
- (3) an increase in the number of fission-product isotopes which can be calculated.

It requires a considerable increase in core space for execution, compared with the previous version. A command macro has been written which generates the required Job Control Language and supplies the necessary data libraries to run standard test cases for a required version of FISPIN. The output can be compared with output from the Risley computer for similar runs. The macro fulfils two purposes:

- (1) to test updated code versions and/or data libraries
- (2) to show new users how to run the code.

1.10.4.2 FISPIN Data Libraries

Four new files for fission-product decay data, cross-sections and yields have been installed, and from these new condensed fission-product libraries have been compiled; one is for thermal reactors and two are for fast reactors. These libraries have been used under version 5.2 for a set of standard test cases, and the results compared with similar tests on the Risley computer. The results are essentially identical.

The FISPIN facility is being used at present for a series of validation runs for the PWR enquiry, in association with CTS Risley, BNFL Windscale, and CEGB Barnwood.

1.11 Selection of low-activity elements for inclusion in structural materials for fusion reactors (O.N. Jarvis)

A study has been undertaken to classify those elements which might be incorporated in a structural material to be used as the first wall of a commercial fusion reactor, under the explicit requirement that 100 years after removal from the reactor the activity of the material should be low enough to permit unshielded handling. The acceptability of 39 elements was summarised in UKNDC(82)P105, p.38 on the basis of induced radioactivity and the surface gamma dose-rate. It was computationally convenient to consider gamma radiation of above 200 keV when computing the dose-rate. The dose-rates from beta activity were ignored.

The study has been extended to include all stable elements, although the cross-section data for the 44 elements not considered previously is very poor indeed (in particular, certain nuclides e.g. ^{166}Ho , ^{186}Re and ^{192}Ir have very long-lived isomeric states which neutron-induced reactions are assumed to populate preferentially - this may not be correct). Bremsstrahlung from β^- particles is now included but the 200 keV photon energy lower limit is retained and the dose-rate from charged particles (mostly β^-) is ignored, on the assumption that thin shielding will be available.

A new table of acceptability may now be constructed as follows:

| | |
|--------------------------------------|---|
| Primary constituents: | those elements (save the actinides) not listed below. |
| Major constituents (10-50%): | Na, Si, Sm, Os |
| Minor constituents (1-10%): | Cu, Zn, Ru, In |
| Trace constituents (0.1-1%): | Cl, Ti, Co, Ni, Rb, Sr, La, Gd, Pt |
| Acceptable impurities (10-1000 ppm): | Al, Ca, Sc, Kr, Zr, Mo, Cd, Sn, Dy, Er, Tm, Re |
| Troublesome impurities (1-10 ppm): | Ar, K, Nb, Ba |
| Unacceptable impurities (<<1 ppm): | Ag, Eu, Tb, Ir, Bi |

A further study in which the arbitrary 200 keV limit is removed is desirable.

1.12 Safeguards research

1.12.1 Fissile material assay by neutron die-away (B.H. Armitage and T.I. Morgan)

The assay of fissile materials by neutron die-away interrogation has a number of potential applications in the U.K. nuclear industry. The feasibility of this method has been studied by Monte Carlo modelling and a design study of a die-away chamber of sufficient size to accommodate 208ℓ barrels has been completed and a chamber constructed. A preliminary examination has been made of the assay of the fissile material content of waste or scrap in barrels. Further work has been undertaken on the feasibility of package monitors for nuclear safeguard purposes. Attention has been given to the reliability and longevity of compact pulsed neutron sources required for neutron die-away interrogation.

1.12.1.1 The design of neutron die-away chambers (T.I. Morgan and B.H. Armitage)

A preliminary report has already been given (UKNDC(82)P105, p.38) of a calculational study of the properties of a neutron die-away chamber of sufficient size to accommodate 208ℓ barrels. The work is now complete, and had as its objective the choice of such design parameters as wall thickness and detector position. The die-away system consists of a compact pulsed neutron tube placed inside a chamber composed of graphite and polyethylene (CH₂) walls. The neutron source produces pulses of 14 MeV neutrons which become moderated and thermalised in the walls of the chamber. The ensuing thermal neutron flux is used to assay fissile material present in the chamber. Fast neutron detector packages in the walls of the chamber are insensitive to thermal neutrons and detect only fast fission neutrons in the period between successive pulses of 14 MeV neutrons. Each fast neutron detector package consists of a BF₃ detector surrounded by polyethylene and wrapped in Cd.

The calculations have been made with the Monte Carlo computer code MONK using the chamber geometry of Fig. 1.5 where the structural materials have been confined to graphite and polyethylene. The procedure consisted of calculating the fission neutron rate for a dilute mixture of ²³⁵U and ²³⁹Pu contained within the volume shown as dotted in the figure. This volume is then treated as a secondary source of fission neutrons to enable the efficiency of the detectors to be determined. Thus, for a given

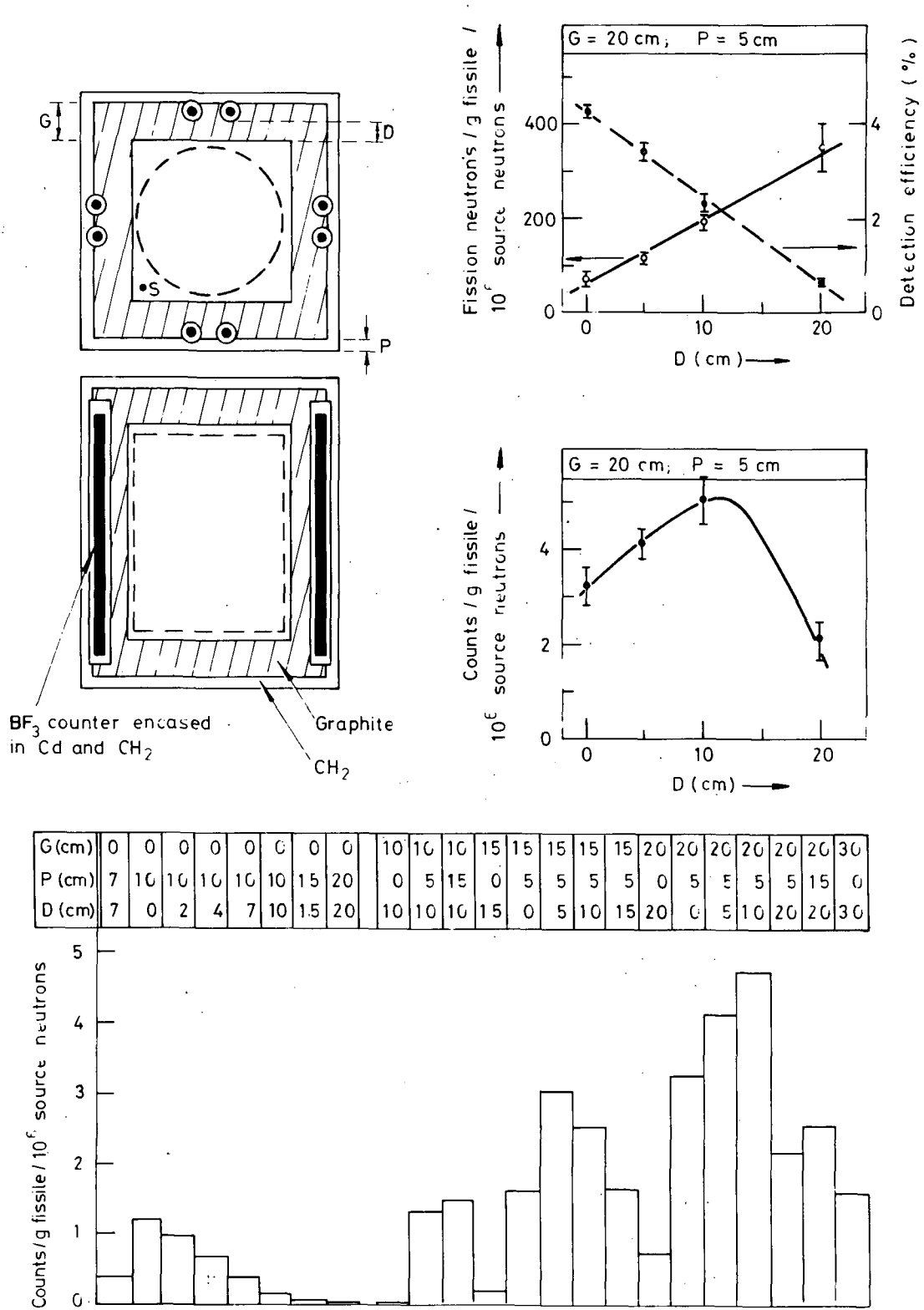


Fig. 1.5 Geometry of model chamber (upper left), example of computational results (upper right), and comparative data for chambers of various wall thicknesses and detector positions (lower).

graphite thickness (G cm) and polyethylene wall thickness (P cm) the number of fission neutrons counted can be obtained as the product of the number of fission neutrons and the detection efficiency.

An example of such a result is shown on the right of Fig. 1.5 where the number of fission neutrons, the detection efficiency and the fission neutron count are plotted against the depth (D cm) to which the detectors are embedded within the walls of the chamber. In the example shown the graphite and polyethylene wall thicknesses are 20 cm and 5 cm respectively, and it is noteworthy that the number of fission neutrons, and also the detection efficiency are strongly dependent on the embedding depth.

The general features of the results are shown at the bottom of Fig. 1.5 where the number of fission neutrons counted per g fissile material per 10^6 source neutrons is plotted for twenty-three values of G, P and D. The results show that the most efficient die-away chambers are made from a combination of graphite and polyethylene, although a relatively thin walled chamber (~ 10 cm) of reasonable efficiency can be constructed entirely from polyethylene. The advantage of embedding the detector packages within the graphite walls has also been demonstrated.

1.12.1.2 Assay of fissile material in 208l barrels (T.I. Morgan and B.H. Armitage)

The main purpose of the die-away chamber is to assay the fissile content of low level waste in barrels. An example of the functioning of the system is shown in Fig. 1.6, where time spectra obtained during an assay of 50s with a 46 mg sample of ^{235}U (93% enrichment) are illustrated. Fast neutron detector time spectra are shown (a) in the presence and (b) in the absence of the fissile sample, while (c) shows the thermal neutron time spectrum within the chamber. The fast neutron detector time spectra show that the system takes ~ 0.5 ms to recover from saturation induced by the 14 MeV pulse from the neutron source. The optimum delay before the recording of fast fission neutron counts is between 0.5 and 0.7 ms.

In the example shown the background subtracted total of fission neutrons recorded within the time interval between 0.7 and 10 ms was 124 for a total of 511 pulses at 10 pulses per sec. It is expected that this performance will be significantly improved when the present four ^3He fast neutron detector packages are replaced with eight more efficient detector packages.

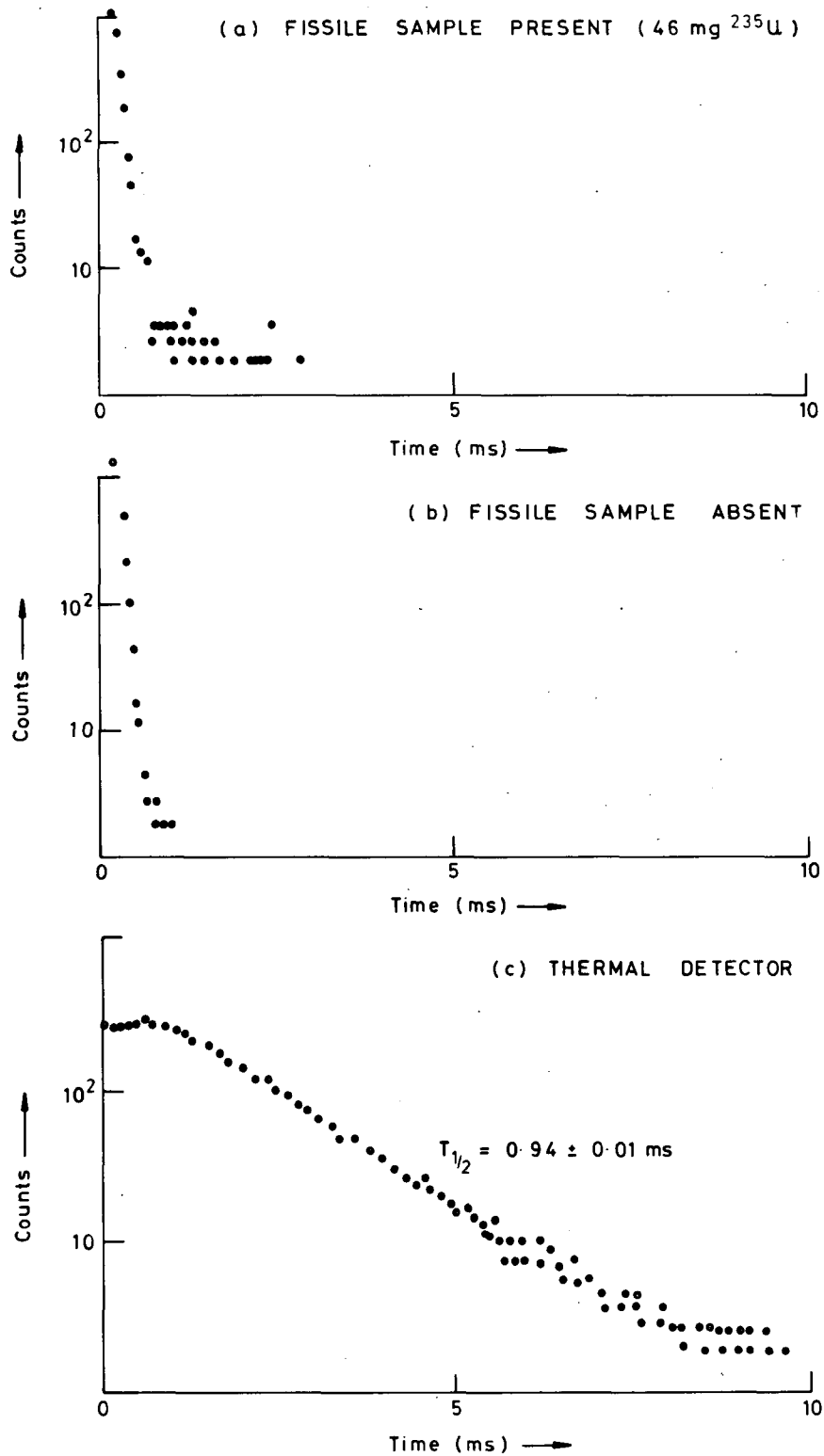


Fig. 1.6 Fast neutron time spectra (a) in the presence and (b) in the absence of a fissile sample together with the thermal neutron time spectrum (c) within the chamber.

A preliminary study has been made of the behaviour of the die-away system when assaying fissile material in matrix filled barrels. The matrices examined so far have been an empty barrel, paper tissues and stainless steel tubes. The first quantity to be measured was the spatial variation of the thermal neutron flux within the volume of the barrel. This was achieved by placing a 1.3 cm dia. 5 cm active length BF₃ thermal neutron detector at various locations within the barrel. A permanently located set of full length Al tubes with axes parallel to that of the barrel was used to position the detector within the matrices. The flux uniformity data given in Table 1.1 was obtained for each matrix at fifteen selected positions within the barrel.

In addition the Table contains data on the variation in the number of fission neutrons counted when a 6.5 g sample of ²³⁵U was placed at the same fifteen positions within the barrel. As can be seen from the Table the fission neutron response was somewhat less uniform than the corresponding thermal flux for the empty and tissue filled barrels, but not for the more highly neutron absorbing stainless steel tube matrix. Finally, it may be noticed that the thermal neutron die-away time is only slightly reduced by the tissue matrix (9 kg) whereas the presence of the more massive stainless steel tube matrix (102 kg) causes a considerable diminution in the die-away time.

Table 1.1
Characteristics of die-away chamber for fissile material in different matrices

| Barrel contents | None | Tissues | Steel tubes |
|---|------|---------|-------------|
| Bulk density (g cm ⁻³) | 0.0 | 0.043 | 0.49 |
| Thermal neutron flux uniformity (%) | ± 5 | ± 9 | ± 22 |
| Fission neutron response uniformity (%) | ± 9 | ± 12 | ± 17 |
| Die-away time (ms) | 0.85 | 0.81 | 0.58 |

1.12.1.3 A monitor for observing enriched uranium in large volume packages (B.H. Armitage)

In an earlier report (UKNDC(82)P105, p.39) it was stated that adequate safeguards for nuclear plants may require the inclusion of a device capable of examining large packages at entry and exit. Such a device may be used to foil attempts to introduce or remove significant quantities of uranium which have been enriched above normal commercial requirements. Fissile material may be surrounded by bulky shielding and it was concluded that either the fissile material may be observed by delayed neutron interrogation or the presence of such bulky shielding should result in a measurable change in the die-away time within the package monitor.

Calculations made with the computer code MONK for a package monitor with a 2 m³ cavity (UKNDC(82)P105, Fig. 1.6) demonstrated that delayed fission neutrons can be suppressed by a certain thickness of polyethylene (CH₂) shielding. Measurements made with a chamber of considerably smaller dimensions (18 cm x 18 cm x 25 cm) demonstrated that 0.35 kg of CH₂ produced a reduction in neutron die-away time of about 2.5%. A conservative estimate for the equivalent amount of CH₂ for the 2 m³ package monitor is such that the suppression of delayed fission neutrons is insufficient to prevent their detection.

Supporting evidence for the above result has been obtained using the time dependent Monte Carlo code MORSE. The calculations have been made for the 2 m³ model package monitor and show that whereas the die-away time for the empty package monitor is 1.0 ± 0.1 ms this value reduces to 0.65 ± 0.15 ms when the uranium sample together with 30 cm thickness of CH₂ is present. This result is compatible with the earlier estimate that the neutron die-away system should be capable of observing the presence of CH₂ shielding in excess of 15 cm thickness.

More recently it has been possible to introduce bulk CH₂ into the die-away chamber designed for the assay of 208ℓ barrels. The results of such a measurement are shown in Fig. 1.7 in which it can be seen that the die-away chamber is sensitive to 6 kg of CH₂, which was present in the form of a rectangular slab (30 cm x 30 cm x 7 cm). Again this result is compatible with the earlier estimates and helps to demonstrate that a package monitor capable of observing kg quantities of U enriched above normal commercial requirements should be a viable proposition.

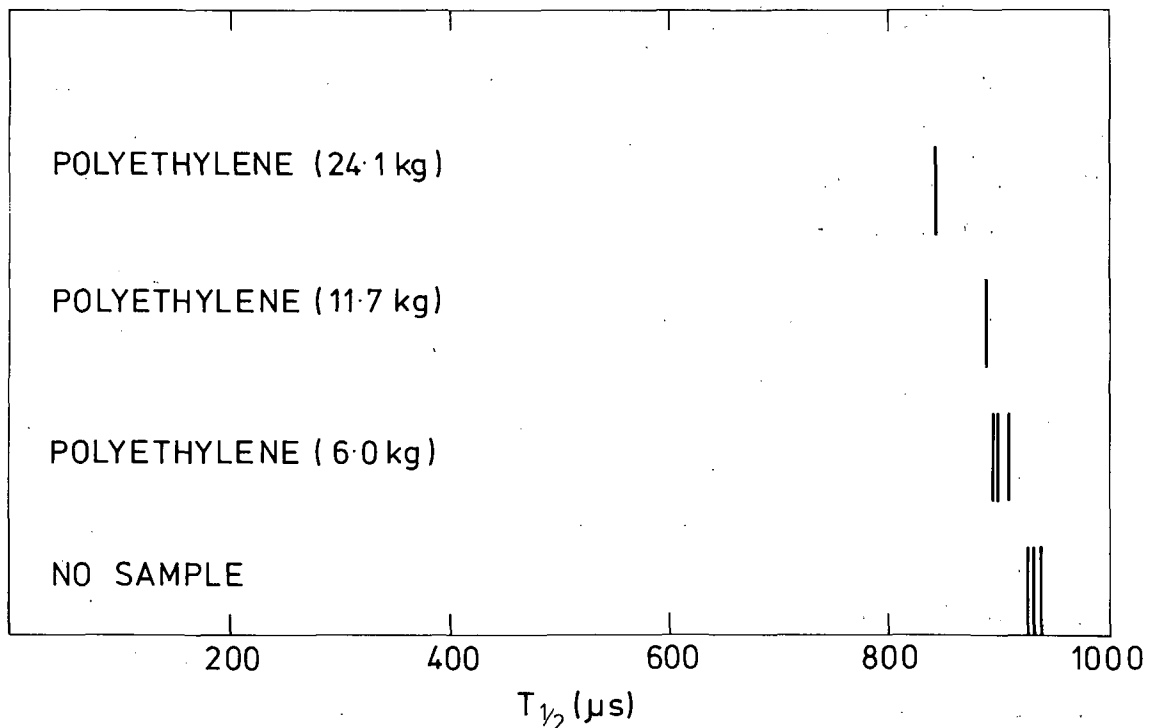


Fig. 1.7 Neutron lifetimes in die-away chamber containing polyethylene neutron shielding material.

1.12.1.4 Pulsed neutron source assessment (B.H. Armitage)

An examination of the probable requirements for neutron interrogation systems in the U.K. nuclear industry has revealed that approximately twelve systems will be required during the next few years. As most of these applications will be in a plant environment, consideration has been given to the reliability and longevity of pulsed neutron sources. The common specification for these sources is $\sim 10^7$ neutrons per pulse, at a repetition rate of at least 10 pulses per second and with a pulse duration of less than 0.1 ms.

An analysis of the behaviour of the Marconi Avionics NK5 pulsed neutron source at Harwell has demonstrated a 56% availability during the first six months of operation. The non-availability of the pulsed neutron source is attributed to electrical break-down in the E.H.T. connections (8%), gas leakage (8%) and an unsuccessful attempt to replace the neutron tube (28%). Following representations, the manufacturers have agreed to take measures to reduce the incidence of such faults, and also to prepare proposals to improve the longevity of neutron producing tubes.

A comparative study of alternative neutron sources (including small Van de Graaff accelerators) is being undertaken, with the eventual objective of being able to recommend a particular system for plant application.

1.12.2 Non-invasive determination of the U content in a centrifuge plant dump tank (M.C. Moxon and E.W. Lees)

Chemical (NaF) absorbers are used in the clean-up and emergency dump systems of some designs of centrifuge plants. The total amount of U absorbed over the lifetime of the plant could amount to a substantial fraction of a Safeguards significant quantity of ^{235}U .

The dump tanks can consist of a thick outer vacuum tank and an inner vessel (both made of Al) the NaF on which the UF_6 is absorbed. Because the tanks are designed to last for the operational lifetime of the plant, removal and/or sampling of the U content is not favoured.

Initial measurements of the U content carried out utilising the passively emitted neutrons and gamma-rays indicated that a quantitative estimate would be difficult to obtain. However preliminary measurements using the gamma-ray transmission technique were more promising. Consequently, these measurements were repeated with better spatial resolution using a stronger (330 mCi) ^{60}Co source and the results are described briefly below.

Fig. 1.8 shows a plan view of the experimental arrangement. The transmitted gamma-rays were detected by a 75 mm diameter x 75 mm NaI crystal with a resolution of ~6%. This resolution is adequate to resolve both the ^{60}Co lines at 1.17 and 1.33 MeV and clearly separates the 1 MeV ^{234}Pa decay line. A vertical scan was made across a diameter of the trap as shown in Fig. 1.9. If C_0 is the unattenuated source count rate and $C(x)$ is the observed count rate at a vertical height x , then

$$\sum_i N_i(x) \sigma_i = \ln |C_0 / C(x)| = A(x) \text{ say}$$

where $N_i(x)$ is the thickness of material i at height x with a gamma-ray attenuation coefficient σ_i .

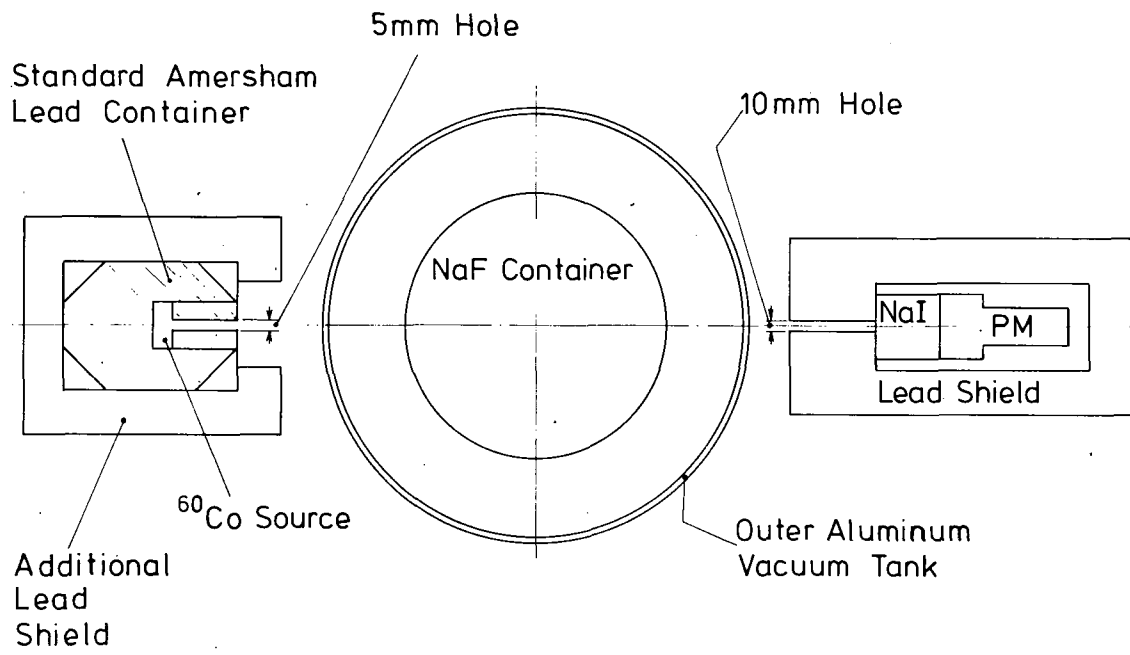


Fig. 1.8 Plan view of the experimental arrangement.

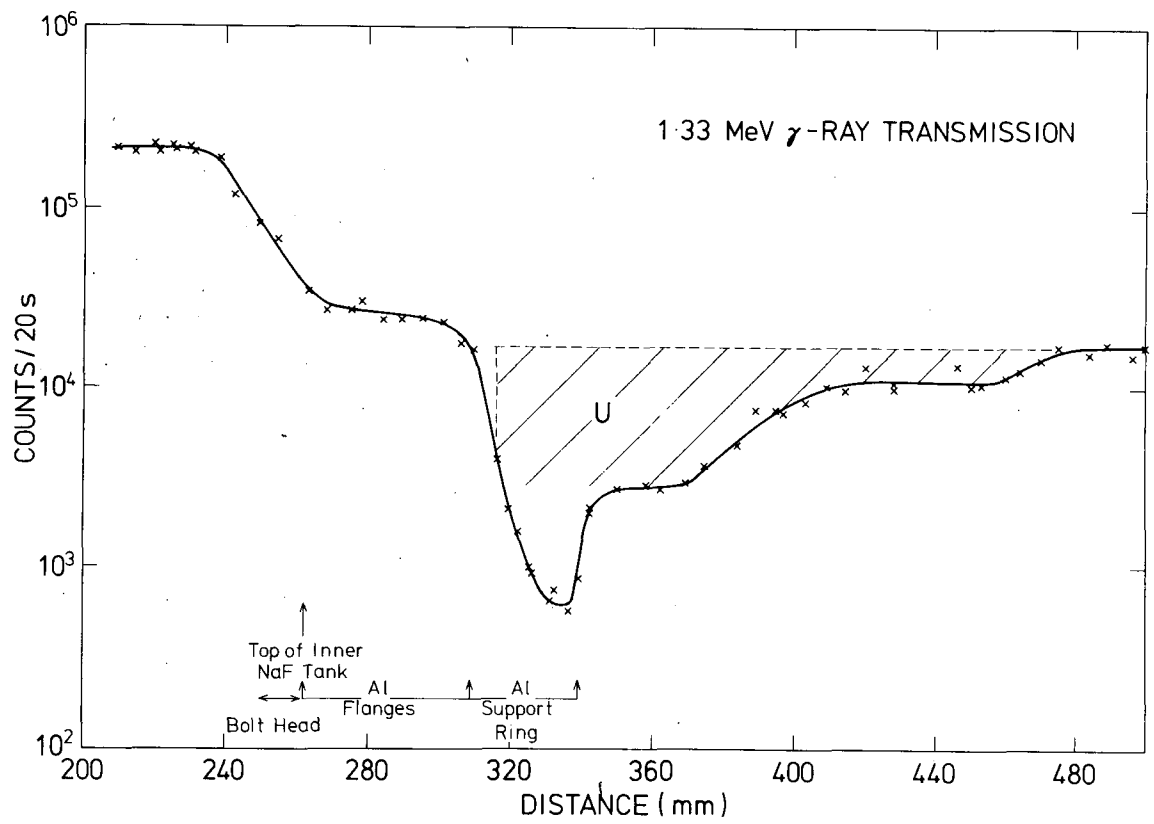


Fig. 1.9 Vertical scan of the transmissions of the 1.33 MeV gamma-ray from a ^{60}Co source across a diameter of the NaF dump trap.

In the region greater than 480 mm, the value of $A(x)$ was fairly close to that calculated for the known NaF concentration and the thickness of the inner tank's Al wall. However, the absolute value is not strictly necessary since the average value of $A(x)$ between 480 and 550 mm can be subtracted to leave the contribution due to UF_6 . Integration of this latter area yielded a value of 12.2 ± 1.4 kg of UF_6 or, equivalently, 8.2 ± 0.9 kg of U. This value is in reasonable agreement with the operators' estimate of 11.2 ± 2.8 kg of U.

In an attempt to improve the precision of the comparison between the gamma-transmission results and the operators' estimates, measurements have been performed recently on a clean-up ("vent") trap. These traps, although narrower in diameter, are similar in design to the dump traps. However, the vent traps are removed regularly from the plant and so the NaF and absorbed UF_6 could be sent for chemical analysis after the gamma-transmission measurements. In the latest measurements an additional scan with a 1 Ci ^{137}Cs source was performed; this will help confirm that the material being measured is U from the known variation of gamma-ray absorption coefficients with gamma-ray energy. Analysis is at present underway.

1.12.3 The ^{252}Cf shuttle (E. Wood, A.R. Talbot, W. Crane)

The ^{252}Cf shuttle system, also known as the "fast shuffler", is recognised⁽¹⁾ as being particularly suited to the measurement of low levels of uranium or plutonium contamination of waste materials arising in the nuclear industry. A prototype shuttle system has been assembled for neutron interrogation of 208l waste drums. An early description of the arrangement now commissioned may be found in UKNDC(81)P100, p.34. The pace of development of the shuttle was reduced to accommodate the construction of the competing system, using a neutron die-away chamber, which is claimed to possess superior attributes. However, to establish the truth of this claim it is desirable that both of the facilities be commissioned and operated in parallel.

The prototype shuttle system is operated entirely under the control of the VAX 11/750 computer. An initial assessment is now being made of its consistency of running, i.e. shuttle transfer times, and of its mechanical reliability. The limit of detection of the present system (3σ , 15 minute measurement) is about 1 g ^{235}U using a 10^7 neutrons s^{-1} ^{252}Cf source. The background count-rate is 6 counts s^{-1} and is proportional to source

strength. Improved shielding should reduce this rate by an order of magnitude. It is conventional to use very strong sources in shuffler systems, e.g. 0.5 mg ^{252}Cf - or 10^9 n s^{-1} , for which detection limits of 1 mg ^{235}U or better can be demonstrated.

(1) T.W. Crane, Los Alamos Scientific Laboratory, report LA-8294-MS (1980)

1.12.4 The determination of the ^{235}U enrichment of UF_6 gas inside pipes at a centrifuge plant (T.W. Packer)

Although the initial aim of the project was to determine the ^{235}U enrichment of the gas (UKNDC(82)P105, p.41), early experiments showed the presence of considerable masses of deposited uranium. Later measurements were therefore aimed at monitoring the history of the plant by determining the ^{235}U enrichment of the deposit.

The number of γ -rays emitted by the UF_6 gas and by any uranium or thorium deposited on the inside of eight product pipes has been determined using a high resolution γ -ray spectrometer. As the centrifuges had been in operation for between 23 and 63 months, there was a considerable deposit on the inside of the pipes. Hence the γ -rays emitted from the deposit were much greater than those emitted from the gas.

The γ -ray spectrometer, incorporating a 50 cm^3 intrinsic germanium semi-conductor detector, was calibrated at Harwell using samples made by depositing different masses per unit area of uranyl nitrate solutions of known but differing ^{235}U content onto filter papers. It was possible to determine the mass per unit area of uranium deposited on the filter paper by determining the number of 63, 93 or 1001 keV γ -rays emitted by ^{238}U daughter products. It was also found possible to determine the ^{235}U enrichment by measuring the ratio of the number of detected 185 keV γ -rays, emitted by ^{235}U , to the number of any one of the detected γ -rays emitted by the ^{238}U daughter products.

However, when applying the same technique for checking the declared enrichment of eight product pipes in a centrifuge plant, these ratios gave low ^{235}U enrichment values. This is thought to be due to the detection of γ -rays emitted by thorium which may have been selectively deposited onto the pipes. This theory was supported by studies on the ratio of the number of detected 185 keV γ -rays, emitted by ^{235}U , to the number of 84 keV γ -rays

emitted by its daughter ^{231}Th . This ratio was higher for the calibration samples than for the deposit.

However, the ratio of the number of 84 keV γ -rays emitted by ^{231}Th to the number of 63 keV γ -rays emitted by ^{234}Th yielded the ^{235}U enrichment of the deposits on the eight product pipes to within 10 to 20% of their declared values in measurement times of approximately 4 hours.

There was also a tendency for the mass of uranium deposited on the pipe to increase with the time that the centrifuge had been in operation, at a rate of approximately $0.1 \text{ mg cm}^2 \text{ yr}^{-1}$, although there was a considerable variation in the mass of uranium deposited on pipes that had been in operation for approximately the same time. The above value corresponds to a deposit that is evenly distributed around and along the pipe.

In order to increase the confidence in the measurement a more detailed study of the mechanism by which uranium and its daughter products are deposited on the pipe is being carried out. In addition, experiments are being undertaken aimed at determining whether the UF_6 gas exchanges with the uranium deposit since this could affect the use of the measurement for checking the history of the plant.

1.13 Plutonium dating (D. West and A.C. Sherwood)

Freshly prepared fuel pins of known age W01, W02 and W03 became available during the year to act as standards. Enquiries about Pu separation dates were made and the material selected before the fuel pins were fabricated. This seemed more appropriate than going to the lengths of getting fuel pins made with special material absolutely homogeneous in age - a desirable feature in a standard.

Table 1.2 contains previous measurements (April 1981) on a variety of fuel pins, together with a single intercomparison of one of them (M120) with W03 carried out in June 1982.

In UKNDC(82)P105, p.50 the comparison of M119 and M120 was described in detail but at that time the measurements on fuel pins M83 and 1054/19 were not discussed as these fuel pins differed in configuration from M119 and M120 and were therefore subject to additional uncertainties from self-absorption of the radiations. The new separation date of M120 (3 May 1977 \pm 12 days) is some four months earlier than the date previously accepted. The age of M83 has been redetermined in terms of this new value giving a separation date of 1 December 1971 \pm 29 days. This is much closer to the recorded date than that measured in April 1981. Although the evaluations

have not been carried out it is clear from Table 1.2 that M119 will still require to have a separation date indistinguishable from that of M120 and that pin 1054/19 will require to have a separation date close to 1 December 1971.

The new dates for both M83 and 1054/19 are much more credible than those measured in April 1981.

Table 1.2
Fuel pin dating results at July 1982

| Fuel Pin | Dia. (mm) | Pellet form | Recorded separation date | Measured in April 1981 | Measured in June 1982 | Reassessed April 1981 values |
|----------|-----------|-------------|---------------------------------|---------------------------|-------------------------|-------------------------------------|
| W03 | 5.8 | Annular | 7 Nov. 1980 ± 1-2 days | | Standard 7 Nov. 1980 | |
| M120 | 5.8 | Annular | Isotopic analysis March 1978 | Standard 15 Sep. 1977 | 3 May 1977 ± 12 days | Standard 3 May 1977 ± 12 days |
| M119 | 5.8 | Annular | March 1978 | 20 Sep. 1977 ± 7 days | | |
| M83* | 5.8 | Powder | Mar/Apr 1972 | 14 Sep. 1972 ± 13 days | | 1 Dec. 1971 ±29 days |
| 1054/19* | 5.1 | Solid | Nov. 1971 | 12 Sep. 1972 ± 13 days | | |

*These pins assumed to have same configuration as pins M119, M120 and W03

1.14 Proposed neutron diagnostic systems for JET (O.N. Jarvis, M.T. Swinhoe, D. West and P. Dixon*)

Over the past three years the Neutron Systems Group has undertaken the design of four sets of neutron diagnostic instrumentation proposed for installation on JET**. The design of a fifth system has just started. These five systems will be described in turn, concentrating mainly on any unusual features they might possess. A possible layout for these systems is illustrated in Fig. 1.10. The actual allocation of space for the

*Engineering Projects Division

**Joint European Torus, Culham

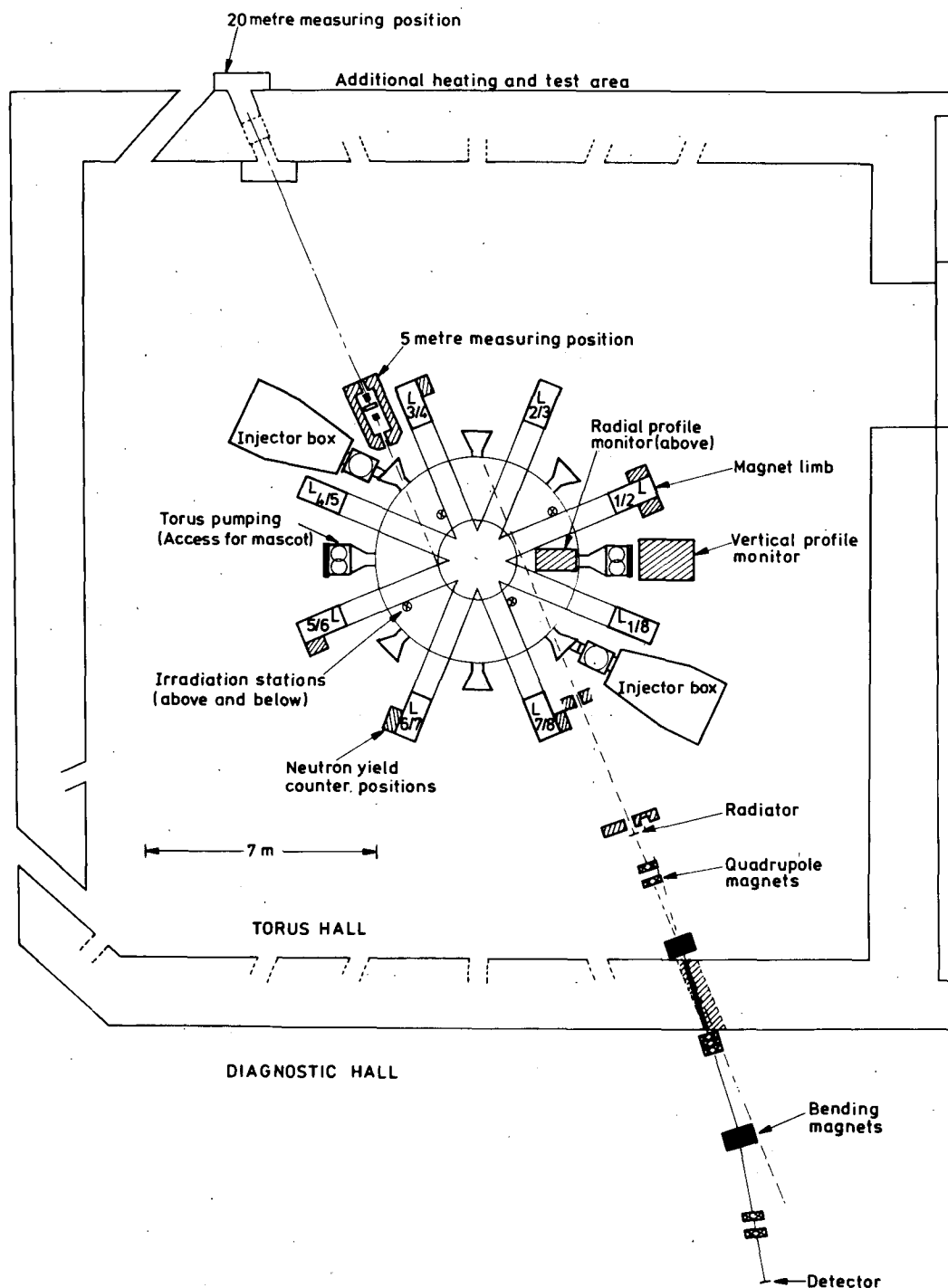


Fig. 1.10 JET torus hall schematic, showing possible locations for the neutron diagnostics

neutron diagnostics has yet to be agreed; the problem of their disposition would be immediately apparent if the many other systems were also to be represented on the figure.

1.14.1 Neutron yield measurements (time-resolved)

The essential feature of a time-resolved neutron yield monitor is an ability to respond linearly to the rate of production of neutrons from JET during the discharge period, with an operational range covering 12 decades. Because the required efficiency is not very high it is acceptable to utilise fission counters. These provide large output signals which can be clipped hard so as to obtain a high count-rate capability.

Two types of fission chamber are to be employed. The more sensitive contains 0.6 g of ^{235}U and is surrounded with a 5 cm thickness of polyethylene moderator, giving a response of about 0.8 counts neutron $^{-1}$ cm $^{-2}$. The less sensitive chamber contains 0.6 g of ^{238}U and no moderator; its response will be about 10^{-4} counts n $^{-1}$ cm $^{-2}$. The ^{235}U counter has a response which is engineered to be reasonably flat between 0.1 and 20 MeV; the ^{238}U counter has a threshold at about 1.5 MeV. These counters will be employed both in pulse-counting and current modes, depending on the neutron flux. Together, they will enable the neutron emission from JET to be monitored from 10^9 n s $^{-1}$ to 10^{21} n s $^{-1}$.

Lead shielding is specified for both counters to reduce their responses to bremsstrahlung radiation arising during minor disruptions and to gamma radiations when the counters are operated in current mode.

Three pairs of fission counters are to be provided, positioned on the vertical magnet limbs at the horizontal mid-plane of the torus (see Fig. 1.10). By suitably distributing the counter positions in azimuth around the torus it should be possible to minimise (or identify) distortions caused by localised emission hot-spots.

The most significant technical problem connected with these counters is the need to operate them without the benefit of preamplifiers, which would be vulnerable to radiation damage (up to 100 Mrad total). Instead, the signals (~ 20 μV fast pulses and d.c. currents down to 100 nA) will be transmitted along 100 m coaxial cables to the diagnostic hall; superscreened cables⁽¹⁾ will be used to reduce the electromagnetic interference (from what can be expected to be a very noisy environment) to an acceptable level.

1.14.2 Neutron yield measurements (time-integrated)

The technique of multi-foil activation analysis (MFA) is well established as a means for determining neutron fluences and energy spectra.

The proposed activation system is complementary to the fission counters in that it gives only the time-integrated neutron yield, and the method is totally insensitive to some of the problems besetting the fission counters (magnetic fields, radiation damage, vibration, electrical interference) as the counting takes place at a remote station during the quiet periods between discharges. Most important, the measurements can be made absolute with high accuracy (~5%) because the eight irradiation stations are located within the bulk of the structure of the torus (see Fig. 1.10) so that corrections for neutron attenuation are negligible and the backscattering is small and calculable.

To exploit the capabilities of the activation method it will be necessary to install a pneumatically operated transport system to move polyethylene capsules rapidly from a hopper to any specified irradiation station and from there to detectors in any of the remote stations for analysis. Three types of detector are proposed: Ge diode, NaI scintillator and delayed neutron counting equipment. Also, a number of delay stations are required to hold irradiated capsules awaiting analysis. A transport system utilising a 20-position carousel is proposed for this application.

The choice of activation reactions poses some difficulty because, on JET, it would be desirable to analyse irradiated samples from all eight irradiation stations following each 10-second discharge, with only 10 minutes permitted for counting the decay emissions. Unfortunately, there are rather few reactions available with the necessary sensitivity since most of those with threshold energies suitable for use with d-d neutrons (i.e. thresholds between 1 and 2.5 MeV) involve radioactive decay half-lives of the order of hours, if not days. The situation for 14 MeV d-t neutrons is much better. The most sensitive of the reactions involves gross gamma-counting of short-lived radiations from fission foils. The foils used in gamma analysis must be allowed to cool for appreciable periods before they can be used again; this implies a need for a large inventory of foils and capsules. Alternatively, routine irradiation and analysis can be based on the technique of counting the delayed neutrons emitted from irradiated fission foils. The longest half-life for delayed neutron emission is about 100 seconds and the overall sensitivity of the method is quite high (comparable with that for gross gamma-counting); it may prove possible to recycle the same foil for use in successive discharges, a very desirable operational simplification. The delayed

neutron counting equipment is being designed by a team from Mol, Belgium.

1.14.3 The profile monitor

The profile measuring system is intended to sample the intensity of neutron emission, as a function of position, from a vertical section of plasma. The measurements should give useful information (in the form of a neutron emission contour plot) on the behaviour of the plasma during MHD fluctuations and, more generally, on the shape of the plasma (which is non-circular). The device is intended to operate from low temperature d-d operation (10^{15} n/shot) up to the highest temperature d-t operation (10^{20} n/shot) with a spatial resolution of about 10 cm, to cover a spatial intensity variation of a factor of 100 and, at high yields, to offer a temporal resolution of a few milliseconds.

The equipment consists of two multi-collimator assemblies positioned at one of the pumping port sectors, the horizontal profile device being supported on the magnet limbs and the vertical profile device being supported on a strong support tower. The entire profile monitoring equipment is designed for operation in the active phase so that a full remote handling capability is essential.

A number of design problems have been encountered with the profile monitor. First, the shielding has to be sufficiently thick that the background flux of neutrons entering through the sides is small compared with that entering via the collimators. Second, the physical separation between collimator channels must be sufficient to reduce the cross-talk to an acceptable level. Third, the plasma must be viewed through a thin window (<6 mm Inconel) otherwise the image of the plasma will be blurred by neutron scattering, much as a rainbow is blurred by viewing through a sheet of frosted glass. Fourth, the neutrons from the plasma must be observed against a background of lower energy neutrons back-scattered from the structural material lying in the field of view of the collimators. Finally, the neutrons must be distinguished against a background of gamma radiation.

For d-d operation a NE213 scintillator/photomultiplier combination offers the necessary efficiency, energy resolution ($\sim 10\%$) and n- γ discrimination properties. For d-t operation a much reduced efficiency is needed and the energy resolution requirement can be relaxed. A promising detector has been investigated by Chrien and Strachan⁽²⁾; it is a

scintillator made from a mixture of LiF and ZnO which utilises the ${}^7\text{Li}(n,n'\alpha)t$ threshold reaction and, like the Hornyak button, is insensitive to gamma radiation.

1.14.4 2.5 MeV spectrometers for deuterium plasmas

The most stringent objective that can reasonably be set for the spectrometers for deuterium plasmas is that of making several determinations of the plasma ion temperature at 2 to 3 keV (and $n = 3 \times 10^{13}$ ions cm^{-3}) in a single 10-second discharge. To achieve this, an instrumental resolution of better than 4% is needed and the efficiency must be such that between 100 and 1000 counts are accumulated in the useful portion of the energy spectrum. Of course, both efficiency and resolution requirements can be relaxed when the ion temperature rises.

It is most unlikely that any single spectrometer can be constructed which will perform acceptably over the entire range of plasma conditions of interest. It is, therefore, necessary to pursue several approaches in the expectation that conditions will be favourable for at least one of them at all times.

Three spectrometers have been identified suitable for use with deuterium plasmas:

- (1) the ${}^3\text{He}$ ionisation chamber, which combines excellent energy resolution (2% at 2.5 MeV) with sufficiently high efficiency for it to be exploited on tokamak devices;
- (2) a thin-radiator "in-line" proton-recoil device, in which the silicon diode detector is positioned to detect forward-scattered protons but must also suffer the unscattered neutron beam passing through it; and
- (3) the thick-target NE213 scintillator, offering poor energy resolution (~10%) but very high efficiency and therefore useful for detecting the 0.5% of 14 MeV neutrons emitted from secondary t-d reactions in the deuterium plasma.

Of these, the ${}^3\text{He}$ ionisation chamber and the NE213 scintillator do not demand the angle of incidence of the neutrons to be defined by collimation whilst the "in-line" proton-recoil device requires only modest collimation ($\pm 8^\circ$). This varying permissiveness in the degree of collimation is seen to be illusory when the further specification is added that the desired spatial resolution at the plasma should be no more than 10 cm.

The present intention is to house the three spectrometers inside a movable shield/collimator assembly positioned against one of the horizontal diagnostic ports and viewing the plasma tangentially. This would be at the 5 metre position (see Fig. 1.10). These detectors share the properties of being of modest dimensions and of not being unduly sensitive to background neutrons. The shielding assembly is being designed for operation with deuterium plasmas only.

1.14.5 14 MeV spectrometers for deuterium-tritium plasmas

The obvious approach to high-resolution spectrometry with 14 MeV neutrons is the conventional "scattering-geometry" proton-recoil arrangement, in which knock-on protons from a thin-radiator are detected in silicon diodes set at a sufficiently large angle ($>10^\circ$) to the incident neutron direction that incident neutrons do not pass through the detector. The solid angle subtended by the detector at the radiator must be kept small if an overall energy resolution of 2% is to be achieved, with the result that the detection efficiency of the spectrometer is very low. Even allowing for the likelihood that tritium operation will not be embarked upon until an ion temperature in a deuterium-only plasma in excess of 5 keV has been attained, the requirement of obtaining several good spectra in a single discharge demands that the plasma to spectrometer separation should be kept as short as possible. The original proposal was therefore to house the proton-recoil spectrometer within a massive (100 tonne) but movable shield unit, provided with full remote handling capabilities and positioned inside the torus hall as close to one of the diagnostic ports as possible.

The approach described above has the obvious disadvantage of being inconvenient and expensive. Consequently, much thought has been given to the design of a more efficient spectrometer which can be located further from the plasma with the biological shield wall providing at least the major portion of the required shielding against background neutrons. Of course, the radiation levels in the diagnostic hall will be much greater for a deuterium-tritium plasma than for a deuterium-only plasma and a substantial secondary shield wall surrounding the spectrometer in the diagnostic hall will be essential.

Two ideas for high-efficiency 14 MeV spectrometers are being investigated. The first possibility is to take advantage of the nuclear reaction induced by high-energy neutrons in a silicon diode. The $^{28}\text{Si}(n, \alpha_0)^{25}\text{Mg}$ reaction leading to the ground state in ^{25}Mg has a 14 MeV

cross-section of about 15 mb and offers an instrumental resolution of slightly less than 1%. Unfortunately, the method has a number of disadvantages and has never yet been applied to a directly comparable problem. Also radiation damage is such that this method is unsuitable for routine use and must be reserved for special investigations where the best possible energy resolution is needed.

The second technique under consideration is the design of an "in-line" proton-recoil technique in which magnetic elements are used to transport the recoil protons to a detector positioned well away from the transmitted neutron flux. Several arrangements are possible, of which the one illustrated in Fig. 1.10 is the most favoured at present because the detector is located conveniently within the diagnostic hall but there is no direct view of the torus from the diagnostic hall thereby reducing radiation leakage into the diagnostic hall. The particular problem of this approach is that the magnetic transport system must be achromatic over an energy band of $\pm 5\%$ (at least) centred on 14 MeV.

-
- (1) E.P. Fowler, *The Radio and Electronic Engineer* 49 (1979) 38.
 - (2) R.E. Chrien and J.D. Strachan, *Rev. Sci. Instrum.* 51 (1980) 1638.

2. CHEMICAL NUCLEAR DATA

2.1 Introduction

The main Chemical Nuclear Data Committee (Chairman: J.G. Cuninghame (AERE), Secretary: R. Bett (AERE)) has held two meetings during the year and the Decay Library Sub-committee (Chairman: B.S.J. Davies (BNL*)), three.

Most of the work of the committee is concentrated on the maintenance and updating of the fission yield file (C3I) and the files for activation product decay data (UKPADD-1), fission product decay data (UKFPDD-2) and heavy element decay data (UKHEDD-1). The current position over these files is as follows:

(a) C3I

Following the retirement of E.A.C. Crouch, work on the updating of this file has ceased. Discussions are currently under way to see if the work can be resumed, perhaps as part of a European effort.

(b) UKPADD-1

Now under revision. The new version, which should be available in 1984, will comprise 410 nuclides.

(c) UKFPDD-2

No work is in progress on this file at present, apart from validation studies. The file is up to date and studies so far have confirmed that its use in, for example, decay heat calculations gives results which are at least the equal of those in which other data files are used.

(d) UKHEDD-1

No work is in progress on this file at present. It is, in any case, up to date and almost certainly the best heavy element data file available today.

Measurement work by members of the committee continues on a variety of subjects, of which the main ones are decay scheme data for short-lived fission products and half-life and branching ratio data for actinides.

A Seminar on Alpha-Spectrometry and Low Level Measurements under the auspices of the International Committee for Radionuclide Metrology (representative: K.M. Glover (AERE)) is being organised at Harwell in May 1983.

*Berkeley Nuclear Laboratories, CEGB

2.2 Fission measurements

2.2.1 Development of a helium jet recoil transport system for VEC* studies of short-lived nuclides (R. Bett, J.G. Cuninghame and H.E. Sims (AERE))

The helium jet system has been rebuilt with extensive modifications. A potassium chloride generator with a centrifugal device for providing KCl particles of the correct size replaces the use of diethyl sulphide as the clustering agent. The tape drive collector has been rebuilt and provided with a remote control system which can be operated by a PET computer through a MOUSE microcomputer. New collimators have been fitted to the beam line and there is now a beam stopper just in front of the target which can also be controlled by the PET/MOUSE. Fully automatic control of irradiation, source and counting is now possible through this computer control, together with automatic data collection by the PDP-11 program MLSPEC (see sect. 2.2.4). The whole system has been tested in a study of neutrondeficient molybdenum isotopes and is now being applied to fission products.

2.2.2 Decay scheme studies on short-lived fission products (J.G. Cuninghame and H.E. Sims (AERE))

Preliminary experiments with fission products generated by the reaction $^{238}\text{U}(^4\text{He},\text{f})$ have given excellent fission product transport to the collecting receiver, using the redesigned helium jet transport system and potassium chloride as clustering agent.

2.2.3 Studies of ^{252}Cf fission products by means of a helium jet transport system (J.G. Cuninghame (AERE); D.L. Stone (pre-university student))

As an alternative to fission products produced from a target irradiated on a VEC beam line, it is possible to use a ^{252}Cf source coupled to the helium jet recoil transport system. The source has a strength of approximately 1.6×10^6 fissions per minute. This mode of operation has been extensively used to explore the effect of changing the operating conditions of the system, particularly the flow rate of the carrier helium and the furnace temperature for production of the KCl particles which carry the fission products to the receiver. As a result of this work we have established a set of best operating parameters for the helium jet.

*Variable Energy Cyclotron, AERE Harwell

Fig. 2.1 is an example of a ^{252}Cf fission product spectrum obtained under these best conditions. The fission products were collected for 10 minutes and the resulting source was then counted for 10 minutes to give this spectrum. The seven fission product peaks marked on the figure have been chosen to cover a range of γ -ray energies and different parts of the fission yield curve. We now know what count rates to expect for them after a 10 minute collection time and they can therefore be used as markers when trying out modifications to the jet transport or to check whether or not any problems have arisen with it.

2.2.4 Control of VEC beam line hardware and data acquisition with a PET/MOUSE microcomputer system (J.G. Cuninghame and H.E. Sims (AERE))

In order to make measurements on very short lived isotopes made by the irradiation of targets on the VEC a large number of operations must be carried out accurately over a short period. The beam stopper, tape drive of the helium jet recoil transport and the counting equipment all have to be switched on or off; the beam current must be continuously recorded and so must all of the times. It is impossible to do all these things manually at the level of accuracy required.

A series of hardware items has been developed which carries out the necessary operations under control of the computer system. First of all, the experimental requirements are entered into the PDP-11/34 computer. On starting the experiment the relevant information is passed from the PDP-11/34 to a PET microcomputer which organises the whole experiment via the MOUSE microcomputer and the dedicated boxes attached to the various pieces of hardware; the PET also instructs the PDP-11/34 to carry out the counting by using the MLSPEC program and displays information on the progress of the experiment on its own screen. At the end of the experiment all the data are collected by the PDP-11/34 and stored on disc.

2.2.5 Software for the acquisition and analysis of γ -spectral data in decay scheme studies on short-lived fission products (J.G. Cuninghame, J.A.B. Goodall and H.E. Sims (AERE); G. Hayton (F. International))

The main problem in making γ -measurements on nuclides with very short half-lives is that one must acquire several γ -ray spectra successively during the time over which the decay occurs. Since the counting time for each spectrum can only be short, poor statistics result. The solution to this problem is to repeat the experiment many times under identical

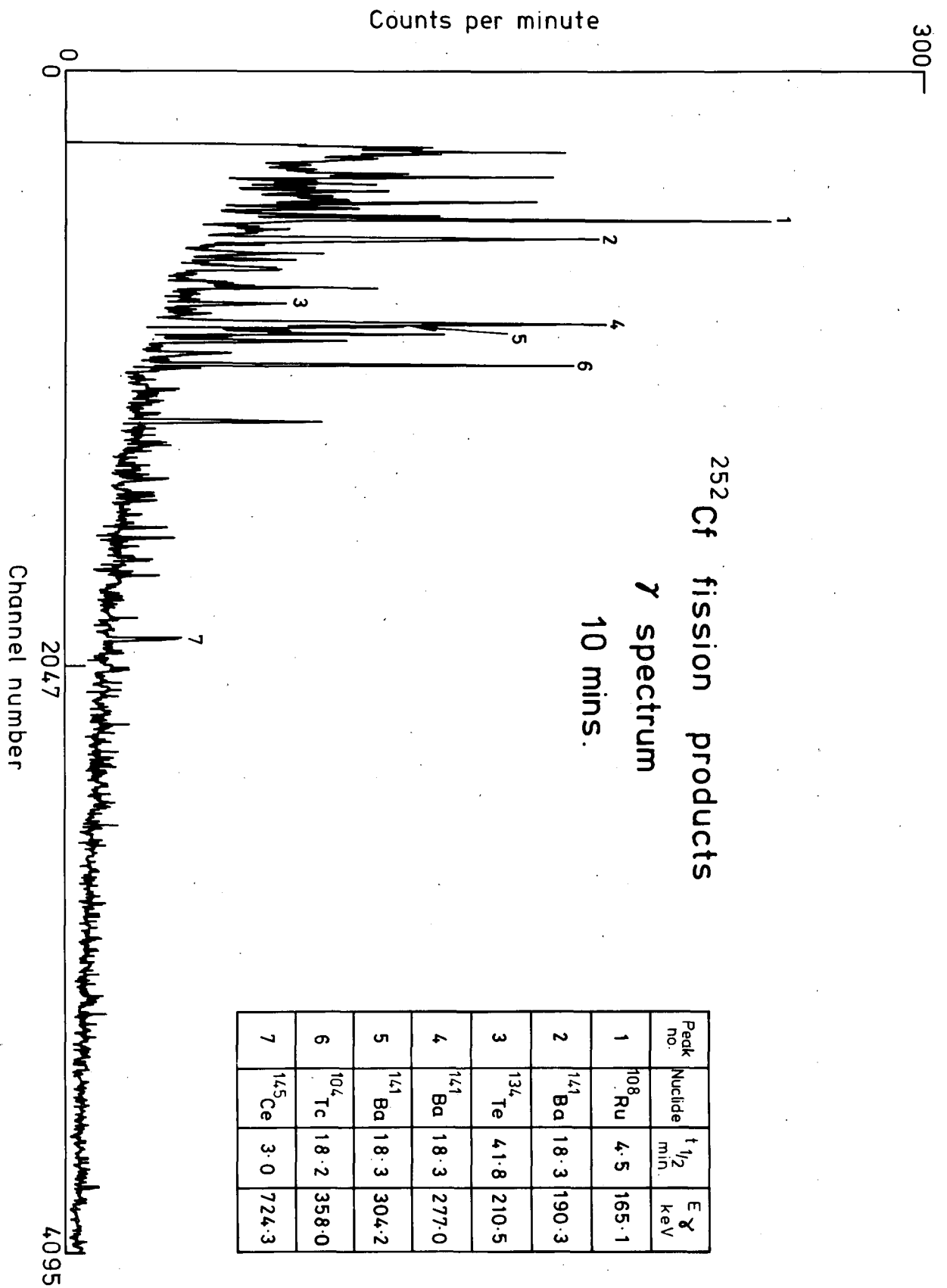


Fig. 2.1 The γ -spectrum from ^{252}Cf fission products (10 min. collection time, 10 min. counting time).

conditions, adding the spectra together until sufficient data have been accumulated.

A program (MLSPEC) has been written for the PDP-11/34 computer in which the alternate use of two 4096 word buffers located in upper core permits up to 50 successive γ -spectra to be accumulated and stored on disc with no break between spectra and with counting times as short as 5 secs. The program can be run over and over again with a fresh source each time, adding the new data to the previous set of γ -spectra until a sufficiently good set has been obtained. This set can then be used as input data for any of our data analysis program, e.g. GAMANAL, PHALIB, or SAMP80. The development of the program SAMP80 is described in sect. 2.2.6.

2.2.6 γ -spectrum analysis using SAMP80 (J.G. Cuninghame, J.A.B. Goodall and H.E. Sims (AERE))

A copy of the program SAMPO was obtained for use on the PDP-11/34 computer. The program was modified to read spectral data in the format produced by our various data acquisition programs and to produce output files of γ -peak areas, background data, etc. identical to those produced by GAMANAL, for display and decay curve analysis by programs such as PHALIB and FATAL. This new version is known as SAMP80. A comparison with GAMANAL has shown that for most spectra SAMP80 and GAMANAL produce similar results; only when the spectrum contains complex multiplets or very poor statistical data is there any advantage of GAMANAL over SAMP80. Since SAMP80 runs on our own PDP-11/34 it has considerable advantages over GAMANAL, which requires the use of the IBM central computer.

2.2.7 Heavy ion reactions on ^{93}Nb and ^{92}Mo (H.E. Sims (AERE); G.W.A. Newton, V.J. Robinson, G.P. Quirk and G. Blower (Manchester University))

The work on the bombardment of ^{93}Nb with ^{16}O ions discussed in UKNDC(82)P105, p.60 has now been analysed in detail, and is being prepared for publication. The yields of 33 product radionuclides were measured at eight ^{16}O beam energies between 117 and 184 MeV. The heavier products (Ag and Pd isotopes) exhibit typical bell-shaped compound nucleus excitation functions, while the lighter ones (isotopes from Y to Ru) give excitation functions which rise monotonically with energy and cannot readily be explained by the compound nucleus model although they account for about one third of the total reaction yield.

In order to explain these latter yields we have developed a model which involves a "soft" but non-fusing collision between the two nuclei.

After a brief encounter, which involves exchange of mass, charge, excitation energy and angular momentum, the nuclei move apart. This model is qualitatively consistent with our experimental observations on the non-compound nucleus yields of the ($^{93}\text{Nb} + ^{16}\text{O}$) system.

Further measurements are being made using ^{12}C , ^{14}N , and ^{20}Ne beams on ^{93}Nb and a variety of the other target-beam combinations. Results so far normally indicate substantial yields of non-compound nucleus products but detailed analysis is not yet complete.

2.2.8 Heavy ion-heavy element reactions (K.M. Glover and K. Howard (AERE))

Progress on this project has been minimal due to shortage of effort.

2.2.9 Absolute determination of the energy of alpha particles emitted by ^{236}Pu (R.A.P. Wiltshire (AERE); A. Rytz (Bureau International des Poids et Mesures))

The only two measurements of the energy of ^{236}Pu alpha particles reported are relative measurements. An absolute energy measurement is being carried out using the uniform-field magnetic spectrometer of BIPM and four sources prepared by Harwell.

2.3 Cross-section measurements

2.3.1 Integral experiments to measure the partial capture cross-sections for the production of $^{242\text{m}}\text{Am}$ and ^{242}Cm from ^{241}Am , and ^{244}Cm from ^{243}Am , using ZEBRA (K.M. Glover, B. Whittaker and R.A.P. Wiltshire (AERE); J.M. Stevenson, A.D. Knipe and D.W. Sweet (AEE Winfrith))

The data from the measurement of the production ratio of ^{242}Cm and ^{244}Cm in a range of fast reactor spectra in ZEBRA are now being analysed (see UKNDC(82)P105, p.62). The results have been converted to one-group production cross-sections, which have been compared with calculated values obtained using neutron spectra from standard ZEBRA analysis methods, together with capture cross-sections from recent differential evaluations of americium data (see Table 2.1). The ratios of calculated/experimental values show means of 0.85 for ^{242}Cm production and 0.95 for ^{244}Cm production, with uncertainties of 5% and 8% respectively. These data give valuable support to the evaluations which, because of shortage of suitable target material for differential cross-section measurements, were almost entirely based on theoretical models.

Table 2.1

Experimental and calculated one-group cross-sections for curium production

| Sample location | ^{242}Cm Production | | | ^{244}Cm Production | | |
|-------------------------------|------------------------------|----------------|--------------------|------------------------------|----------------|--------------------|
| | Experimental (E) | Calculated (C) | C/E | Experimental (E) | Calculated (C) | C/E |
| ZEBRA 12 core centre | 1.48 | 1.28 | 0.86 | - | - | - |
| ZEBRA 14 core centre | 1.28 | 1.16 | 0.91 | 1.61 | 1.60 | 0.99 |
| ZEBRA 16 core centre | - | - | - | 1.99 | 1.72 | 0.86 |
| ZEBRA 21 | | | | | | |
| mid-core radius | 1.18 | 1.03 | 0.87 | 1.34 | 1.43 | 1.06 |
| edge of breeder island | 2.20 | 1.88 | 0.86 | 2.79 | 2.58 | 0.92 |
| Near centre of breeder island | 3.92 | 3.13 | 0.80 | - | - | - |
| Centre of breeder island | 4.07 | 3.32 | 0.82 | 4.85 | 4.52 | 0.93 |
| Mean and standard deviation | | | 0.85 ± 0.04 | | | 0.95 ± 0.08 |

The ^{242m}Am production rate in ^{241}Am samples irradiated in ZEBRA core 21 will be measured on the 50 mg samples over an extended period.

2.3.2 PFR high power reaction rate experiment (K.M. Glover and R.A.P. Wiltshire (AERE))

Samples of ^{241}Am and ^{243}Am irradiated in the Dounreay Prototype Fast Reactor to measure the production rates of ^{242}Cm and ^{244}Cm have been decanned, identified, and will be processed during 1983.

2.3.3 ^{235}U fission mass and counting comparison and standardisation (R.A.P. Wiltshire, M. King and W. Snooks (AERE); B.L.H. Burbidge (AEE Winfrith))

The accuracy of the ^{235}U fission cross-section does not meet the requirements for reactor calculations. A major factor affecting the accuracy of the $^{235}\text{U}(n,f)$ measurement is the uncertainty in the mass of the ^{235}U deposit. A counting comparison and standardisation of ^{235}U fission deposits prepared in laboratories in Europe and in the USA is being co-ordinated by W.P. Poenitz of Argonne National Laboratory. Harwell was invited to participate. Two ^{235}U deposits with active diameter 20 ± 1 mm were prepared by vacuum evaporation on to stainless steel substrates. The isotopic composition was measured by mass spectrometry and the deposits were assayed in defined solid angle counters at Winfriths and at Harwell.

The characterised deposits were sent to ANL for the fission cross-section intercomparison measurements. Evaluation of the mass assay data is in progress. The combined uncertainties take account of uncertainties arising from deposit diameter, uniformity, isotopic impurities, dead time correction, back scatter and self-absorption corrections.

2.4 Half-life measurements

2.4.1 ^{235}Np decay data (B. Whittaker (AERE) and J.L. Campbell (University of Guelph, Canada))

There is increasing interest in the use of ^{235}Np as a yield tracer in studies of the behaviour of ^{237}Np in the environment, but there is a lack of reliable decay data for ^{235}Np . The principal mode of decay is by electron capture with an alpha branching ratio of 1.4×10^{-5} . The reaction $^{238}\text{U}(p,4n)$ at 53.4 MeV can be used to produce ^{235}Np , but ^{234}Np is produced at the same time by the (p,5n) reaction (^{234}Np has a half-life of 4.4 days and also decays by electron capture, the K shell X-rays having the same energy as those of ^{235}Np). A 5 μCi ^{235}Np source has been prepared on a mylar substrate for studies of the fine structure in the K X-ray spectrum. The intensities of the alpha particles emitted by ^{235}Np will be measured at Harwell. The half-life of ^{235}Np is also being determined at Harwell by measuring the ratio of the ^{235}U K_{α} and K_{β} lines from ^{235}Np decay to the 59.5 keV ^{237}Np line from ^{241}Am which is being used as an internal standard. The measurements are being made using a coaxial Ge(Li) detector linked to a Canberra series 80 MCA. Two samples have been used for the measurements, a solid sample of ^{235}Np accurately spiked with ^{241}Am deposited on a thin mylar substrate and a solution of ^{235}Np also accurately spiked with a known quantity of ^{241}Am . The samples are being measured at monthly intervals. Based on twelve data points a preliminary value of 385 ± 4 days is obtained for the half-life of ^{235}Np . This compares with half-life of 396.1 ± 1.2 days obtained by Landrun in 1970.

2.4.2 ^{237}Np half-life and I_{α} (D. Brown, K.M. Glover and B. Whittaker (AERE)) (WRENDA 1287)

There is no progress on this topic due to lack of effort.

2.5 Fission product decay data

2.5.1 Data Library Sub-committee

Committee members: B.S.J. Davies (Chairman, CEGB), A. Tobias (Secretary, CEGB), V. Barnes (BNFL), K.M. Glover (AERE), M.F. James (AEEW), A.L. Nichols (AEEW), H.E. Sims (AERE) and D.G. Vallis (AWRE).

The Data Library Sub-committee (DLSC) is responsible for development and maintenance of the UK Chemical Nuclear Data Libraries, the current state of which is shown in Table 2.2.

Considerable effort has been expended upon production of a Winfrith report (AEEW-R 1407) describing the contents of UKHEDD-1, a library of evaluated heavy element decay data. The computer-based library files are in ENDF/B-V format; they list references used to evaluate each decay scheme and identify their inadequacies. The data include half-life, total decay energies, branching ratios, alpha, beta and gamma energies and intensities, spontaneous fission decay data, average energies, internal conversion coefficients and associated uncertainties. Extensive tabulations of the data are presented in the report by means of various listing programs. The final draft has undergone peer review and is in the process of reproduction.

Work has been started on the development of a new decay data library for activation products (UKPADD-2) in ENDF/B-V format. This constitutes an up-date of the existing library UKPADD-1 and will include data for about 410 nuclides. Of these, 165 are in UKFPDD-2 and a further 17 in UKHEDD-1; these will be used directly in UKPADD-2 so that there remain 228 nuclides to be evaluated. Initially 50 nuclides from ^3H to ^{49}Ca are being assessed.

A general report describing the decay data libraries UKPADD-1, UKFPDD-2, UKHEDD-1 and the fission yield library CROUCH-3I has been published at Berkeley Nuclear Laboratories (RD/B/5095 N81).

The contents of the Spring 1982 version of ENSDF* has been examined with the result that data for use in a revised fission product decay data library UKFPDD-3 has been identified. Spectral data for about 30 short-lived fission products have been extracted from the literature.

2.5.2 CASCADE (H.E. Sims (AERE) and G. Evangelides (Daresbury Laboratory))

The CASCADE suite of programs is now virtually complete. A detailed comparison of CASCADE output with the heavy element decay data file UKHEDD-2 for selected nuclides has been carried out by A.L. Nichols (AEE Winfrith) as a means of validation with satisfactory results. It is hoped that the CASCADE manuals will be available shortly.

*Evaluated Nuclear Structure Data File, National Nuclear Data Centre, Brookhaven National Laboratory

Table 2.2

UK Chemical Nuclear Data Libraries: status table, October 1982

| Data | Present status | File development |
|--|--|---|
| 1. Fission product decay data | Exists as UKFPDD-2 (ENDF/B-IV format); replaces UKFPDD-1 Total no. of nuclides = 855 Radioactive nuclides = 736 Ground state = 715 1st excited state = 133 2nd excited state = 5 Nuclides with spectra = 390 Total no. of γ lines = 11978 Total no. of β^- lines = 3592 Total no. of β^+ lines = 91 | Data acquisition for future revision |
| 2. Activation product decay data | Available in ENDF/B-IV format for 91 nuclides as UKPADD-1 | Evaluation of 15 nuclides has been completed for UKPADD-2 |
| 3. Heavy element and actinide decay data | Completion of UKHEDD-1, including spontaneous fission data, in June 82 Data in ENDF/B-V format for: Total no. of nuclides = 125 Ground state = 11 1st metastable state = 13 2nd metastable state = 1 Total no. of α lines = 767 Total no. of β^- lines = 527 Total no. of β^+ lines = 39 Total no. of γ lines = 3474 Total no. of discrete electrons = 6755 Total no. of X-rays = 381 | |
| 4. Fission yields | Available in ENDF/B-IV format, based on Crouch's second round of adjustments (Crouch 3). 60 new compilations have been added. Yields to isomeric states have been calculated on basis of ENDF/B-IV ratios and are included | A publication describing this evaluation is urgently required |
| 5. Delayed neutrons | Tomlinson data are still recommended | Delayed neutron emission probabilities and half-lives or precursors have been evaluated. The DLSC requires access to these data. Neutron spectra await evaluation |
| 6. (α ,n) cross sections | A library now exists for all α emitters in oxide fuel - for use with UKHEDD-1 | Report in preparation by Barnes (BNFL) |
| 7. Gamma spectra from (n, γ) reactions | None in library | Data being compiled by Davies (BNL) |

Spectral data from the decay data files may be accessed via the retrieval system described by Tobias (RD/B/5170 N81, 1981).

3. REACTOR PHYSICS DIVISION, AEE WINFRITH

(Division Head: Dr. C.G. Campbell)

3.1 The UK Nuclear Data Library and allied topics (M.F. James, R.W. Smith and C.J. Dean)

(a) Following the results of the intercomparison of doppler-broadened cross-sections computed by the computer programs SIGMA1 and MLCS with SIGAR7 in early 1982 and the use of SIGAR7 with the Winfrith resonance parameter evaluation of ^{58}Fe several important modifications have been made to SIGAR7 during the last nine months. These are:

- (1) The automatic provision of extra energy mesh points, where necessary, to improve the cubic spline fit when there are very narrow resonances. Negative cross sections were occurring for certain narrow resonances when using the cubic spline option with the earlier point selection procedure.
- (2) For the Reich-Moore option modifications have been made to allow for the energy shift in the peaks of narrow non s-wave resonances away from the eigenvalues (very important for the case of ^{58}Fe resonance parameters). Two options are available: either the eigenvalues or the resonance peak energies can be supplied as input. A paper was presented at the 1982 Antwerp Conference.
- (3) An improved treatment for calculating the energies of the minima and maxima of s-wave resonances (allowing for distant resonances).
- (4) The program now uses double precision arithmetic throughout.

This programme of developments has been satisfactorily concluded. The program and its user guide will now be made generally available at the earliest opportunity.

(b) The work on the resonance parameter evaluation of the isotopes of iron has been in abeyance. Although the work on ^{54}Fe is almost complete, that for ^{56}Fe and ^{57}Fe remains in progress; however the new Geel measurements reported at Antwerp will now be included for consideration.

(c) A tape file of data for natural iron, for inclusion in the JEF library and produced in accordance with the recommendations of Moxon et al., has been forwarded to the NEA Data Bank.

3.2 Studies of the $^{93}\text{Nb}(n,n')^{93\text{m}}\text{Nb}$ reaction (W.H. Taylor, M.F. Murphy and M.R. March)
(WRENDA 718)

Measured values of the absolute $^{93}\text{Nb}(n,n')^{93\text{m}}\text{Nb}$ reaction rates in the fissile region of the experimental fast reactor ZEBRA have been compared with values calculated using both the latest Strohmaier⁽¹⁾ and older Hegedus⁽²⁾ values for the cross-section for the reaction. The measured values were normalised to the measured $^{239}\text{Pu}(n,f)$ and $^{54}\text{Fe}(n,p)^{54}\text{Mn}$ reaction rates and values for these rates were calculated using cross-section data from the ENDF/B-V dosimetry file. The ratio of the calculated values to the measured values are included in Tables 3.1 and 3.2.

Table 3.1

Reaction rate ratio $^{93}\text{Nb}(n,n')^{93\text{m}}\text{Nb}/^{239}\text{Pu}(n,f)$ in ZEBRA

| Measured value | Calculated value | |
|----------------------|------------------|---------|
| | Measured value | |
| 0.0201 ± 1.9% random | Strohmaier | Hegedus |
| 4.6% systematic | 0.97 | 0.74 |

Table 3.2

Reaction rate ratio $^{93}\text{Nb}(n,n')^{93\text{m}}\text{Nb}/^{54}\text{Fe}(n,p)^{54}\text{Mn}$ in ZEBRA

| Measured value | Calculated value | |
|--------------------|------------------|---------|
| | Measured value | |
| 2.84 ± 2.1% random | Strohmaier | Hegedus |
| 4.7% systematic | 1.06 | 0.86 |

It will be seen that better agreement with measurement is obtained using the Strohmaier data.

The above work has been done to support the measurements of the differential cross-section for the $^{93}\text{Nb}(n,n')^{93\text{m}}\text{Nb}$ reaction which have been made using the Dynamitron machine at the Birmingham Radiation Centre (BRC). This has been done with the joint efforts of AERE, AEEW and BRC and is reported by AERE in sect. 1.7 above.

(1) B. Strohmaier, private communication (1982).

(2) Threshold Reaction Neutron Cross Sections EANDC 95 "U".

4. DIVISION OF RADIATION SCIENCE AND ACOUSTICS,

NATIONAL PHYSICAL LABORATORY

(Supt. Dr. W.A. Jennings)

4.1 International intercomparisons of neutron source strength (E.J. Axton and A.G. Bardell)

- (a) BIPM* intercomparison of NBS $10^7 \text{ s}^{-1} \text{ }^{252}\text{Cf}$ spontaneous fission source. Co-ordinator NPL, twelve participants. The source has now been returned to NBS for final re-measurement. Chemical analyses of the MnSO_4 solution have been carried out by CBNM** and VGKRI.
- (b) BIPM intercomparison of NBS $10^9 \text{ s}^{-1} \text{ }^{252}\text{Cf}$ source. Co-ordinator PTB, three participants. This source is currently being returned from NPL to NBS for final re-measurement.
- (c) BIPM intercomparison of NRC*** $10^6 \text{ s}^{-1} \text{ Ra/Be } (\alpha, n)$ source. Co-ordinator NRC. This is a bilateral intercomparison with VNIIM of the source used in the 1st BIPM intercomparison, 1962-5.
- (d) Intercomparison of $10^6 \text{ s}^{-1} \text{ }^{252}\text{Cf}$ source. This is a bilateral intercomparison between NPL and INEL****. Measurements have been completed.

4.2 International intercomparison of neutron fluence rate organised by BIPM (J.B. Hunt, V.E. Lewis and T.B. Ryves)

Details of the intercomparison have been given previously (UKNDC(80)P96, p.89; UKNDC(82)P105, p.72). The current situation is summarised below:

- (a) $^{115}\text{In}(n, n')^{115\text{m}}\text{In}$ intercomparison at 2.5, 5.0 and 14.8 MeV. Co-ordinator CBNM, ten participants (including China). Measurements completed, analysis in progress.

*Refer to UKNDC(82)P105, p.71 for abbreviations.

**Central Bureau for Nuclear Measurements, Belgium.

***National Research Council of Canada.

****Idaho National Engineering Laboratory, USA.

- (b) $^{115}\text{In}(n,\gamma)^{116\text{m}}\text{In}$ intercomparison at 144 and 565 keV.
Co-ordinator NPL, six participants.
Measurements in progress.
- (c) ^{235}U fission chamber at all energies, ^{238}U fission chamber at 2.5, 5.0 and 14.8 MeV.
Co-ordinator AERE/NPL, eight participants, including linacs.
Measurements to start in 1983.
- (d) Nb/Zr intercomparison at 14.8 MeV only.
Co-ordinator NPL, nine participants.
Completed; see sect. 4.3 for further details.

4.3 International intercomparison of d+t neutron fluence and mean energy (V.E. Lewis)

This was co-ordinated by NPL and held under the auspices of BIPM. Measurements by nine participants were carried out in 1981 and the analysis was completed early in 1982. Simultaneous irradiation of niobium and zirconium was used, with the postal return of irradiated samples to NPL for the activity measurements. The fluence results were fairly consistent, especially if allowance was made for special factors affecting two slightly discrepant results. The mean energy estimates (from 14.0 to 14.8 MeV), compared by the ratios of Zr to Nb activities, generally agreed with the original NPL calibration.

This intercomparison was a good test of the Nb/Zr transfer system and has showed the technique to be satisfactory.

4.4 The $^{65}\text{Cu}(n,2n)$ cross section at 14 MeV (G. Winkler* and T.B. Ryves)

A precision measurement of this cross-section by the activation technique has been made in Vienna. This new value has been incorporated in a re-evaluation of the $^{65}\text{Cu}(n,2n)$ cross-section at 14.70 MeV, also making use of the recently measured ^{64}Cu decay scheme branching ratios (see sect. 4.6) to update all the experimental data in the literature. The previous results of the simultaneous evaluation⁽¹⁾ are little changed, apart from the $^{65}\text{Cu}(n,2n)$ cross-section, which has dropped 2% and has a much reduced uncertainty.

*Institut für Radiumforschung und Kernphysik, Vienna

(1) J.G. Hayes and T.B. Ryves, Ann. Nucl. Energy 8 (1981) 469.

4.5 The indium cross-sections at 14 MeV (T.B. Ryves and Ma Hongchang*)

A comprehensive set of measurements by the activation technique of the various reaction cross-sections of indium at 14 MeV has been completed and analysis of the data is now proceeding. During the course of this work it was necessary to measure some of the half-lives and decay scheme data of the radionuclides found in the various reactions.

4.6 Nuclear decay scheme measurements (P. Christmas, D. Smith, M.J. Woods, R.A. Mercer, T.B. Ryves, G. Winkler**)

Half-life measurements have been continued for $^{152,154}\text{Eu}$; preliminary values are $(13.2 \pm 0.1)\text{y}$ and $(8.5 \pm 0.1)\text{y}$ respectively.

A paper describing further work on ^{137}Cs has been accepted for publication ⁽¹⁾, with the following abstract:

Evidence is presented to support the view that the approximate shape factor $C = q^2 + bp^2$ does not adequately describe the second-forbidden beta-decay of ^{137}Cs . An improved formula is given, with single-particle estimates of the nuclear matrix-element ratios.

According to this model the coefficient of p^2 involves considerable cancellation between matrix elements; when due allowance is made for this, good fits to the experimental data are obtained, leading to better estimates of the decay scheme parameters.

The value $(85.21 \pm 0.07)\%$ was obtained for the γ -ray intensity per disintegration.

The branching ratios in the decay of ^{64}Cu , which decays by the emission of positrons and electrons and also by electron capture, have been determined by six distinct but partially correlated measurements. From the data, best estimates, including covariances, were obtained by a generalised least-squares criterion. The ratio of electrons to positrons was determined by β spectrometry and separately by $4\pi\beta\gamma$ coincidence counting using a gas proportional counter. The total activity and total β branching ratio were determined by $4\pi\beta\gamma$ coincidence counting using a liquid scintillation technique. The positron branching ratio was estimated by

*Institute of Atomic Energy, Beijing

**Institut für Radiumforschung und Kernphysik, Vienna

Ge(Li) γ -ray spectrometry, firstly by comparison of emission rates of annihilation quanta from sources of ^{64}Cu and ^{22}Na of known activity, and secondly by counting the total γ -rays from a copper foil of known activity which had been irradiated in a standard thermal neutron field. The yield of the low intensity 1.34 MeV γ -ray was also determined. Preliminary results are given in Table 4.1.

Table 4.1
The decay of ^{64}Cu

| Mode | Intensity (%) | Endpoint energy (keV) |
|------------------------|-------------------|-----------------------|
| β^- decay | 39.04 ± 0.30 | 577.8 ± 1.0 |
| β^+ decay | 17.86 ± 0.12 | 651.4 ± 1.0 |
| Electron capture | 43.11 ± 0.20 | - |
| 1.34 MeV γ -ray | 0.471 ± 0.011 | - |

- (1) H. Behrens and P. Christmas, The Beta Decay of ^{137}Cs , Nuclear Physics, to be published.

5. BIRMINGHAM RADIATION CENTRE*, UNIVERSITY OF BIRMINGHAM

(Director: Professor J. Walker)

5.1 Neutron spectrometry with ^3He detectors (J.G. Owen, D.R. Weaver and J. Walker)
(WRENDA 1184)

Measurements and analysis of the response function and efficiency of our second ^3He spectrometer have continued throughout the year, as has the analysis of the $^3\text{He}(n,p)^3\text{H}$ events in short rise-time channels of the older detector (UKNDC(82)P105, p.75). The calibration measurements have absorbed the available accelerator time and no new measurements of delayed neutron spectra have been made. However, we have summed all previously reported ^{235}U spectra to produce a delayed neutron pulse height distribution corresponding to a broad spread of energy in the incident fast neutrons. This distribution was unfolded and the result is shown in Fig. 5.1.

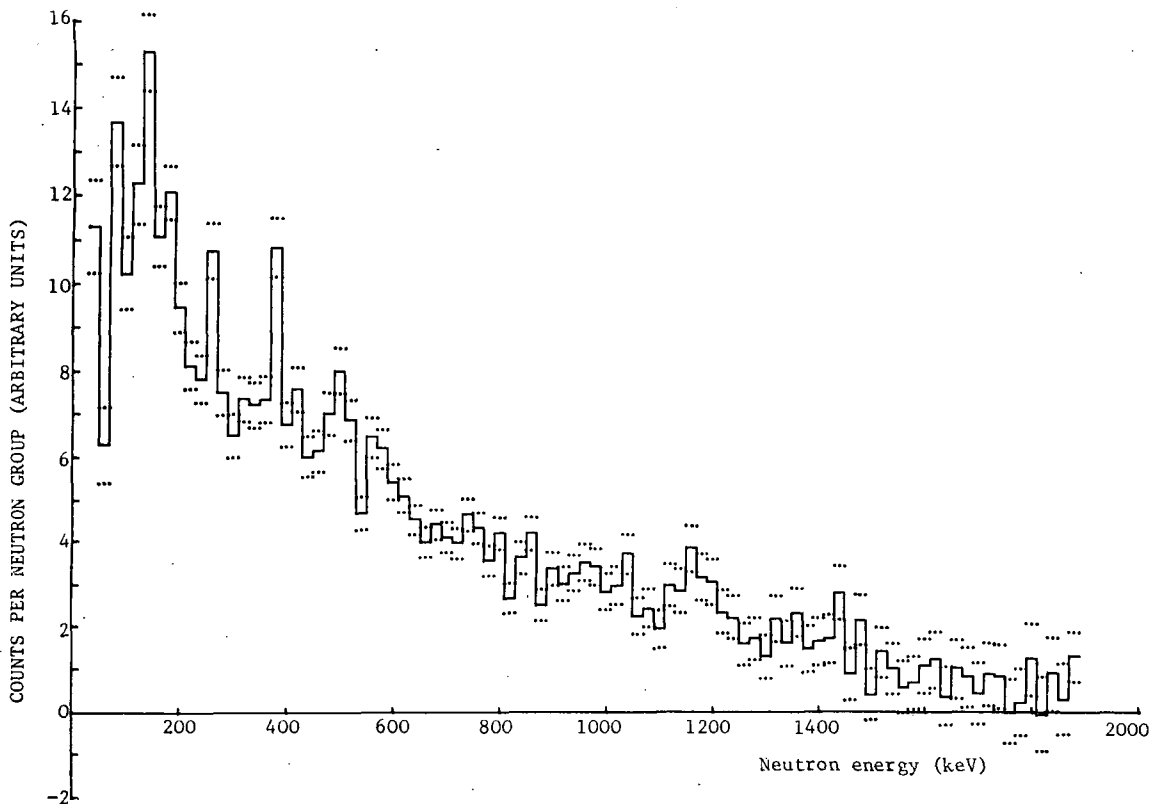


Fig. 5.1 The combined delayed neutron spectrum for fast neutron fission of ^{235}U . Errors represent ± 1 s.d.

*Operated jointly by the Universities of Birmingham and Aston in Birmingham.

5.2 Neutron spectra from (α ,n) sources
(WRENDA 31, 255)

A letter detailing the neutron spectrum measurement of the National Physical Laboratory (NPL) Am/Li source referred to in last year's report (UKNDC(82)P105, p.74) has now been published⁽¹⁾ and has led to our being asked to co-ordinate an international group of measurements of this source by those laboratories involved in delayed neutron spectrum measurements. It is hoped that this will provide a comparison of the techniques used, and in particular give some indication of the reasons for differences in delayed neutron spectra measurements by different types of spectrometer.

We have also completed spectrum measurements of an NPL Am/F source, but final analysis awaits the complete determination of the detector response function; a preliminary report was presented at the IAEA meeting on Nuclear Data for Science and Technology⁽²⁾.

(1) D.R. Weaver, J.G. Owen and J. Walker, Nucl. Instr. Meth. 198 (1982) 599-602.

(2) J.G. Owen, D.R. Weaver and J. Walker, Neutron spectrum from Am/F and Am/Li (α ,n) sources, Int. Conf. on Nucl. Data for Sci. and Tech., Antwerp, Sept. 1982.

6. DEPARTMENT OF PHYSICS, UNIVERSITY OF BIRMINGHAM

6.1 Measurements relating to tritium production in fusion reactor breeder blankets (D.A. Naylor and M.C. Scott) (WRENDA 54, 58, 88, 89, 93)

Earlier work on fusion reactor breeder blanket neutronics centred on neutron spectrum measurements in a spherical assembly of LiF⁽¹⁾. However, this assembly did not lend itself to studying the effect of first wall materials and blankets, so a new integral assembly has been made, consisting of six 1 x 1 x 0.15 m aluminium clad slabs of LiF. At the same time, we have started to measure tritium production directly by irradiating pellets of LiOH placed within the LiF assembly and determining the tritium produced using the same techniques as Swinhoe and Uttley⁽²⁾. In order to make the results absolute, viz. tritium atoms per unit mass of LiOH per source neutron, the neutron yield from the high current tritium target was monitored using a ²³⁸U fission counter which had previously been calibrated using the associated particle technique on a thin target. Allowance has been made for reflection from the assembly.

Some preliminary results of measurements of the dependence of tritium production on axial distance into the LiF assembly using both ^{nat}Li and ⁷Li pellets are shown in Fig. 6.1, where they are compared to Monte Carlo calculations using the ENDF/B-IV data set. Note, however, that only the slopes should be compared, since some correction factors for the absolute values of the measured results have still to be evaluated. It can be seen, however, that the shapes of both the ^{nat}Li and ⁷Li results are in good agreement except near the source, where the experimental slope is less than that predicted. Possible reasons for this are under investigation.

Although tritium production measurements are essential as an overall cross-section check, they are very time-consuming because of the high integrated currents required (>15 mA hours). In many studies a measure of the change in the ratio of tritium production in ⁶Li to production in ⁷Li would be of interest. The use of lithium in, say, scintillation counters, should allow this measurement to be made in principle, but in practice there are a number of interfering processes (e.g. γ -interactions) which make it difficult. However, it may be possible to use the ²³⁵U and ²³²Th fission cross-sections to simulate the ⁶Li and ⁷Li tritium production cross-sections respectively. We have therefore investigated the use of ²³⁵U and ²³²Th fission chambers as a method for estimating the lithium

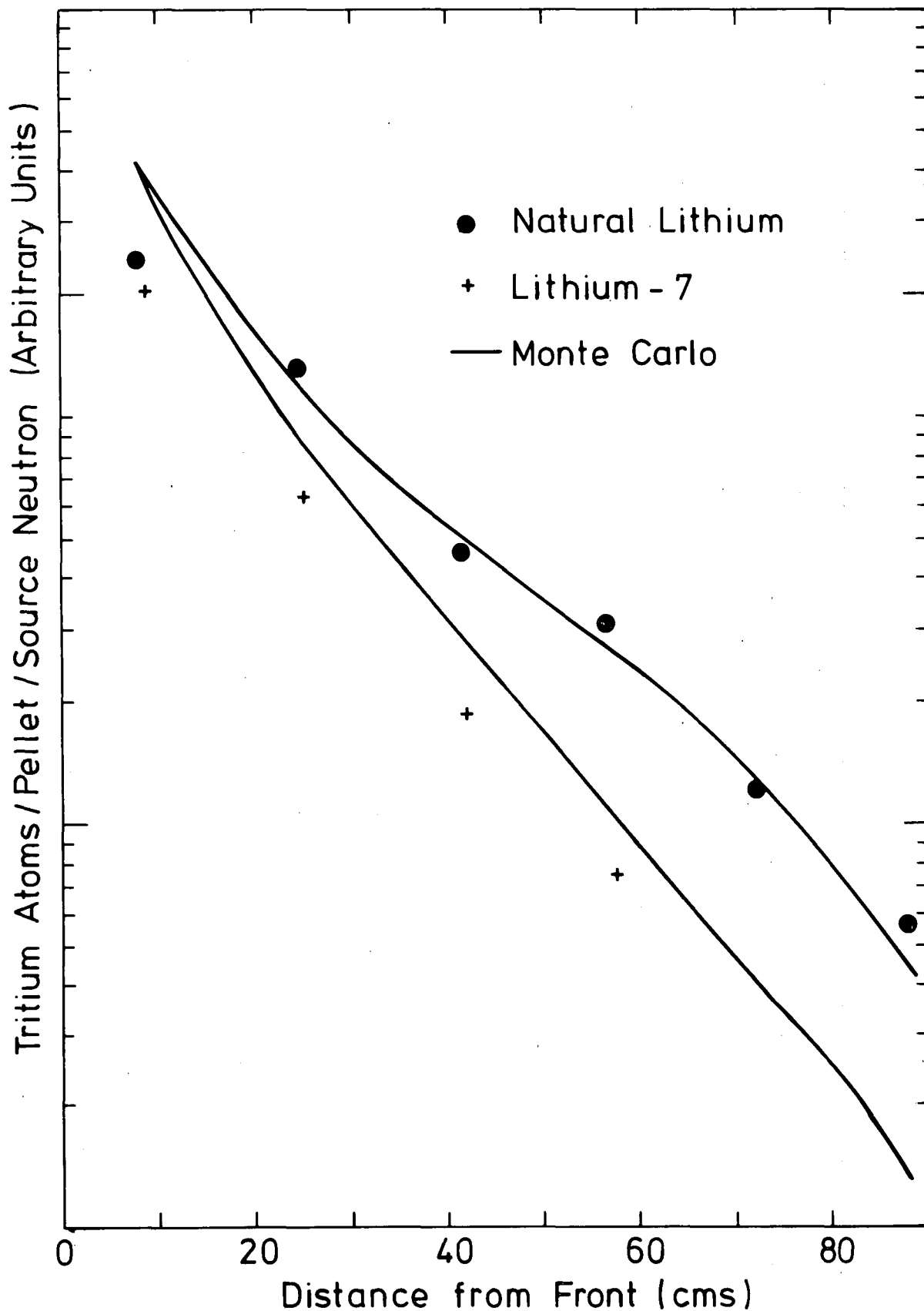


Fig. 6.1 Dependence of tritium production on axial distance into LiF assembly measured using both $^{nat}\text{LiOH}$ and $^7\text{LiOH}$ pellets.

reaction rate ratio, and have made measurements in a number of LiF assemblies, incorporating Be, Fe and graphite to simulate reflectors and first wall materials. Whilst it is clear that cross-section differences between ${}^6\text{Li}$ and ${}^{235}\text{U}$ and between ${}^7\text{Li}$ and ${}^{232}\text{Th}$ will mean that the ${}^6\text{Li}/{}^7\text{Li}$ and ${}^{235}\text{U}/{}^{232}\text{Th}$ ratios do not vary in exactly the same way, the similarities are sufficient to make this a useful method for parameter studies and for mapping in difficult geometries, e.g. round beam injector ducts. Fig. 6.2 compares the fission rate ratio ${}^{235}\text{U}/{}^{232}\text{Th}$ with the tritium production rate ratio ${}^6\text{Li}/{}^7\text{Li}$. The upper part gives the calculated ${}^6\text{Li}/{}^7\text{Li}$ ratio as a function of axial distance into a bare LiF assembly for a point source at the centre of the front face, and the lower part compares the ${}^{235}\text{U}/{}^{232}\text{Th}$ ratio with the ${}^6\text{Li}/{}^7\text{Li}$ ratio through the quantity $R = ({}^{235}\text{U}/{}^{232}\text{Th}) / ({}^6\text{Li}/{}^7\text{Li})$. The absolute value of R depends on the thickness of the fissile deposit in the fission chambers, so R is normalised to an average value of 1. It can be seen that there is only an $\sim 30\%$ variation in R for a variation of more than a factor 10 in the ${}^6\text{Li}/{}^7\text{Li}$ ratio.

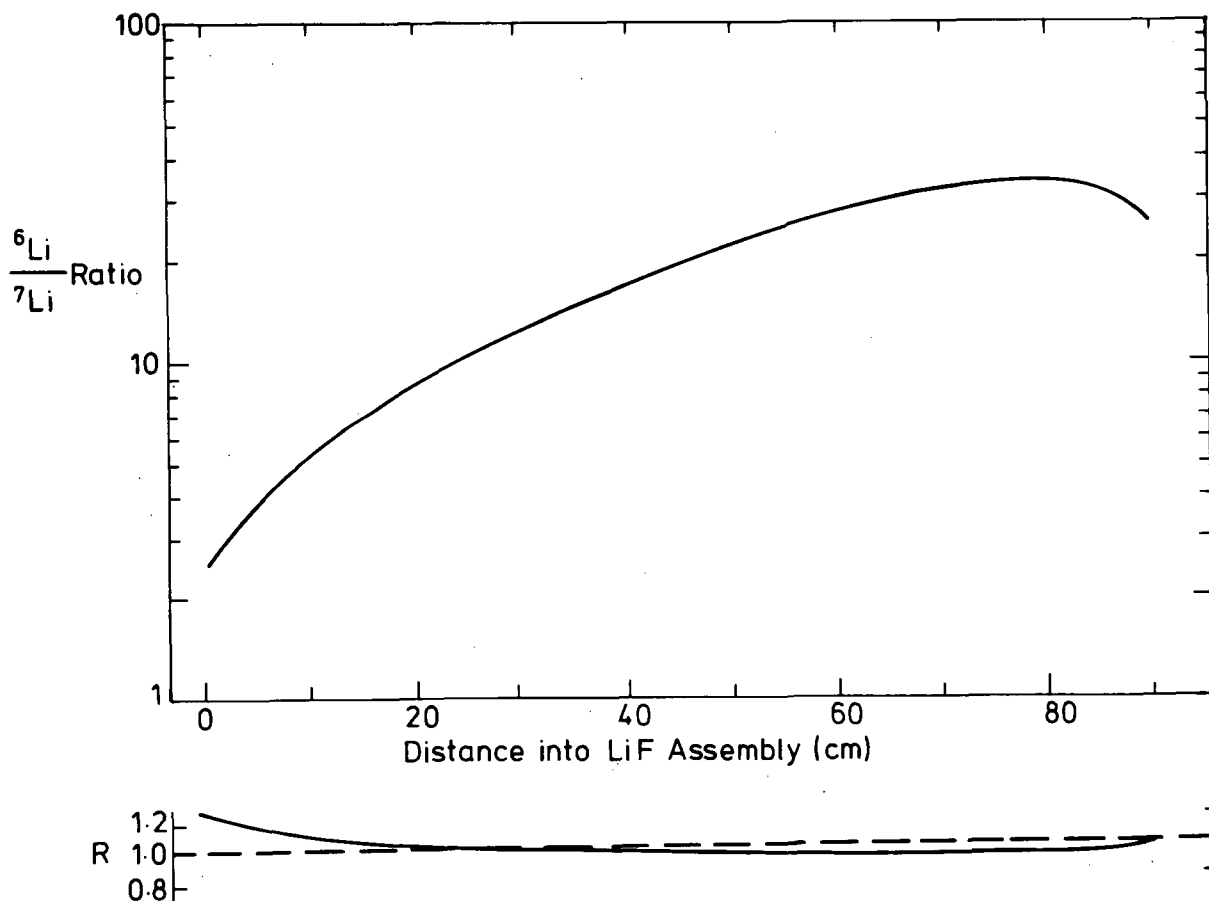


Fig. 6.2 The simulation of ${}^6\text{Li}/{}^7\text{Li}$ tritium production cross-sections by ${}^{235}\text{U}/{}^{232}\text{Th}$ fission cross-sections. The lower part gives the ratio R of fission cross-section ratio to tritium production ratio for the variation in tritium production ratio shown in the upper part.

- (1) L.J. Perkins, N. Evans, R. Koochi-Fayegh, M.C. Scott and B.Y. Underwood, Nucl. Sci. Engng. 78 (1981) 30-43.
- (2) M.T. Swinhoe and C.A. Uttley, Proc. Int. Conf. Nuclear Cross Section for Technology, Knoxville, 1979, ed. J.L. Fowler et al. (NBS Special Publication 594, 1980) p.246. (work also reported in AERE-R 9929 (1980)).

7. DEPARTMENT OF PHYSICS, UNIVERSITY OF ASTON IN BIRMINGHAM

7.1 The absolute measurement of (n,p) and (n, γ) cross sections in the energy range 2 to 4.5 MeV (H.A. Hussain and S.E. Hunt)
(WRENDA 339, 591, 593, 595, 644, 645, 979, 981)

Neutrons of energies from 2.0 to 4.5 MeV were obtained from the $^2\text{H}(d,n)^3\text{He}$ reaction using a 2 MeV deuteron beam from the Joint Birmingham Dynamitron accelerator. The energy of the neutrons was determined by the angle subtended by the sample at the target with respect to the deuteron beam, and the neutron flux was estimated from the proton yield of the associated $^2\text{H}(d,p)^3\text{H}$ reaction. Activation techniques were used and the cross sections calculated from the observed γ activity. The results are shown in Table 7.1.

7.2 The gamma rays associated with the inelastic scattering of 14 MeV neutrons in large samples of iron and concrete (A.J. Cox and B. Al-Shalabi)
(WRENDA 477, 479 and 480)

This work is an investigation of the effect of neutron multiple scattering on the cross-sections for the production of gamma rays by neutrons in fusion reactor structural materials, specifically iron and concrete. Energy spectra and angular distributions of the emergent gamma rays from inelastic neutron scattering in slabs of various thicknesses have been measured using a NaI(Tl) detector. The neutrons were produced using the $^3\text{H}(d,n)^4\text{He}$ reaction, with the deuterons being accelerated by a SAMES type J accelerator and by the 3 MeV Dynamitron at the Joint Aston and Birmingham Universities' Radiation Centre. An associated particle time-of-flight technique was used to gate the gamma ray signals in order to reduce the background. The angular resolution of the system was $\pm 4^\circ$ while the overall time resolution of 3.5 ns enabled the gamma ray and neutron pulses to be completely resolved. The iron scattering samples were in the form of rectangular slabs 120 x 220 mm with various thicknesses ranging from 20 to 76 mm. The concrete samples were rectangular plates with dimensions 230 x 150 mm. The thickness of each plate was 25 mm, and the different samples studied consisted of 2, 5, 8 and 10 plates giving a sample thickness of 50, 125, 200 and 250 mm respectively. The concrete samples used were of ordinary concrete (type 5) which had been ultrasonically treated to increase its density to about 2500 kg m^{-3} . This treatment has no effect on the chemical composition of concrete, which was assumed to be 15.1% hydrogen, 55.7% oxygen, 3.2% aluminium, 14.9% silicon and 3.6% calcium constituting about 93% of the concrete composition^(1,2). These percentages were used in the calculation of the differential cross-sections.

Table 7.1

Measured (n,p) and (n, γ) reaction cross-sections

| Neutron energy (MeV) | Energy spread (MeV) | Reaction cross-sections (barn) | | | | | |
|----------------------|---------------------|-------------------------------------|-------------------------------------|-------------------------------------|-------------------------------------|--|--|
| | | $^{27}\text{Al}(n,p)^{27}\text{Mg}$ | $^{47}\text{Tl}(n,p)^{47}\text{Sc}$ | $^{58}\text{Ni}(n,p)^{58}\text{Co}$ | $^{64}\text{Zn}(n,p)^{64}\text{Cu}$ | $^{115}\text{In}(n,\gamma)^{116\text{m}_1}\text{In}$ | $^{197}\text{Au}(n,\gamma)^{198}\text{Au}$ |
| 2.050 | 0.08 | | | | 0.0094 | | |
| 2.116 | 0.08 | | | | 0.0133 | | 0.0539 |
| 2.188 | 0.08 | | | | 0.0102 | | - |
| 2.266 | 0.08 | | | | 0.0114 | | 0.0452 |
| 2.351 | 0.08 | | 0.0372 | 0.086 | - | | 0.041 |
| 2.442 | 0.09 | | 0.0312 | 0.1027 | 0.026 | 0.140 | 0.0371 |
| 2.539 | 0.12 | | - | - | - | 0.1235 | - |
| 2.552 | 0.14 | | - | 0.122 | 0.0317 | - | - |
| 2.757 | 0.24 | | 0.0373 | 0.1403 | - | - | - |
| 2.871 | 0.27 | | - | 0.1541 | 0.0512 | 0.102 | 0.0262 |
| 2.992 | 0.32 | 0.00171 | 0.0405 | - | 0.0569 | - | - |
| 3.115 | 0.36 | 0.00375 | 0.0407 | 0.1885 | - | 0.089 | - |
| 3.237 | 0.4 | 0.00374 | - | 0.2137 | - | - | 0.021 |
| 3.356 | 0.46 | 0.00511 | 0.0502 | 0.2376 | - | 0.0732 | - |
| 3.472 | 0.52 | - | 0.0565 | 0.246 | 0.07608 | - | - |
| 3.586 | 0.56 | 0.00606 | 0.0595 | 0.279 | - | - | 0.0207 |
| 3.7 | 0.6 | 0.00589 | 0.0685 | - | - | 0.0459 | - |
| 3.816 | 0.64 | 0.00630 | 0.0612 | 0.305 | - | - | - |
| 3.933 | 0.68 | 0.00955 | 0.0613 | 0.365 | 0.1047 | 0.0432 | - |
| 4.049 | 0.7 | 0.0118 | 0.0641 | 0.342 | - | - | - |
| 4.159 | 0.72 | 0.0117 | 0.0638 | - | - | 0.0408 | - |
| 4.259 | 0.74 | 0.0106 | - | 0.382 | 0.1078 | - | - |
| 4.344 | 0.76 | - | 0.068 | 0.4014 | 0.1121 | 0.033 | - |
| 4.413 | 0.76 | - | 0.0672 | 0.405 | - | - | - |
| 4.463 | 0.76 | 0.0174 | - | 0.421 | - | - | - |
| 4.504 | 0.76 | 0.0204 | - | - | 0.1248 | 0.0292 | - |

The overall uncertainty in the cross-section measurements for the (n,p) reactions was about 4% throughout, that for $^{115}\text{In}(n,\gamma)^{116\text{m}_1}\text{In}$ approximately 16% and for $^{197}\text{Au}(n,\gamma)^{198}\text{Au}$ approximately 8.5%.

A typical iron spectrum is shown in Fig. 7.1. Two lines can be seen in the spectrum at 0.84 and 1.24 MeV which are identified as the gamma rays from the first two excited states in ^{56}Fe . Fig. 7.2 shows the angular distributions for the 0.84 MeV gamma ray for the various sample thicknesses. The differential cross-sections were first corrected for contributions from competing reactions (e.g. $(n,2n)$) and then fitted by the least-squares method to an even order Legendre polynomial series. Data obtained by other authors ^(3,4,5) are also shown.

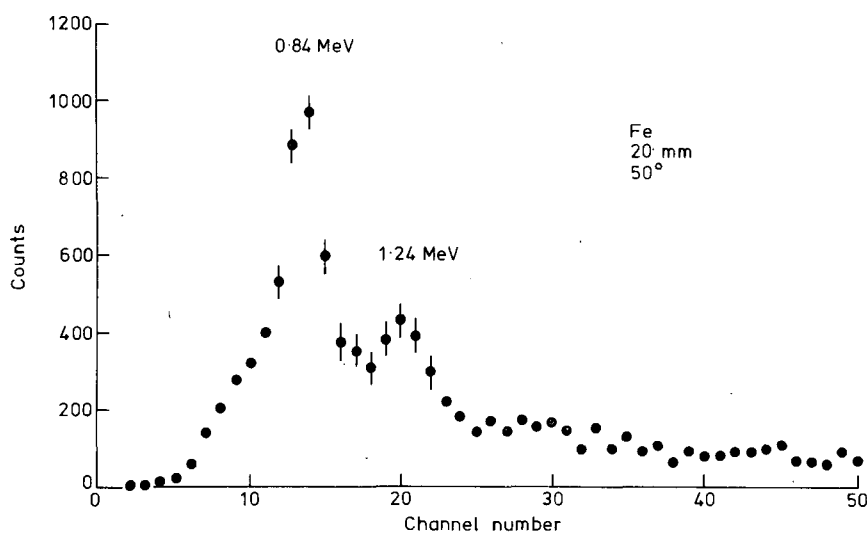


Fig. 7.1 Typical spectrum of γ rays at 50° from 14 MeV neutrons on a 20 mm thick iron sample.

The results for concrete are given in Table 7.2 in the form of differential cross-sections for the production of gamma rays of energies between 1 and 6 MeV in 1 MeV bins. Fig. 7.3 shows the angular distribution for the production of 2-3 MeV gamma rays from concrete samples of different thicknesses. Contradicting the normal assumption, the angular distribution is very anisotropic and the anisotropy increases with increasing sample thickness. The solid lines in Fig. 7.3 are least-squares fits of the experimental results using even order Legendre polynomials. In each case the uncertainties were calculated by combining the component errors in quadrature.

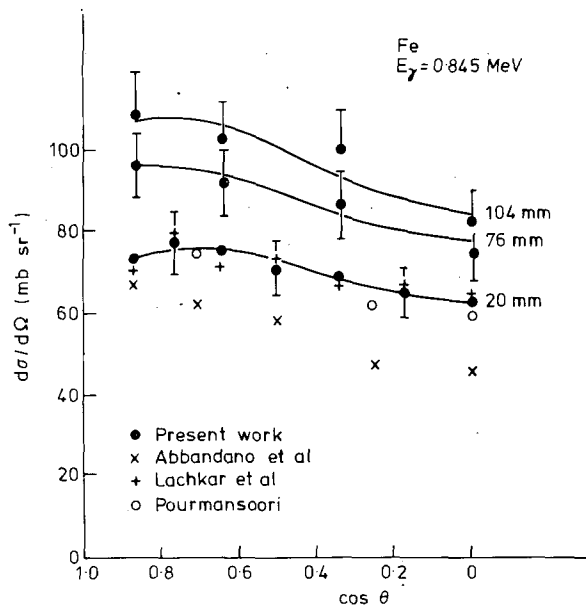


Fig. 7.2 Angular distributions of 0.845 MeV γ rays from the $^{56}\text{Fe}(n,n'\gamma)$ reaction with 14 MeV neutrons for various sample thicknesses.

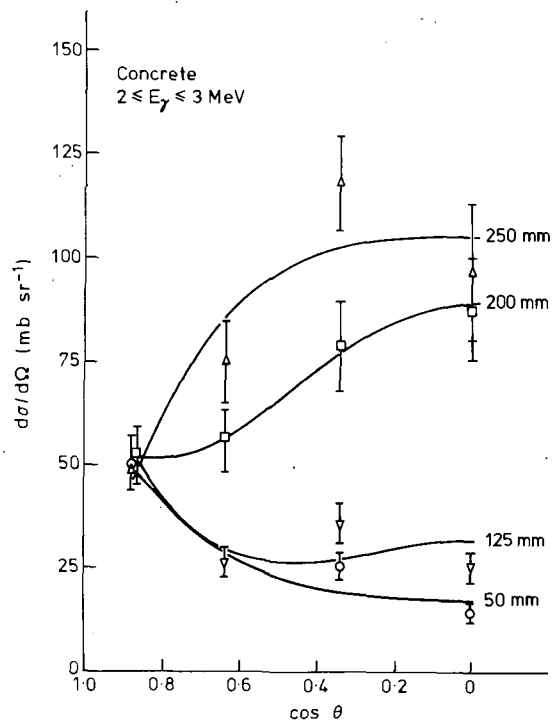


Fig. 7.3 Angular distributions of 2-3 MeV γ rays from 14 MeV neutrons on concrete samples of various thickness.

There is a general increase in the effective gamma ray production cross-section as the thickness of the sample increases due to multiple scattering effects, and in the region covered by the present work this increase is described for both iron and concrete by the equation

$$\sigma = \sigma_0 \exp \{ \alpha x \}$$

where σ is the effective cross-section for a sample, x mean free paths thick, and σ_0 is the cross-section for zero thickness. Fits of the experimental results yield a value for α of 0.17 ± 0.1 per mean free path.

-
- (1) A.M. Neville, Properties of Concrete (Pitman, London, 1963).
 - (2) Engineering Compendium on Radiation Materials, ed. R.C. Jaeger, vol.2 (Springer-Verlag, Berlin, 1975).
 - (3) F.C. Engeser and W.E. Thompson, J. Nucl. Energy 21 (1967) 487.
 - (4) B. Jonsson, K. Nyberg and I. Bergquist, Arkiv For Fysik 32 (1969) 295.
 - (5) J. Lachkar, J. Sigaud, Y. Patin and G. Haugat, Nucl. Sci. Engng. 55 (1974) 168.

Table 7.2

Differential cross-sections $d\sigma/d\Omega$ for the production of gamma rays at angle θ by 14 MeV neutrons in concrete samples of thickness t

| θ° | t (mm) | $d\sigma/d\Omega$ (mb sr ⁻¹) for gamma ray energy bins | | | | |
|----------------|-------------|--|--------------|--------------|------------|------------|
| | | 1-2 MeV | 2-3 MeV | 3-4 MeV | 4-5 MeV | 5-6 MeV |
| 30 | 50 | 13.3 ± 2.1 | 50.0 ± 7.0 | 55.9 ± 6.1 | 30.5 ± 2.7 | 26.9 ± 2.2 |
| 30 | 125 | 15.4 ± 2.5 | 52.8 ± 7.4 | 80.7 ± 8.9 | 50.4 ± 4.5 | 42.5 ± 3.4 |
| 30 | 200 | 20.9 ± 3.3 | 52.3 ± 7.3 | 72.4 ± 8.0 | 44.8 ± 4.0 | 43.0 ± 3.4 |
| 30 | 250 | 17.9 ± 2.9 | 48.1 ± 6.7 | 53.0 ± 5.8 | 23.8 ± 2.1 | 23.6 ± 1.9 |
| 50 | 50 | 17.4 ± 2.8 | 26.5 ± 3.7 | 30.7 ± 3.9 | 17.0 ± 1.5 | 13.0 ± 1.0 |
| 50 | 125 | 18.4 ± 3.0 | 26.4 ± 3.0 | 39.4 ± 4.3 | 24.4 ± 2.2 | 22.7 ± 1.8 |
| 50 | 200 | 34.8 ± 5.6 | 56.4 ± 7.9 | 65.7 ± 7.1 | 54.0 ± 4.9 | 61.2 ± 4.9 |
| 50 | 250 | 51.4 ± 8.2 | 75.0 ± 10.5 | 77.1 ± 8.5 | 33.5 ± 3.0 | 30.8 ± 2.5 |
| 70 | 50 | 10.6 ± 1.7 | 25.1 ± 3.5 | 32.0 ± 3.5 | 17.2 ± 1.5 | 14.8 ± 1.2 |
| 70 | 125 | 19.3 ± 3.1 | 35.6 ± 5.0 | 36.0 ± 4.0 | 16.6 ± 1.5 | 15.0 ± 1.2 |
| 70 | 200 | 52.9 ± 8.3 | 78.3 ± 11.0 | 92.5 ± 10.2 | 54.3 ± 4.9 | 52.2 ± 4.2 |
| 70 | 250 | 78.4 ± 12.5 | 118.6 ± 16.6 | 110.8 ± 12.2 | 45.1 ± 4.6 | 49.8 ± 4.0 |
| 90 | 50 | 11.3 ± 1.8 | 14.1 ± 2.0 | 13.6 ± 1.5 | 11.8 ± 1.1 | 15.4 ± 1.2 |
| 90 | 125 | 31.2 ± 5.0 | 25.6 ± 3.6 | 32.2 ± 3.5 | 15.6 ± 1.4 | 16.2 ± 1.3 |
| 90 | 200 | 75.3 ± 12.0 | 78.6 ± 12.3 | 64.6 ± 7.1 | 21.1 ± 1.9 | 24.9 ± 2.0 |
| 90 | 250 | 77.9 ± 12.5 | 96.8 ± 13.6 | 70.7 ± 7.8 | 49.8 ± 4.5 | 30.7 ± 2.5 |

7.3 Measurements of $^{28}\text{Si}(n,p)^{28}\text{Al}$ and $^{64}\text{Zn}(n,2n)^{63}\text{Zn}$ excitation functions (R.A. Jarjis*)
(WRENDA 295,296)

It is widely recognised that improving the accuracy of cross-section standards and experimental procedures are important steps to fulfil current data requirements. This has motivated the present investigation in which a novel experimental technique is applied to the measurement of selected reaction cross-sections. Activation cross-sections for the $^{28}\text{Si}(n,p)^{28}\text{Al}$ and $^{64}\text{Zn}(n,2n)^{63}\text{Zn}$ reactions were measured using the concentric ring technique⁽¹⁾. Discs made of pure elemental silicon or zinc were enclosed in concentric geometry within copper and aluminium rings, and activated with $^3\text{H}(d,n)^4\text{He}$ neutrons. Neutron energies were determined using the method of $^{63}\text{Cu}(n,2n)^{62}\text{Cu}$ and $^{27}\text{Al}(n,p)^{27}\text{Mg}$ cross-section ratios^(1,2). Our measured Si and Zn cross-sections shown in Fig. 7.4 were determined relative to the $^{27}\text{Al}(n,p)^{27}\text{Mg}$ and $^{63}\text{Cu}(n,2n)^{62}\text{Cu}$ cross-sections respectively. Cross-section data for the reference reactions have been

*Present address: Nuclear Physics Division, AERE Hawell

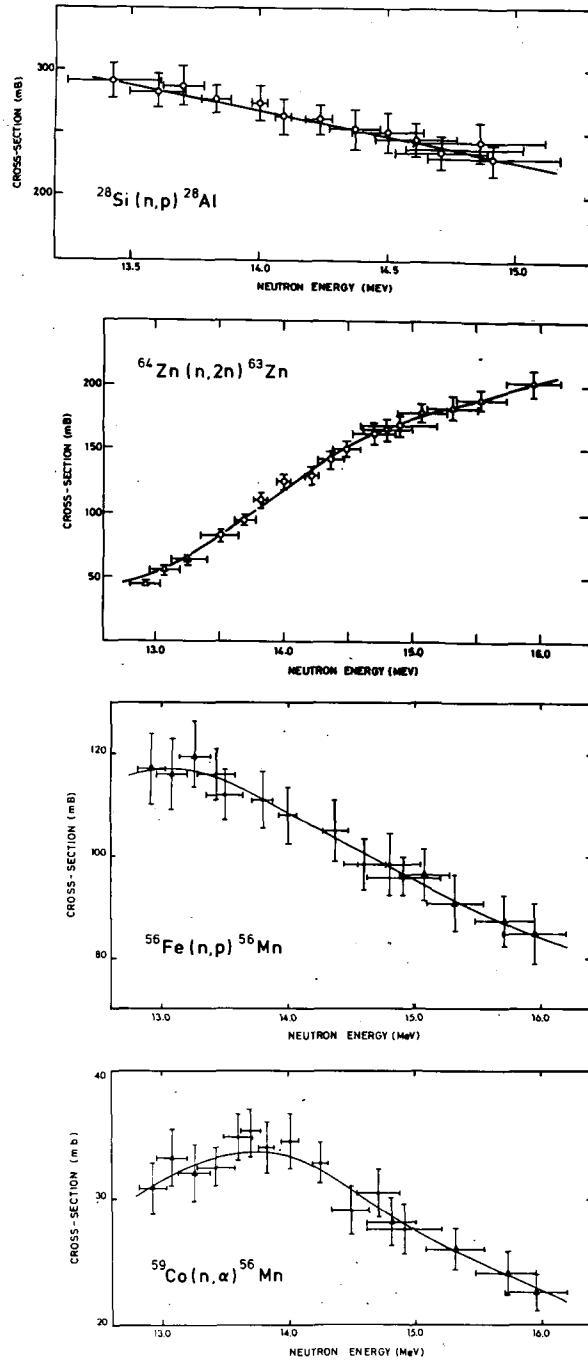


Fig. 7.4 Excitation functions of the $^{28}\text{Si}(n,p)$, $^{64}\text{Zn}(n,2n)$, $^{56}\text{Fe}(n,p)$ and $^{59}\text{Co}(n,\alpha)$ reactions.

reported by us previously⁽³⁾.

Most of the $^{28}\text{Si}(n,p)^{28}\text{Al}$ data have been reported at selected neutron energies. Our data agree with the latest results of Kaji et al.⁽⁴⁾ (252 mb at 14.1 MeV) and Robertson et al.⁽⁵⁾ (265 mb at 14.78 MeV). Statistical

calculations indicate that the reaction cannot be accounted for entirely by compound nucleus formation (210 mb at 14.1 MeV⁽⁴⁾). The present $^{64}\text{Zn}(n,2n)^{63}\text{Zn}$ results are in remarkable agreement with the carefully measured data of the Japanese group⁽⁶⁾ (13.4 - 14.8 MeV). This and the fact that the reaction has a reasonably high cross-section and gives a simple gamma spectrum indicate that the reaction is a good candidate for fast neutron monitoring applications. Compound nucleus calculations⁽⁶⁾ have overestimated the cross-section of this reaction by ignoring the $^{64}\text{Zn}(n,p)^{64}\text{Cr}$ reaction.

-
- (1) R.A. Jarjis and S.E. Hunt, Int. J. Appl. Radiat. Isot. 26 (1975) 57.
 - (2) R.A. Jarjis, Nucl. Instr. Meth. 184 (1981) 439.
 - (3) R.A. Jarjis, J. Phys. G. 4 (1978) 445.
 - (4) H. Kaji et al., Sci. Rep. Tohoku Univ. Ser. 1, 58 (1975) 54.
 - (5) J.C. Robertson, B. Audric and P. Kolkowski, J. Nucl. Energy 27 (1973) 531.
 - (6) H. Kaji et al., Sci. Rep. Tohoku Univ. Ser. 1, 58 (1975) 40.

7.4 Application of a neutron monitoring antimony ring for the measurement of $^{56}\text{Fe}(n,p)^{56}\text{Mn}$ and $^{59}\text{Co}(n,\alpha)^{56}\text{Mn}$ cross-sections (R.A. Jarjis*) (WRENDA 486-490, 528)

The excitation function of the $^{121}\text{Sb}(n,2n)^{120g}\text{Sb}$ has been reported by us previously⁽¹⁾. The data show a broad maximum with a cross-section of about 1 barn in the 14 MeV region. These qualities are attractive for fast neutron flux monitoring which was conducted in the present work under improved geometry and using the antimony reaction. Antimony rings were activated in concentric geometry with discs made of iron or cobalt, and the induced activities were determined using a NaI(Tl) detector. Our measured cross-sections are shown in Fig. 7.4.

The $^{56}\text{Fe}(n,p)^{56}\text{Mn}$ data are in good agreement with the excitation functions of Liskien and Paulsen⁽²⁾ and Santry and Butler⁽³⁾. There is also good agreement with the careful measurements of Kudo⁽⁴⁾ (107.1 ± 3.1 mb at 14.8 MeV). Statistical model calculations have underestimated the $^{56}\text{Fe}(n,p)^{56}\text{Mn}$ cross-section⁽⁵⁾; this points to the

*Present address: Nuclear Physics Division, AERE Harwell

existence of a direct interaction contribution. In order to predict total (n,p) cross-sections, Levkovskii⁽⁶⁾ has proposed an exponential equation containing the neutron asymmetry parameter. This formula produces a value of 100 mb for 14-15 MeV neutrons, in very good agreement with the present data.

Similarly, the corresponding (n, α) formula⁽⁶⁾ predicts a cross-section of 26 mb for ⁵⁹Co, which is again close to our experimental data. Our results also agree with the recent mixed powder results of Ghorai et al.⁽⁷⁾, but there are some disagreements with the general excitation function trends of refs. 2, 3 and 8. On a theoretical basis there are strong indications that the reaction proceeds by compound nucleus formation. An isotropic α -particle angular distribution has been reported⁽⁹⁾, and statistical model calculations predict cross-section of 27 mb at 14.0 MeV⁽¹⁰⁾.

-
- (1) R.A. Jarjis, Nucl. Instr. Meth. 184 (1981) 439.
 - (2) H. Liskien and A. Paulsen, J. Nucl. Energy, A/B 19 (1965) 73.
 - (3) D.C. Santry and J.P. Butler, Can. J. Chem. 42 (1964) 1030.
 - (4) K. Kudo, Nucl. Instr. Meth. 141 (1977) 325.
 - (5) H. Kaji et al., Sci. Rep. Tohoku Univ. Ser. 1, 58 (1975) 54.
 - (6) V.N. Levkovskii, Sov. J. Nucl. Phys. 18 (1974) 361.
 - (7) S.K. Ghorai, J.E. Gaiser and W.L. Alford, Ann. Nucl. Energy 7 (1980) 41.
 - (8) F. Gabbard and B.D. Kern, Phys. Rev. 128 (1982) 1276.
 - (9) E. Saetta-Menichella et al., Nucl. Phys. 51 (1964) 449.
 - (10) U. Facchini et al., Nucl. Phys. 51 (1964) 460.

8. DEPARTMENT OF PHYSICS, UNIVERSITY OF EDINBURGH

8.1 The polarisation and differential cross-section for elastic scattering of 3 MeV neutrons by heavy nuclei (J.R.M. Annand, R.B. Galloway and H. Savalooni)
(WRENDA 1008, 1213, 1214)

Simultaneous measurements (see UKNDC(82)P105, p.76) of the angular dependence of polarisation due to elastic scattering and of the elastic differential cross-section for 3 MeV neutrons scattered by W, Hg, Tl, Pb, Bi and U have been made; the data have been compared with the results of optical model and Hauser-Feshbach calculations and optimum optical model parameters found (see Table 8.1). The calculations for W show little resemblance to the observed polarisation distribution. The Hg data is fitted quite acceptably. For Tl the parameters giving the best fit to the polarisation data do not give the best fit to the differential cross-section. Neither the Pb nor Bi polarisation data is fitted well around $40^\circ - 60^\circ$, while the U polarisation data is not fitted well by the calculations. Coupled channels calculations for W and for U made significant differences to the polarisation distributions but without achieving a good fit.

Table 8.1
Optimised optical potential parameters

| Parameter | W | Hg | Tl | Pb | Bi | U |
|---------------|-------|-------|-------|-------|-------|-------|
| V | 44.02 | 45.84 | 43.94 | 43.60 | 43.71 | 45.08 |
| r_R | 1.26 | 1.25 | 1.30 | 1.30 | 1.30 | 1.22 |
| a_R | 0.64 | 0.67 | 0.62 | 0.63 | 0.63 | 0.73 |
| $(r_R)_{rms}$ | 1.06 | 1.06 | 1.08 | 1.08 | 1.08 | 1.04 |
| J_V/A | 398 | 406 | 430 | 427 | 428 | 372 |
| W | 9.91 | 7.69 | 18.99 | 9.75 | 15.77 | 6.12 |
| r_I | 1.28 | 1.25 | 1.32 | 1.32 | 1.32 | 1.21 |
| a_I | 0.66 | 0.46 | 0.20 | 0.19 | 0.19 | 0.37 |
| $(r_I)_{rms}$ | 1.37 | 1.34 | 1.33 | 1.33 | 1.33 | 1.24 |
| J_W/A | 97.9 | 71.2 | 56.3 | 27.9 | 44.3 | 27.4 |
| V_S | 4.18 | 3.86 | 3.20 | 6.89 | 6.96 | 2.86 |
| r_S | 1.26 | 1.25 | 1.30 | 1.30 | 1.30 | 1.22 |
| a_S | 0.13 | 0.52 | 0.55 | 0.22 | 0.23 | 0.82 |

Measurements are now being made on scatterers with mass number around 120.

An account has been published of the tests on the stability of the 22 liquid scintillation counters used in the fast neutron polarimeter⁽¹⁾.

(1) J.R.M. Annand and R.B. Galloway, Nucl. Instr. Meth. 201 (1982) 381.

8.2 Polarisation of neutrons from the ${}^7\text{Li}(d,n){}^8\text{Be}$ reaction (R.B. Galloway and A.M. Ghazarian)
(WRENDA 98)

The polarisation of the ground state neutrons from the ${}^7\text{Li}(d,n){}^8\text{Be}$ reaction induced by 500 keV and 450 keV deuterons has been determined for reaction angles from 25° to 125° . The polarisation was evaluated from the asymmetry in scattering by ${}^4\text{He}$ in the form of a gas scintillation counter at a pressure of 75 atmospheres. Scattered neutrons were detected in a pair of NE213 liquid scintillation counters symmetrically placed at a scattering angle of 55° in the scattering plane. Any instrumental asymmetry was cancelled by frequent interchange of the neutron detectors in the computer controlled measurement sequence. Rejection of excited state neutrons was by pulse-height discrimination. Pulse-shape discrimination rejected gamma-ray events and the requirement of coincident detection of ${}^4\text{He}$ recoil and scattered neutron rejected neutron background.

The measurements were made, firstly, in a search for a reaction that would provide 14 MeV polarised neutrons from a low energy accelerator for elastic scattering studies, and secondly, because early DWBA calculations for deuteron induced reactions at less than 1 MeV on light nuclei gave an expectation of polarised emitted nucleons and such calculations had not been subjected to experimental test.

The angular distribution of polarisation and differential cross-section have been compared with DWBA calculations (see Fig 8.1).

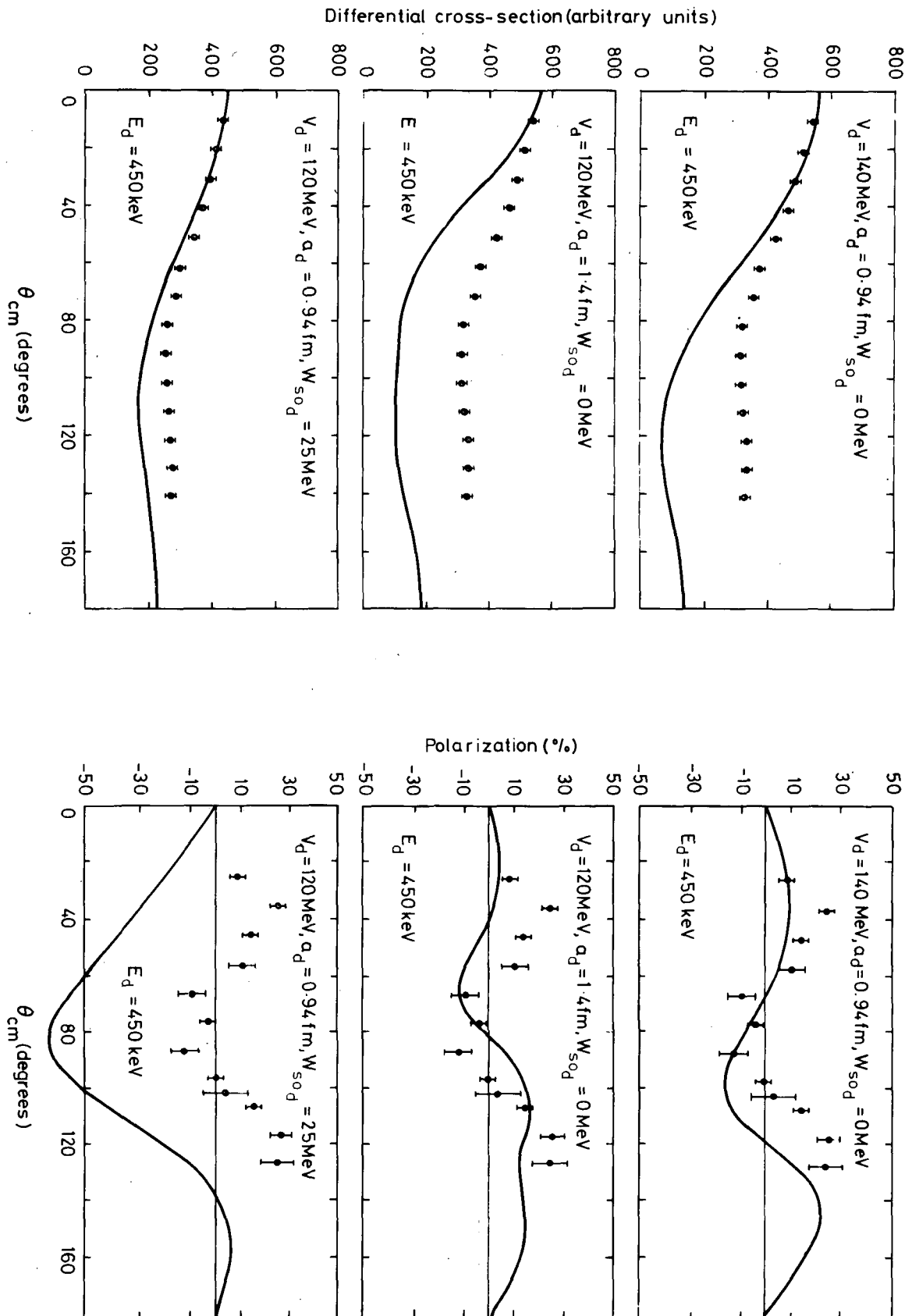


Fig. 8.1 Differential cross-sections and polarisations for the ${}^7\text{Li}(d,n)$ reaction. Solid circles: measured cross-sections and polarisations for 450 keV deuterons - the arbitrary units of the cross-section vertical scale are the same in the three figures. Solid curve: DWBA calculation, deuteron optical model parameters (real depth, surface diffuseness and spin-orbit imaginary depth) being given. The DWBA cross-sections are normalised to the data at 0° .

9. DEPARTMENT OF PHYSICS, UNIVERSITY OF LIVERPOOL

9.1 Nuclear structure data evaluation (N.J. Ward and F. Kearns)

During the last year, data evaluation work at Liverpool has proceeded steadily in the $A = 65 - 75$ mass region assigned to the U.K.

In May 1982 the IAEA advisory group on Nuclear Structure and Decay Data met to discuss the progress of the international effort over the last two years and make recommendations for the future. It was agreed that it was important for the network to completely finish the first cycle of mass-chain evaluations before moving on to the second.

Mass-chain schedule

Evaluation of data for nuclides with masses 68, 70, 71, 72, 73 and 75 were completed and published in Nuclear Data Sheets before January 1982. During the course of 1982 the review of data for $A = 69$ nuclides was published (N.D.S. 35, 101) and that for $A = 66$ nuclides was submitted for publication. Mass-chains at present under review are:

A = 65 submission planned for summer 1983

A = 67 submission planned for early 1983

A = 74 temporarily reassigned to the Kuwait Nuclear Structure Data Evaluation Group

This will mark the completion of the first cycle of mass-chain evaluations assigned to the U.K.

Future plans

As a result of the discussion at the IAEA advisory group meeting the Liverpool group has agreed to assume temporary responsibility for one or two mass-chains not previously assigned to any other group; it is hoped to begin work on the review of data for $A = 165$ nuclides during the course of the next year.